2023

Geological Survey Paper 13:

Structural Geology of the Southern Tyennan Domain, Tasmania—An Overview, Synthesis and Structural Implications

Author: D. R. Gray and M. J. Vicary
Date: 16/03/2022
Email: info@mrt.tas.gov.au
Website: www.mrt.tas.gov.au

REPORT No.: GSP13

Mesoscopic recumbent folds within intensely foliated quartzite from a ridgeline defining the northwest corner of the "folded zone" middle shell of the De Witt-Propsting mega-sheath fold. The folds are plunging to the northwest in the direction of the photo. The Lawson Range occupies the ridgeline on the horizon.

Tasmanian Government
Mineral Resources Tasmania
mrt

CONTENTS

Abstract

The Southern Tyennan Domain occupies the southwest part of the Proterozoic core of Tasmania. It has a complex structural architecture consisting of a stacked series of isoclinal macro-folds within a composite, layered metamorphic "sheet" made up of high-grade schist, low-grade phyllite, low-grade quartzite and platy quartzite. Contacts between the high-grade and low-grade units are high-strain, mylonitic zones (HSZ) that in many cases have brittle/cataclastic overprints from Late Cambrian and younger deformations. Shear sense indicators suggest a complex movement picture with the overall emplacement shear sense towards the southwest (~250°).

Structurally the Southern Tyennan domain is dominated by two regional-scale isoclinal, mega-sheath folds that have ~25 km length widths (sheath 'y' dimension) and ~20 km sheath lengths (sheath 'x' dimension). They are the structurally higher, east-closing De Witt-Propsting mega-sheath fold and the underlying west-closing South West Cape mega-sheath fold. Together they form a complementary isoclinal sheath-fold pair within quartzite and platy quartzite/quartzite respectively. In map view, the mega-sheath folds have approximately north-south-elongated elliptical sections, or sheath shell profiles, that are bisected by the broadly west-south west trending mineral lineation (Lm). The sheath form of the De Witt-Propsting and South West Cape mega-sheath folds are defined by doubly plunging, closed-loop outcrop patterns. The apparent antiformal form of the De Witt-Propsting sheath core reflects an east-closing geometry, whereas the apparent synformal, downward facing form of the South West Cape sheath core reflects a west-closing geometry. Both mega-sheath folds show complex refolding and overprinting fabrics within their cores reflecting decoupling of the inner sheath shell(s) accompanied by shear-related translation relative to the outer sheath shells.

The Nye Bay fold-nappe overlying the Mulcahy Bay-Port Davey isoclinal fold stack in high-grade schist forms an outboard carapace to the De Witt-Propsting mega-sheath fold. The high-grade schist occurs within the core of the fold-nappe with the map pattern indicating attenuation of the schist to the north beyond the Lawson Range. The Nye Bay fold nappe is interpreted as a bending fold formed at the leading-edge of the ascending composite sheet (allochthon). Roll-over of the sheet edge is caused by tractional forces at the base of the overlying ophiolite sheet effectively pinning the leading edge, with bending caused by continued bouyant ascent of the allochthon. This is analogous to stubbing your toe (toe-stub mechanism).

The eastern part of the Southern Tyennan domain, incorporating the asymmetric-fold domain including the Arthur Range, represents the lowest part of the structural architecture. It shows a reverse stacking of low-grade platy quartzite overlying quartzite overlying low-grade pelite. Structurally it consists of an 'S'-vergent, asymmetric, isoclinal third-order macro-fold pair bounded by a regional scale shear zone. This is shown in the Solly River Valley and Crest Range where the asymmetric-fold domain structurally overlies, with a high strain transition into, a low-grade pelite sequence. This low-grade sequence consists of dolomitic phyllite and dolomite, a possible equivalent of the para-autochthonous Scotchfire metamorphic sheet.

A Mid- to Late Cambrian northwest-trending, fault-bounded wrench or strike-slip graben in the Joe Page Bay and Melaleuca Inlet part of Bathurst Harbour truncates the early mega-fold architecture. This graben has structural and sedimentation characteristics similar to the wrench basins along the San Andreas fault-system in the western United States.

Devonian folding overprints and refolds the Cambrian age fold-nappe and mega-sheath fold architecture with dominant northwest- and north-south trending folds and smaller domains of northeast- and east-west trending folds. The younger Devonian fold plunges and axial surface traces are controlled by the major Cambrian fold geometries and broad structural architecture.

Tasmanian Government

Mineral Resources Tasmania

Department of State Growth
www.mrt.tas.gov.au

Structural Geology of the Southern Tyennan Domain, Tasmania - an Overview, Synthesis and Structural Implications

David R. Gray[1] and Michael J. Vicary[2]
[1] *Consultant Structural Geologist to Mineral Resources Tasmania*
[2] *Geological Survey Branch - Mineral Resources Tasmania*

ARTICLE INFO

Published: 16 March 2023
Publisher: Mineral Resources Tasmania
Report No.: GSP13

KEYWORDS

Structural Geology
Isoclinal folds
Mega-sheath folds
Southern Tyennan region
High P metamorphism

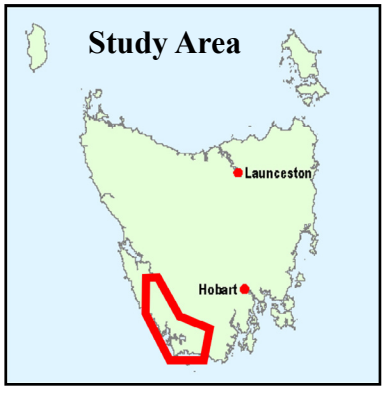

1.0 INTRODUCTION

The Southern Tyennan domain is a structurally complex, litho-tectonic sequence of high-grade garnet schists overlying low-grade phyllite±quartzite, overlying low-grade quartzite (Figure 1). These units represent shear zone-bounded slabs of Proterozoic age continental margin deposits that were subducted to depths of 20 to 60 km beneath an advancing ophioloite sheet during a Cambrian arc-continent collision along the margin of Gondwana (see Berry & Crawford, 1988; Berry, 2014, fig. 4.10).

This Tasmanian Geological Survey Paper is part of a series of Papers revisiting the structural geology of the Tyennan Proteterozoic nucleus of Tasmania (Figure 1). The aim of this study has been to re-examine the structure of the Tyennan Proterozoic rocks in the context of Cambrian continental margin subduction-obduction. Deformation of this former Cambrian continental margin beneath the advancing ophiolite sheet has involved crustal-scale stacking of sheets of different metamorphic grade, isoclinal folding and internal sheet deformation, with sheets welded along their contacts by shear zones and/or brittle faulting. In Tasmania, subsequent erosional removal of the ophiolite sheet has provided an exposed 50-100 km window into these underlying rocks.

In map projection the Southern Tyennan domain has a ~100 km length and ~50 km width representing an oblique crustal view of complex structures within the subducted and obducted Proterozoic continental margin sequence (Figure 2).

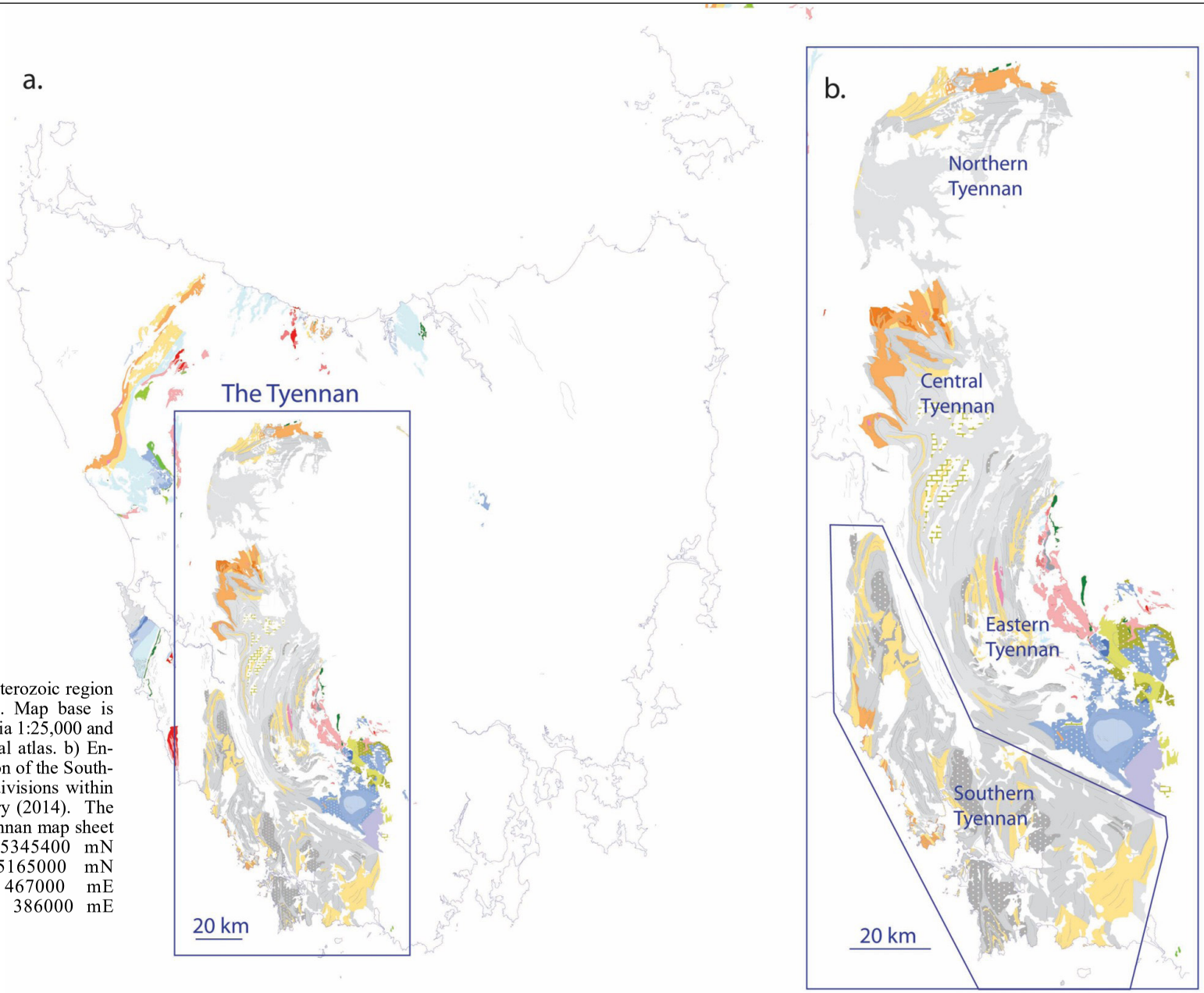

Figure 1. The Tyennan Proterozoic region of Tasmania shown in a). Map base is Mineral Resources Tasmania 1:25,000 and 1:250,000 digital geological atlas. b) Enlarged map with the location of the Southern Tyennan region. The divisions within the Tyennan are after Berry (2014). The approximate Southern Tyennan map sheet polygon boundaries are 5345400 mN (northern boundary), 5165000 mN (southern boundary), 467000 mE (eastern boundary) and 386000 mE (western boundary).

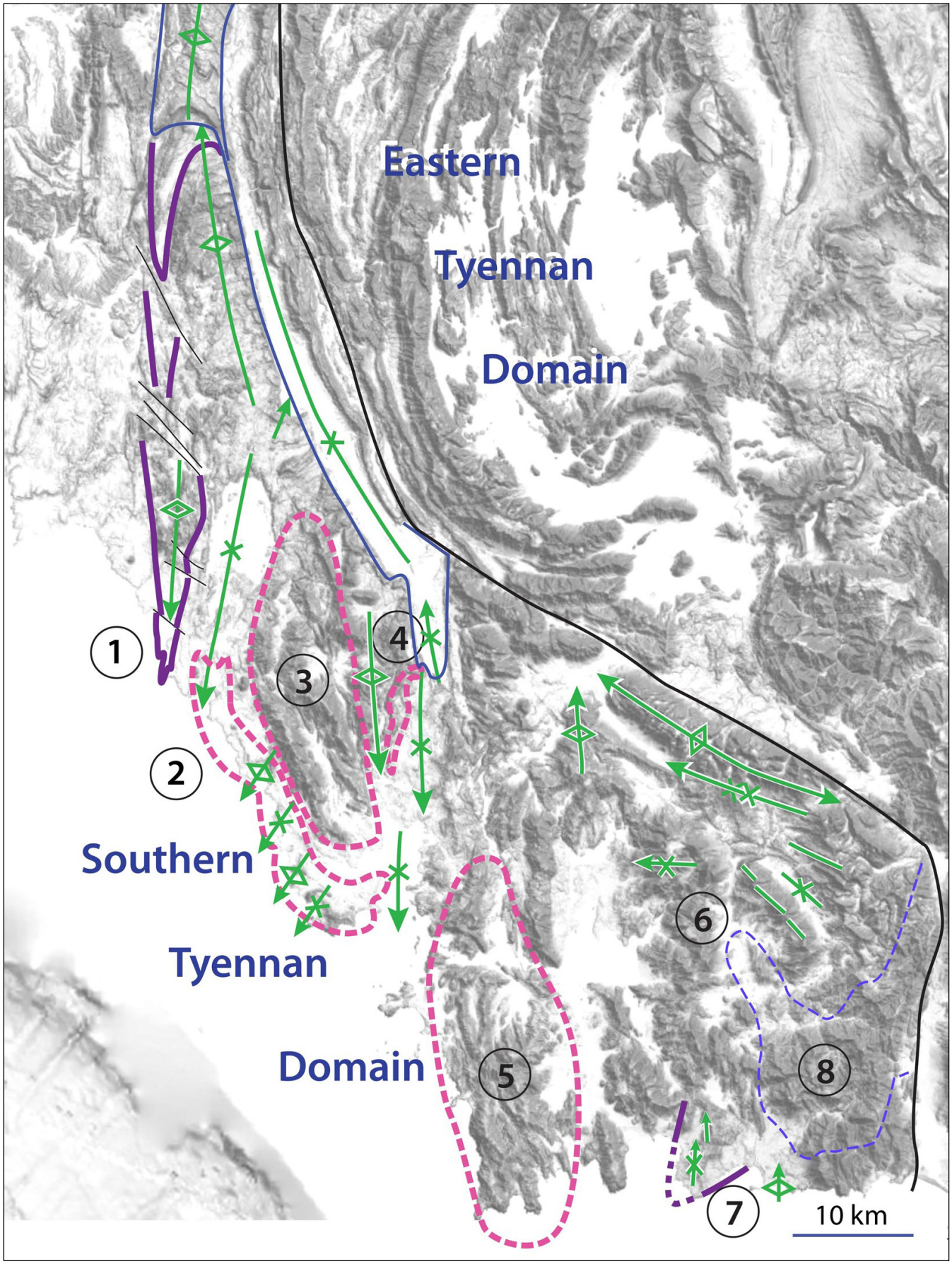

Figure 2. Major structural elements of the Southern Tyennan domain with ListMap greyscale digital elevation model as base map. Purple lines are So/Sm form lines that outline the Nye Bay-Charles Range fold-nappe (element 1) and the Red Point macro-fold (element 7). Pink dashed lines show the approximate extent and positions of the isoclinal fold stack (element 2) and the De Witt-Propsting mega-sheath fold (element 3), the Davey River sheath nose (element 4), the South West Cape mega-sheath (element 5). Element 6 represents the remaining area to the east, which is the isoclinal macro-fold domain. Element 8, outlined by the blue dashed line, sits at the lowest structural level and is a possible Scotchfire metamorphic sheet equivalent. The axial surface traces of younger, Devonian folds that fold the older Cambrian macro-structures are shown by the green line traces. The black is the faulted boundary between the Southern and Eastern Tyennan domains.

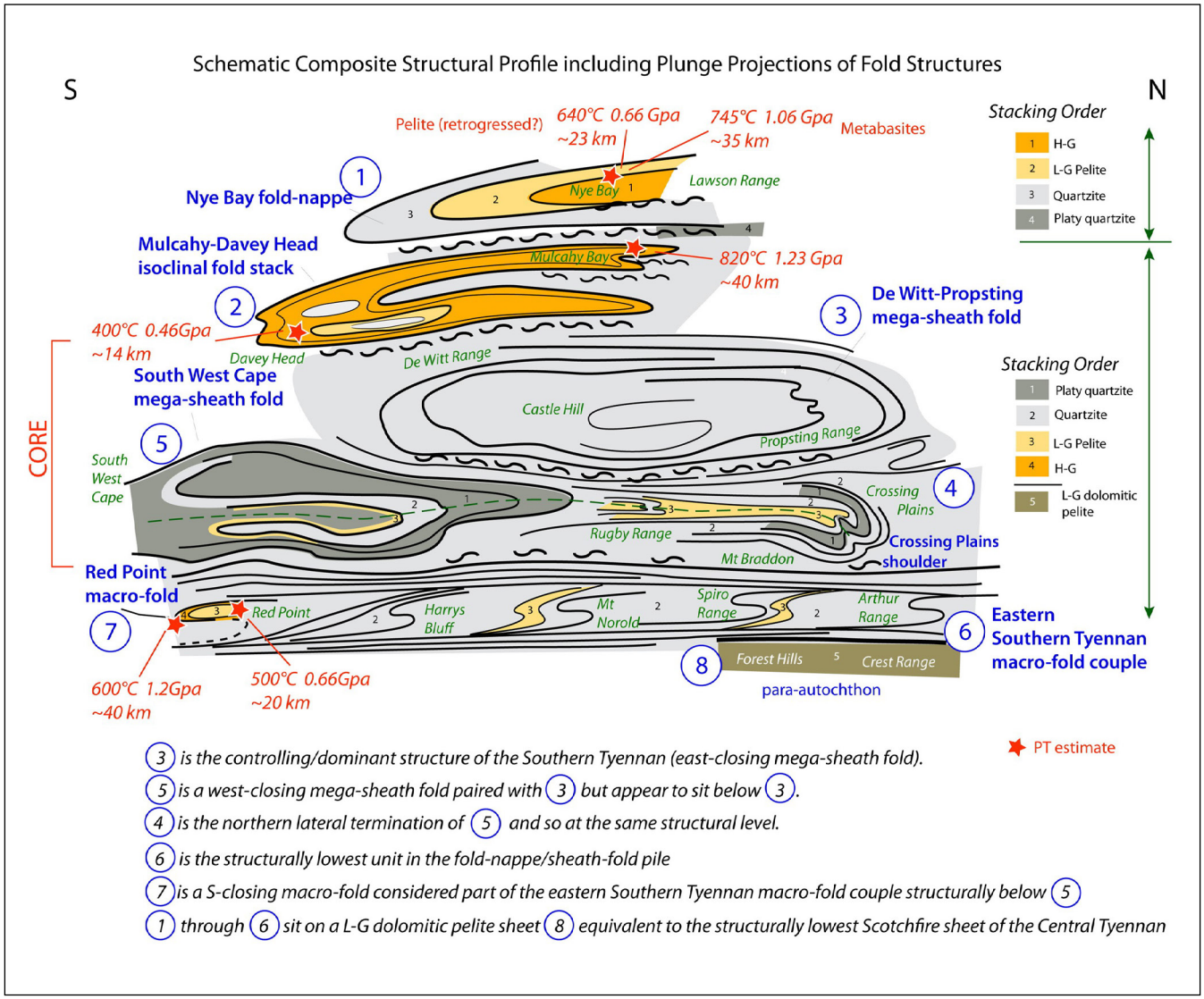

Figure 3. Schematic approximate down-plunge structural profile of the major structural elements that make up the Southern Tyennan domain (Figures 2 and 4). The profile is a tilted map view looking to the west with north on the diagram right. The profile captures a 70 km width with an approximate deformed crustal thicknerss of 20 km. The litho-tectonic units and stacking order are shown for the respective upper and lower limbs of the De Witt-Propsting mega-sheath fold. Unit numbers 1 to 4 are from top of stack to bottom of the stack with an order reversal between the upper and lower limbs. Orange: high-grade (H-G) schist; low-grade (L-G) pelite; light grey: low-grade (L-G) quartzite; dark grey: platy/schistose quartzite; khaki: low-grade dolomitic pelite as element 8 in the far eastern part of the Southern Tyennan domain incorporating the Spiro and Arthur Ranges.

P, T determinations from the high-grade schists (orange unit) and an estimate of the maximum depth of subduction are shown in red text and their approximate positions in the structural stack shown by the red stars.

The major structural elements of this crustal-scale architecture (Figures 2 and 3) include:

1. Nye Bay-Charles Range Fold-nappe: a south-closing, west-plunging macro-isoclinal fold with reclined geometry.
2. High-grade isoclinal macro-fold stack: in-folded sequence of high-grade schist, low-grade pelite and low-grade quartzite.
3. De Witt-Propsting mega-sheath fold: a closed macro-fold outcrop pattern within the low-grade quartzite sequence.
4. Davey River sheath-fold nose: the east-closing nose of the De Witt-Propsting mega-sheath fold exposed on the western limb of the anticline.
5. South West Cape mega-sheath fold: a closed macro-fold outcrop pattern largely within the low-grade platy quartzite, quartzite-pelite sequence.
6. Eastern Isoclinal fold domain, including the Arthur Range.
7. Red Point macro-isocline: an interpreted south-closing, west-plunging macro-fold cored by low-grade pelite enveloped by high-grade schist.
8. Low-grade dolomitic pelite sheet that sits beneath the Eastern isoclinal fold domain and is the structurally lowest part (base) of the Southern Tyennan domain. It is a likely equivalent to the Scotchfire metamorphic sheet of the Central Tyennan (Gray and Vicary, 2021b)

This paper represents a synthesis of the regional structure of the Southern Tyennan domain. The definition and description of the individual component structural elements listed above are presented in a series of more detailed Mineral Resources Tasmania Geological Survey Papers. These are:

1. Geological Survey Paper 8 (Gray and Vicary 2022a) on the structure of the Arthur Range including the regional scale, isoclinal fold-pair of the eastern Southern Tyennan domain (see 4 below) and the Devonian fold-thrust system.
2. Geological Survey Paper 9 (Gray et al., 2022) on the Nye Bay-Charles Range fold-nappe (element 1) with transition along the lower limb into the high-grade isoclinal fold stack (element 2) involving the high-grade schist sequence. The isoclinal fold-stack forms a structural carapace to the mega-sheath folds within the quartzite sequence below (Figure 3).
3. Geological Survey Paper 10 (Gray and Vicary 2022b) on the dominant De Witt-Propsting and South West Cape complementary sheath-fold pair (Elements 3, 4 and 5) that comprise the core of the Southern Tyennan domain.
4. Geological Survey Paper 11 (Gray and Vicary 2022c) on the eastern part of the Southern Tyennan domain dominated by a regional scale, asymmetric fold pair. This includes the Arthur Range regional scale, asymmetric fold pair (see 1 above).
5. Geological Survey Paper 12 (Gray and Vicary 2022d) on the structure of the Red Point macro-fold and contained Red Point Metamorphic Complex.

2.0 BACKGROUND TO THE SOUTHERN TYENNAN DOMAIN

2.1 Geographic Elements

The Southern Tyennan domain (Figure 4) is bounded on the north by the Olga Valley extending to the glacial moraines north of the Arthur Ranges, on the east from Federation Peak to the Ironbound Range on the south coast, on the south from New River Lagoon/Prion Bay to South West Cape and the west from South West Cape to Top Rocks/Elliott Bay on the Southern Ocean to the Charles Range (Figure 4).

A unique aspect of the Southern Tyennan domain, unlike all other parts of the Tyennan nucleus, is approximately 120 km of almost continuous coastal exposure from Top Rocks in the north through Nye Bay, Mulcahy Bay, Wreck Bay to Port Davey and then south to South West Cape and east through Cox Bluff to Red Point to Prion Bay (Figure 5). This coastal strip is essentially made up of 2-dimensional coastal platforms of limited width (< 100 m) and depth (cliff heights generally <50 m) extending inland to scrubby belts and poorly exposed button grass plains with low rounded hills and knolls with weathered quartzite and the occasional "good" outcrops.

The Southern Tyennan however, apart from the Arthur Range, is not as well exposed as other parts of the Tyennan massif, particularly the low coastal ranges with elevations generally <500 m. These include the Charles-Lawson Range (< 500 m), the Propsting Range (< 850 m), the De Witt Range (< 750 m), the South West Cape Range (< 450 m), the Melaleuca Range (500-600 m) and the Pasco Range (~300 m). Outcrop is patchy at best.

The Western Arthur Range has general elevations from 1000-1150 m whereas the Eastern Arthur Range has general elevations 1000-1100 m but includes Federation Peak at 1225 m.

Further to the west the Spiro Range (~700 m) with Mt Pollux (916 m) and Mt Castor (773 m) leads to a series of hills including Mt Norold (978 m), Harrys Bluff (739 m) and High Round Mountain (760 m) that southwards become the Ray Range. These ranges reflect the broad, open folds within the underlying quartzites. Ranges extending from Bathurst Harbour include the Rugby Range (600-700 m) to the north and the Bathurst Range (600-800 m) to the south, including Mt Counsel (806 m).

2.2 Litho-tectonic Units

Lithologies of the Southern Tyennan domain have been defined and described by Taylor (1959), Spry & Baker, (1965), Hall et al. (1969), and Williams (1982) with an overview presented by Turner (1989, p.36) for the regions of 1) the Arthur Range to Port Davey and 2) the Southwestern Area between the De Witt Range and the Charles Range.

Four major litho-tectonic units or stacked structural sheets have been recognised, including 1) high-grade schist, 2) low-grade pelite, 3) low-grade quartzite and 4) low-grade schistose to platy quartzite (Figure 3). The high-grade schists include albite and garnet bearing schists and gneiss, intercalated with thin quartzite bands, quartz-albite rocks and feldspar-rich rocks with garnet amphibolite bands (Meffre et al., 2000; Mulder et al., 2015; Gray et al., 2022). The low-grade pelite consists of black-chloritic phyllite and quartz-mica phyllite (McNeill, 1985; Mulder et al., 2015; Gray et al., 2022). The quartzite is mostly massive and non-micaceous with ripple marks and cross-bedding preserved in places (McNeill, 1985; Turner, 1989; Gray et al., 2022). The schistose quartzite is micaceous and foliated and intercalated with minor bands of chloritic phyllite and sericite-quartz schist.

In the Southwest High-grade Coastal belt west of the Propsting Range a stacking order was defined in the core to flanks of the Charles Range Anticline as well as the coastal sequence from Top Rocks to Mulcahy Bay as part of the core and limbs of the Nye Bay fold-nappe

Figure 4. ListMap topographic relief map showing the major geographic elements of the Southerrn Tyennan domain, including the coastal embayments, headlands, the ranges and rivers. This part of the Tyennan nucleus has approximately of 120 km coastal exposure in cliffs and shoreline platforms.

(Gray et al., 2022). The uppermost unit is the high-grade schist exposed in the core of the fold Nye Bay fold-nappe overlying low-grade pelite, overlying low-grade quartzite towards Top Rocks, overlying platy-schistose quartzite exposed in the core of the Charles Range Anticline (Figure 5). This is the West stacking order observed west of the Mulcahy high-strain zone (Figure 5). East of the Mulcahy high-strain zone the sequence occurs in reverse order as seen in the Davey Creek and Mt Braddon Synclines where the structurally highest unit is the schistose to platy quartzite in the core of the synclines, underlain by low-grade quartzite followed by low-grade pelite (i.e. the East stacking order, Figure 5). High-grade schist is only exposed on the south coast in the Red Point area (Figure 5).

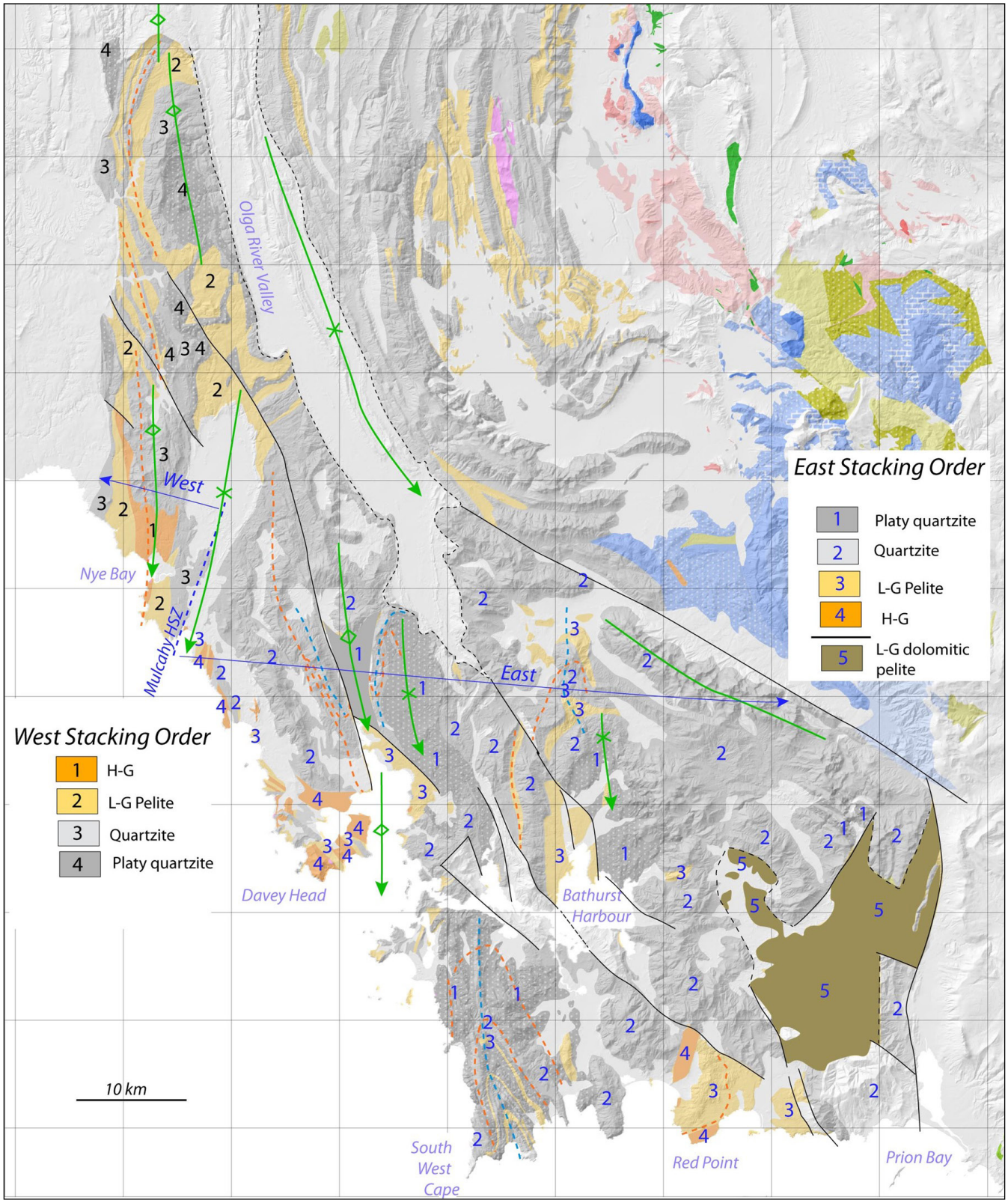

Figure 5. Geological map of the Southern Tyennan domain showing the distribution of the litho-tectonic units and the stacking order from point to point based on the regional folding relationships, namely lowest units in anticline cores versus uppermost in synclinal cores. The stacking order changes across the Mulcahy shear zone from a West Stacking order with high-grade schist at the top to an East Stacking order with high-grade schist at the base. Map base is the 1:25,000 and 1:25,000 digital geological atlas from Mineral Resources Tasmania draped on the digital elevation model (DEM). This interpretation assumes lateral continuity of units across the entire Southern Tyennan domain.

2.3 Structural-tectonic Elements

The Southern Tyennan domain has been subdivided into several major structural-geographic elements (Figure 2). These include the major Mt Eleanor Anticline, the Southwest coastal high-grade belt, the De Witt-Propsting-Davey Gorge mega-sheath fold system, the South West Cape mega-sheath fold system, the Eastern asymmetric fold pair system, the Arthur Range fold-thrust system and the Red Point high-grade complex (Figure 3).

These structural-geographic elements define a Southern Tyennan domain structural architecture composed of the following regional scale structures (Figures 2 and 3):

1. Nye Bay fold-nappe with south-closing reclined geometry;
2. Mulcahy Bay-Port Davey isoclinal fold stack with macro-augen form;
3. De Witt-Propsting mega-sheath fold;
4. Davey River sheath nose;
5. South West Cape mega-sheath fold;
6. Eastern isoclinal macro-fold domain, including the Arthur Range;
7. Red Point macro-fold.

2.4 Nature of the Layering, Foliations and Lineations

The schists, quartzites and phyllites of the Southern Tyennan region show varying degrees of deformation from relatively undeformed, with preserved bedding features (So), to highly deformed rocks, with high strain fabrics typified by strong to intense foliation and transposition layering/foliation (Sm), rodding fabrics within the transposition layering (So/Sm), mesoscopic isoclinal folds, rootless isoclinal fold pairs, and multiple crenulation cleavages (Scc).

There are six types of layering and foliation:

1. Bedding So: relatively undeformed bedding;
2. Bedding-parallel foliation So/Sm: compositional banding sub-parallel to a strong to intense foliation that is folded by recumbent isoclinal folding;
3. Intense foliation (Sm): the dominant foliation that is axial surface to the major recumbent isoclinal macro-folds. Associated with this layering is a marked rodding fabric within the Sm layering. This is the regional foliation that envelopes macro- to meso-fold "pods". The pods occur at all scales;
4. Crenulation cleavages (Scc) associated with development of transposition layering in the basal high strain zones and to younger folding events[;
5. Shear Band foliation (Sb) or S-C' fabrics as a form of extensional crenulation cleavage that reflects shear-induced, foliation-oblique late-stage flattening. These zones are essentially secondary shear zones that record the overall shear sense and/or emplacement direction;
6. Spaced cleavage (Scl) a younger Devonian cleavage that overprints all three foliations listed above.

There are four types of lineations:

1. A mineral lineation (Lm) generally defined by mica and/or elongated quartz grains in the quartzite;
2. An elongation or stretching lineation (Lelong) most commonly shown by elongated quartz grains;
3. A rodding lineation (Lrod) that changes from an initial intersection lineation at high angle to the regional stretching direction, to a "herringbone" pattern where flattened mesoscopic fold hingelines become curvilinear and pulled apart, to eventually develop a strong, sub-parallel alignment with the regional stretching direction (Lstretch);
4. A crenulation lineation (Lcren) as tiny puckers or wrinkles within the foliation.

2.5 Key Structural Relationships

Mapping in the Davey River quartzite region of the Southern Tyennan domain (Maclean and Bowen, 1971) documented two relationships that are important in understanding the structural and tectonic evolution of the Tyennan nucleus.

2.5.1 Timing of Lineation Lm

The foliation (Sm) and the contained mineral lineation (Lm) are folded by the major early isoclinal macro-folds and by many of the mesoscopic isoclinal folds (Figure 6). This timing holds throughout the Tyennan nucleus (Turner, 1989, p.45). Recognition of multiple foliations as well as angular discordance or different orientations from isocline lower to upper limb suggest reworking of the rock fabric and lineation across the folded layering in isoclinal refolding of these folds (Maclean and Bowen, 1971, p.101).

The mineral/stretching lineation Lm represents the bulk rock stretching direction in the first phase of deformation within the dominant foliation Sm and the sub-parallel transposition layering So/Sm.

2.5.2 Curvilinear Fold Hinges and Scale Invariant Sheath Folds

The Davey River region quartzites show 1) curvilinear isocline fold hingelines typical of small-scale sheath folds (Figure 7a), and 2) fold hinges with variation in amount and direction of fold plunge from similar generation of folds, reflecting different hinge segments of sheath folds within different layers (Figure 7b). Maclean and Bowen (1971, p.101) describe situations where "adjacent axes in an outcrop may at times vary in orientation by up to 90° with individual axes varying in plunge by up to 60°." They note that despite this fold axis variability "all axes lie on the axial surface, and usually become more regular in the vicinity of major closures where they parallel the major structure".

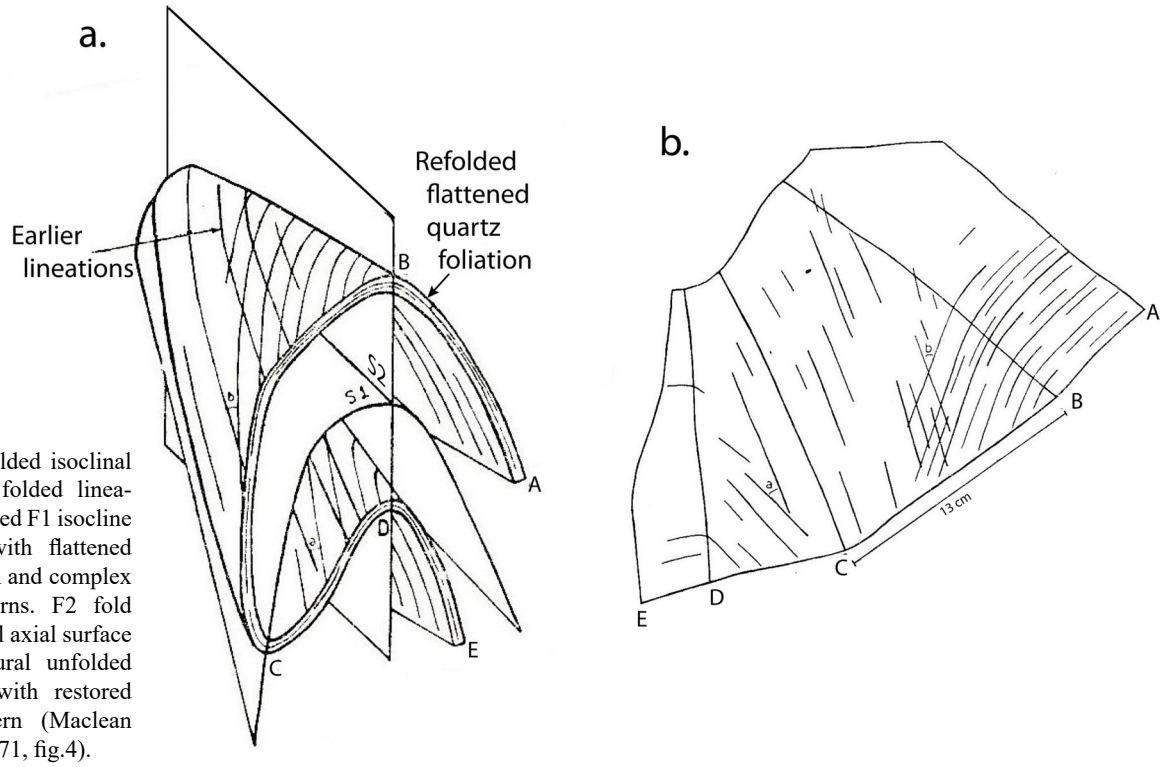

Figure 6. Refolded isoclinal F1 fold with folded lineations. a) Refolded F1 isocline in quartzite with flattened quartz foliation and complex lineation patterns. F2 fold has sub-vertical axial surface (S2). b) Flexural unfolded layering Sm with restored lineation pattern (Maclean and Bowen, 1971, fig.4).

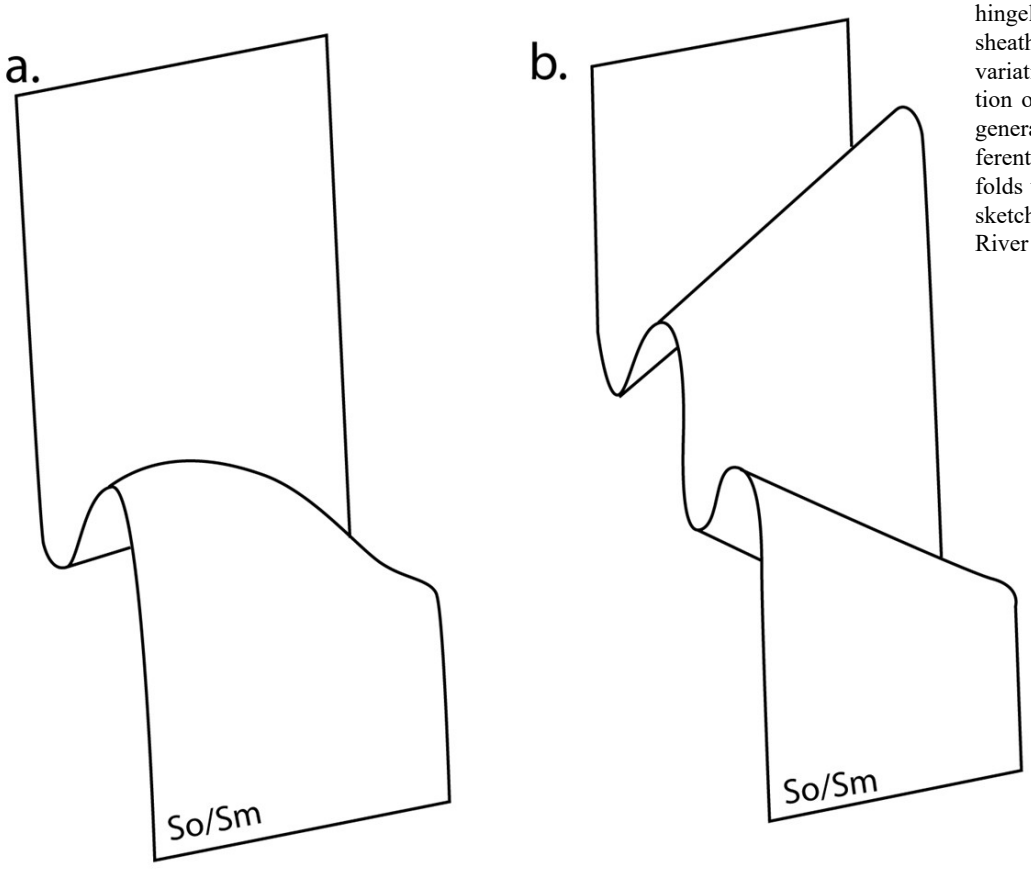

Figure 7. Modes of F2 fold hingeline variation (Maclean and Bowen, 1971, fig. 6b). a) Curved hingeline typical of developing sheath fold. b) Fold hinges with variation in amount and direction of fold plunge from similar generation of folds reflecting different hinge segments of sheath folds within different layers. The sketches are based on the Davey River region quartzites.

A broad parallelism between hinge-elongation in sheath folds with the direction of bulk rock stretch (Lstretch), recorded by the lineation Lm, can be seen at all scales reflecting the scale invariance of sheath folding (cf. Alsop and Holdsworth, 1999, 2004). Sheath folding at the small scale (Figure 8) was also observed in the core of the De Witt-Propsting mega-sheath fold. A foliated and folded quartzite sample from the Castle Hill ridgeline shows multi sheath lobes as "F2" folds with an axial surface crenulation cleavage Scc. Two stacked sheath lobes (Figures 8a and b) are separated by an extremely attenuated return-pinchout. They have sheath noses with hingelines drawn out or elongated sub-parallel to the mineral lineation ribbing on the folded Sm (Figure 8a). The profile view (Figure 8c) shows a flattened chevron form with a pointed hinge and long limbs. The core of the sheath (Figures 8c) shows smaller chevrons with 'M' symmetry.

2.6 Significance of Southern Tyennan Domain Metamorphism

Spry and Baker (1965), Williams (1982), McNeill (1985), Meffre et al. (2000) and Chmielowski (2009) have investigated the metamorphism of the Southern Tyennan domain (Figure 4a), Mulder (2013) and Mulder et al. (2015), the Red Point Metamorphic Complex on the south coast.

2.6.1 Textures and Micro-structural Implications

In the coastal belt the high-grade schists at Nye Bay show a chronology of crystallisation and deformation that indicates the metamorphic maxima, based on the formation of sillimanite, occurred late syn- to early post formation of the dominant foliation Sm (McNeill, 1985).

Similar porphyroblast-fabric relationships (Figure 9) occur within schists of the Red Point metamorphics along the southern coastline (Mulder et al., 2015). These have a dominant S2 schistosity that overprints and envelopes garnet and albite porphyroblasts containing relicts of earlier internal foliation. The internal foliation is an older S1 foliation that is approximately orthogonal to the overprinting intense mica fabric of S2 (Figure 9).

2.6.2 Estimated PT Conditions: Attained Depth of subduction (or position in subducted slab) or complications from effects of retrogression

Metamorphic P, T estimates based on the composite assemblage biotite-garnet-kyanite-muscovite¬-albite-quartz-sillimanite (Figure 10) are from McNeill (1985), Chmielowski (2009), Chmielowski and Berry (2012) and Mulder et al. (2015).

The PT conditions of the metamorphic maximum fall in the stability fields of quartz-muscovite and sillimanite, and above the granite-melting curve. Conditions are therefore in the range 0.6 Gpa and 630° C to approximately 0.9 Gpa and 730° C (Figure 11). Temperatures are above the kyanite-sillimanite boundary, and close to, or above the melting curve; that is, approximately 650° C.

The combined results from geobarometry and geothermometry, including all data from the garnet-biotite thermometer, indicate temperatures of 635 ± 50° C and pressures of 0.75 ± 0.01 GPa. Garnet zoning may indicate retrograde re-equilibration, resulting in lower temperature estimates.

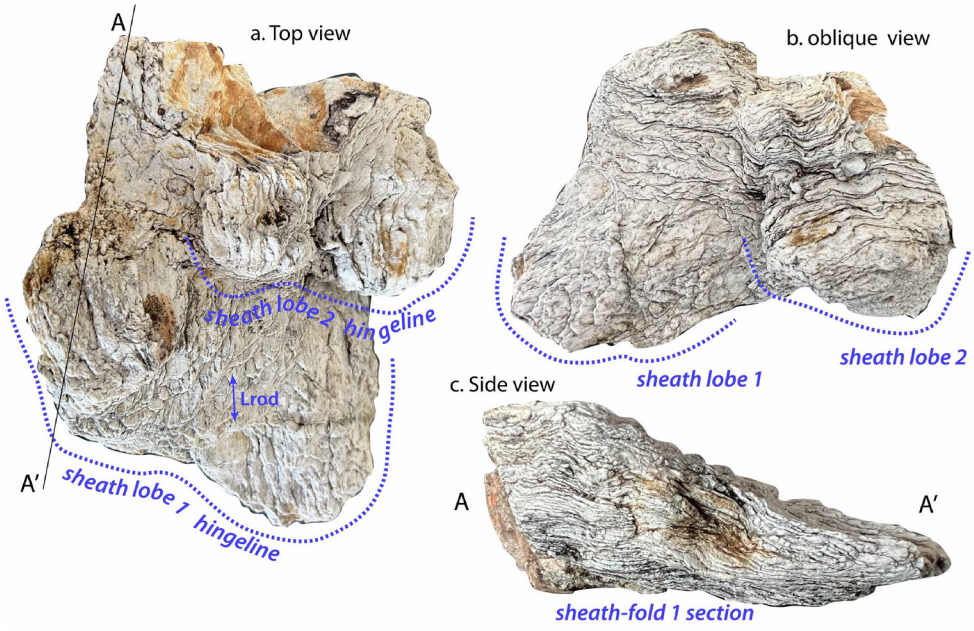

Figure 8. Mesoscopic sheath fold sample in transposed quartzite layering showing two sheath-lobes both with axial surface crenulation cleavage (Scc2). a) Top view showing the sheath lobes labelled 1 and 2 with hingelines depicted as blue dashed heavy lines. b) oblique frontal-side view showing fold lobes. c) Left-frontal side view (profile) of sheath fold 1. The sample is from Castle Hill within the core of the De Witt-Propsting mega-sheath fold (see Section 4.3).

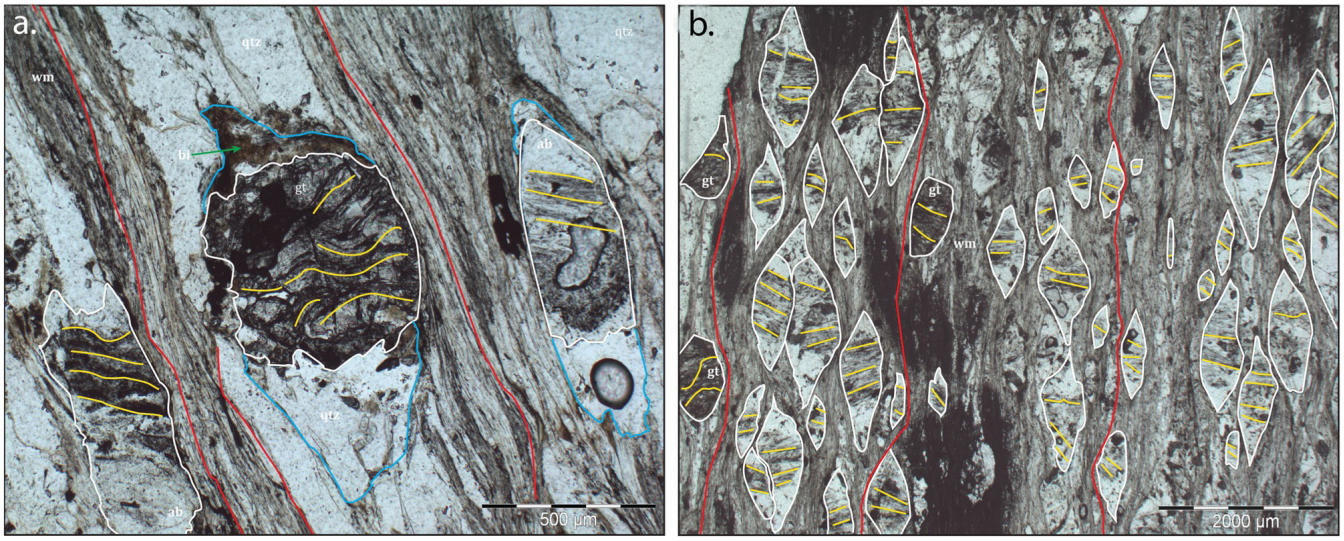

Figure 9. Dominant schistosity S2 fabric relationships. a) Intense transposition layering defined by alternating zones of white mica (wm) and quartz (qtz) enclosing garnet and albite with quartz ±biotite pressure shadow growths (fig. 5a, Mulder et al., 2015). b. Dominant foliation as intense mica alignment defining schistosity in pelitic schist enclosing canoe-shaped albite pophyroblasts with quartz overgrowths as tails (fig. 5d, Mulder et al., 2015). S1 - yellow lines. S2 - red lines. Quartz-biotite pressure shadows - blue lines.

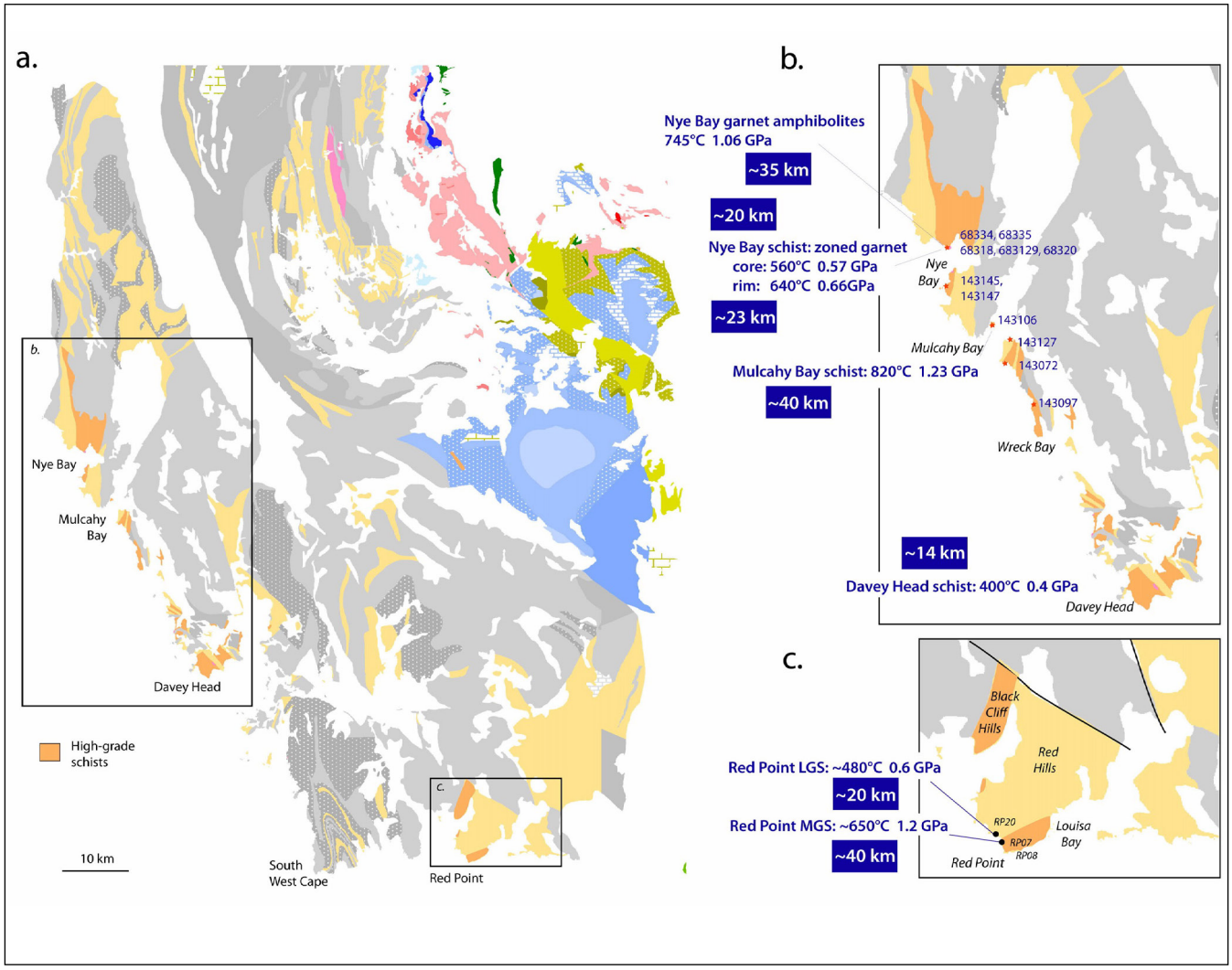

Figure 10. Metamorphic PT data with sample locations for the Southwest High-grade belt and Red Point Mertamorphic Complex. Lithological map base is from Mineral Resources Tasmania 1:250,000 digital atlas series. a) Southwest High-grade Coastal Belt PT calculations and sample locations. Data are from Chmielowski (2009) and Williams (1982). Lithological map base is from Mineral Resources Tasmania 1:250,000 digital atlas series. b) Red Point Metamorphic Complex PT calculations and sample locations. Data are from Mulder et al. (2015). Lithological map base is from Mineral Resources Tasmania 1:250,000 digital atlas series.

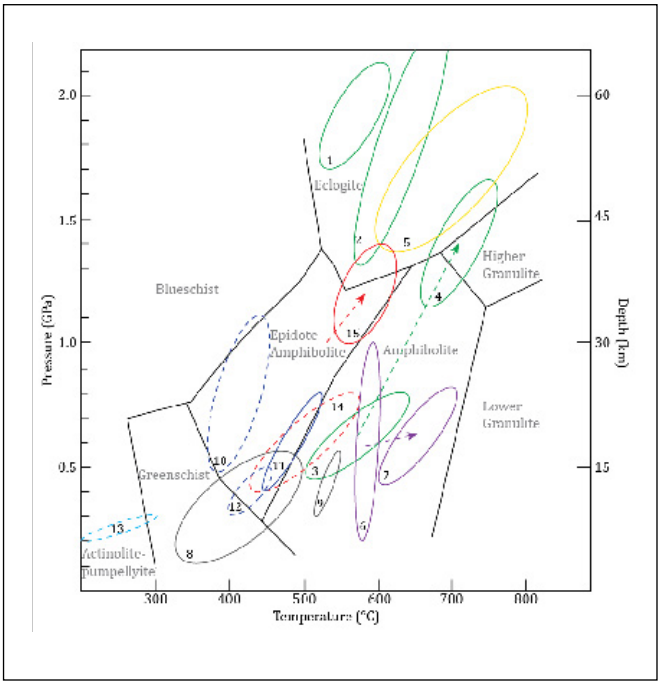

Figure 11. Comparative pressure-temperature plot (Mulder, 2013, Figure 5.13; modified from Chmielowski, 2009) showing the Cox Bight-Red Point PT estimates for the low-grade sequence LGS (dashed red 2σ uncertainty error ellipse 14) and the medium-grade sequence MGS (red 2σ uncertainty error ellipse 15).

Other data include Franklin Metamorphic Complex (1) white schist, (2) eclogite, (3) schist, garnet cores, (4) schist, peak; Forth Metamorphic Complex (5) schist peak; Port Davey Metamorphic Complex (6) schist, garnet cores, (7) schist peak; Strathgordon Metamorphic Complex (8) and (9) schist peak; Arthur Metamorphic Complex (10) blue amphibole bearing allochthon, (11) amphibolite; Port Sorell (13) phyllite.

Garnets from Nye Bay are large (~2cm) with two distinct habits: 1) euhedral shape with inclusion free cores and rims dusty with fine grained inclusions, and 2) patchy shape with abundant quartz inclusions that show a marked density change across the core-rim boundary (Chmielowski and Berry, 2012) Geothermobarametric calculations using THERMOCALC (Chmielowski and Berry, 2012) give:

- Garnet cores: initial garnet growth at 560° C and ~0.56 GPa.
- Garnet rim: late growth with a slight increase in both temperature (<100° C) and pressure (~0.04GPa), with conditions changing from the kyanite field into the sillimanite field (Figure 11), consistent with the observations of sillimanite-rimming kyanite (McNeill, 1985).

Possible retrogression in the pelitic lithologies suggests that the associated mafic/amphibolitic lithologies may provide the best estimate of the metamorphic maximum (McNeill, pers. com., 2022). These metabasites have a hornblende-plagioclase (An40)-garnet assemblage supporting amphibolite facies conditions (McNeill, 1985), but the metamorphism involves a transition from the kyanite field to the sillimanite field by increasing P+T (Figure 11). Garnet-clinopyroxene geothermometry and application of the albite-jadeite-quartz geobarometer on Nye Bay garnet amphibolites give 745° C and 1.06 GPa (McNeill, unpublished data).

2.7 Early Mapping

Tasmanian Geological Survey regional mapping in the late 1950's by Stefanski (1957a,b) and Taylor (1959) provided the first geological maps of the southern and eastern parts of the Southern Tyennan domain (Figure 12). Subsequently maps of the entire Southern Tyennan were produced by BHP as part of Exploration Licenses in the early 1960's (Figure 13, Hall, 1965). This early work provided the first understanding of the geology of the Southern Tyennan part of the Tyennan nucleus where 1) litho-sequences included quartzite (pq), quartz schist (pqs), phyllite (pp), graphitic phyllite (pgs), chloritic schist (pcs) and knotted garnet-albite schist (pks) (Hall et al., 1969), and 2) much of the regional structure was due to Devonian interfering north-south and north-west-southeast trending fold systems.

Subsequently Tasmanian Geological Survey mapping has included 1) the Port Davey area, undertaken by Peter Williams in 1976 to produce the Geological Atlas 1:50,000 Davey Map Sheet (Williams, 1978), and 2) the Ironbound Range through to Harry's Bluff undertaken by Paul Lennox in early 1980 (Lennox, 2013).

Honours thesis mapping was undertaken in the Davey River area (MacLean and Bowen, 1971), the Nye Bay area (McNeill, 1985) and the Cox Bight-Red Point area (Mulder, 2013). Peter Williams also undertook PhD mapping of the mid Cambrian intra-rift sequence Clytie Cove Group through Bathurst Harbour (Williams, 1980).

University research has included 1) mapping from Nye Bay to south of Mulcahy Bay in 1997 by Ron Berry, Sebastian Meffre and Mike Hall that resulted in publication Meffre et al (2000), and 2) complete coastal mapping from Elliott Bay in the north to Towterers Beach in the South by Mike Hall in the summers of 1997, 2004, 2005 and 2006. This included mapping lithologies and taking structural measurements, data that was utilised to compile the Rookery, Propsting, Elliot and Mulcahy 1:25,000 digital map sheets (Hall & Vicary, 2010a, b, c and d).

2.8 Current Work

This Southern Tyennan region structural investigation and synthesis is based on:

1) Photographs and structural data collected by the authors on two helicopter day-trips into the Southwest on 22/2/2019 and 26/3/2020. Hand-held, serial photographs taken every 10 seconds from the helicopter provided another dataset of the changing regional structure to aid structural profile and cross section construction.

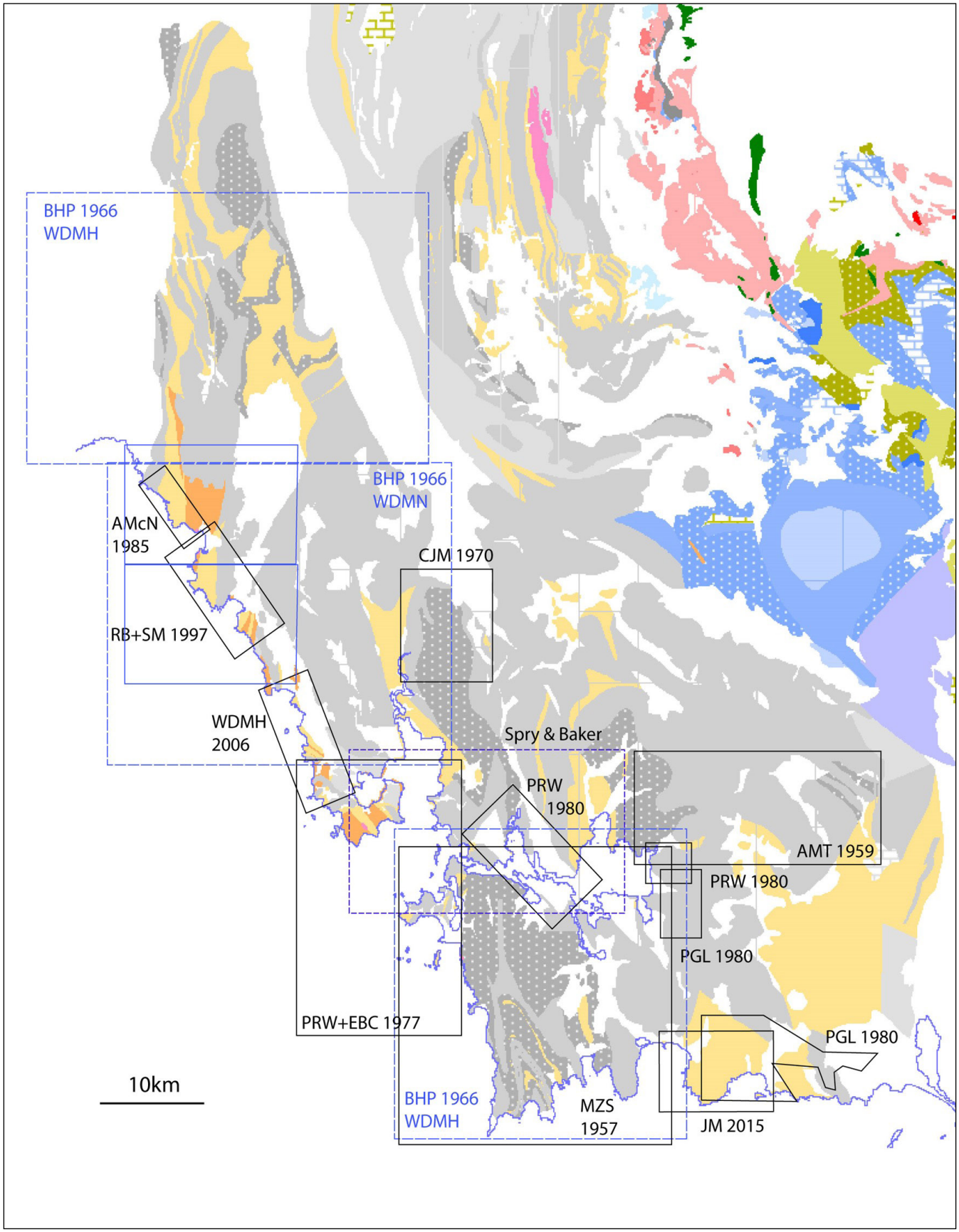

Figure 12. Index map for structural data sources for the Southern Tyennan domain. Geological mapping was initiated in the late 1950's by the Tasmanian Geological Survey followed by extensive mapping undertaken by BHP exploration in the mid-1960's. Compilation of the Davey 1:50,000 Geological Map sheet was completed in 1976. Map base is the 1:25,000 and 1:250,000 digital geological atlas from Mineral Resources Tasmania.

WDMH: Mike Hall; AMcN: Andrew McNeill; RB: Ron Berry; SM: Sebastien Meffre; CJM: Colin MacLean; PRW: Peter Williams; EBC: Elizabeth (Sib) Corbett; MZS: Stefanski; AMT: Taylor; JM: Jacob Mulder; PGL: Paul Lennox; Spry & Baker: Allan Spry and Bill Baker.

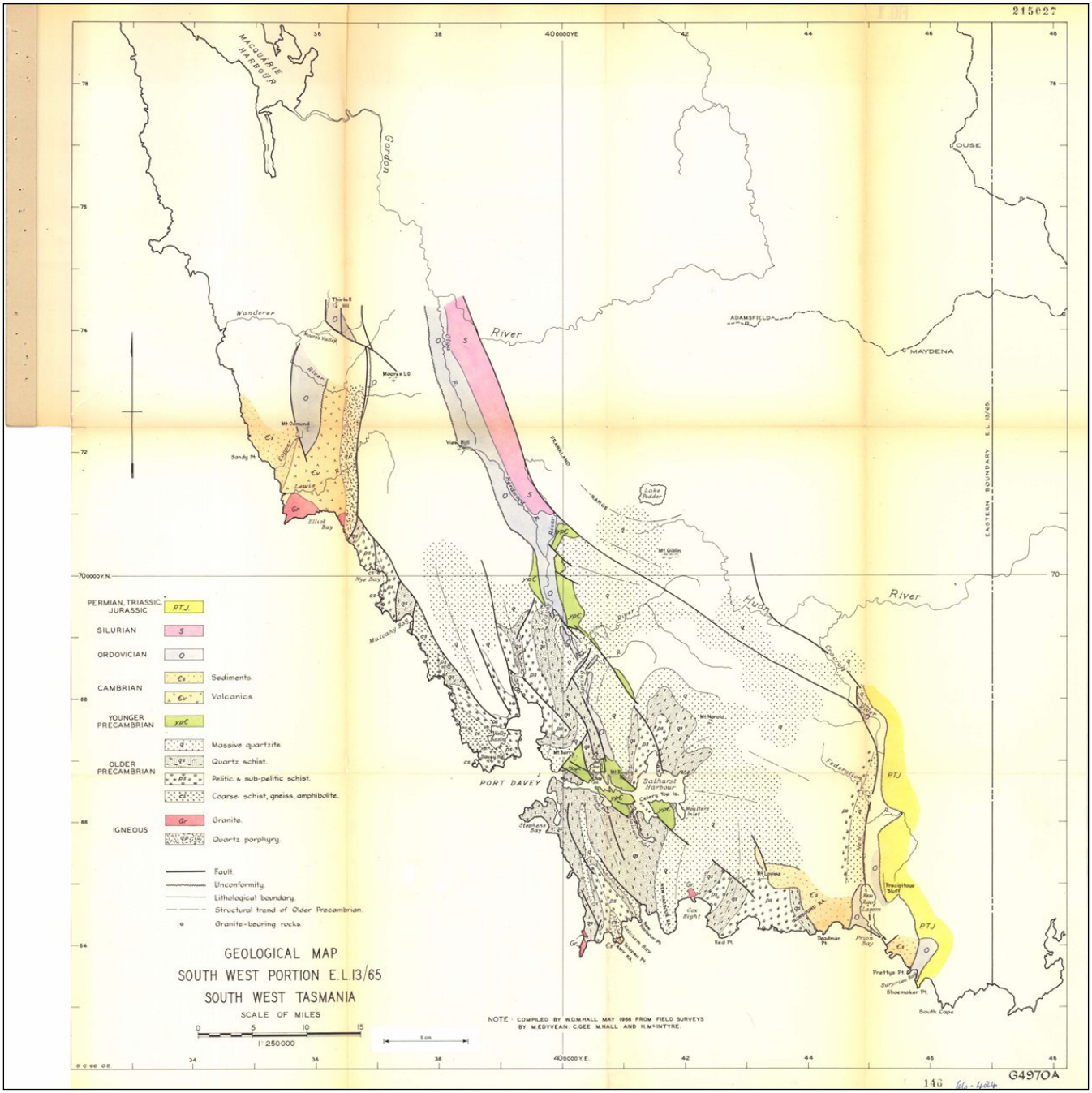

Figure 13. Early geological map of Southwestern Tasmania by BHP Exploration for the southwest portion of EL 13/65 (Hall, 1965). The map shows the broad distribution of geological/lithological units, the major fault lines and an overall younger fold pattern based on the mapped lithological contacts.

2) Analysis, re-interpretation and compilation of all existing structural data from both published and unpublished sources. The unpublished data included PWS Permit Reports, field maps primarily from Mike Hall and included field notebook data from Berry (1997), Hall (2005, 2006 and 2008), Miller (2004), Willliams (1976) and Lennox (1980).

Much of the data is from the unpublished BHP maps compiled by Hall (1965) and Hall et al. (1969), and coastal mapping by Hall in 1997, 2004, 2005 and 2006, Nye Bay by McNeill (1985), Nye Bay to Mulcahy Bay by Ron Berry and Sebastien Meffre in 1997 (Berry, 1997), Top Rocks to Towterer Beach by Hall and Miller in 2004, the Davey 1:50,000 sheet by Williams (1978), parts of the unpublished Bathurst sheet by Stefanski (1957b) and Lennox (2013), and Cox Bight to Red Point by Mulder (2013) and Mulder et al. (2015).

All map grids and grid references in the text have a GDA94 datum with MGA coordinates in Zone 55.

All structural data utilised and/or presented are true north unless otherwise stated.

The following structural terminology is used:

So/Sm	metamorphic foliation parallel to bedding (commonly a transposition layering)
So/Sm env	enveloping surface to folded So/Sm
Sm	dominant or main metamorphic foliation
Sb	shear band (S-C' structure)
AST	fold axial surface trace
AS/Sm	dominant foliation sub-parallel to fold axial surfaces
Sm/Sb	dominant foliation developing from Sb, shear band foliation
Scc:	crenulation cleavage
Scl	Devonian overprinting low-grade cleavage
S1	early slaty cleavage
Lm	dominant lineation
Lstretch	stretching lineation
Lelongation	mineral elongation lineation
TD	transport direction
Lint	intersection lineation
Lrod	rodding lineation developed from deforming Lint
FA	fold axis
F1, F2, F3	local age of fold axes (oldest to youngest)
FA^Lm	FA rotation sense defined by closing the acute angle between Lm and FA. Rotation can be either clockwise or anti-clockwise about the median lime ML
Sm^Sb	angle between Sm and Sb
HSZ	high strain zone
LSD	limb separation
HSD	hinge separation distance
ML	median line of sheath fold (see Figure 15c)

3.0 SOUTHERN TYENNAN GEOLOGY SUMMARY/OVERVIEW

3.1 Map Pattern and Regional Relationships

The map pattern of the Southern Tyennan domain (Figures 2 and 14) is dominated by a central belt of quartzite defined by two en echelon mega-folds including 1) the closed-loop De Witt-Propsting mega-sheath-fold and its Davey River sheath-nose as lateral termination, and 2) the South West Cape mega-refold within structurally intercalated low-grade quartz-mica schist, slabby to platy quartzite, quartzite and pelite (phyllite) (Figures 14 and 15).

An upper, structurally higher carapace to the De Witt-Propsting structure includes the Nye Bay fold-nappe, which is transitional along its lower limb into a closed-loop isoclinal fold stack from Mulcahy Bay to Port Davey. These structures are within structurally intercalated high-grade schist overlying low-grade phyllite, overlying low-grade quartzite overlying platy quartzite. The high-grade schist occurs within the core of the fold-nappe with the map pattern indicating attenuation of the schist to the north beyond the Lawson Range.

The eastern part (Figure 2), incorporating the eastern fold domain and including the Arthur Range, represents the structurally lower limb of the De Witt-Propsting mega-sheath fold. It shows a reverse stacking of low-grade platy quartzite overlying quartzite overlying low-grade pelite and consists structurally of an isoclinal macro-fold pair.

A mid-Cambrian northwest-trending, fault-bounded wrench or strike-slip graben in the Joe Page Bay and Melaleuca Inlet part of Bathurst Harbour (Williams, 1980) truncates the early mega-fold architecture (Figure 14). This structure has structural and sedimentation characteristics similar to the wrench basins along the San Andreas fault-system in the western United States (see Section 5).

The map-scale structure is further defined by younger north-northwest-, north-south, north-northeast- and northeast trending major regional folds (Figure 14). These folds refold the early meso- to macro- isoclines of F1/F2 generation.

In the northern segment the regional structure is dominated by the southern continuation of the Charles-Elliott Range Anticline expressed as the major north-trending, north-plunging Mt Eleanor Anticline (Figure 14). This anticline is cut by an apparent conjugate brittle fault system of NW- and NE-trending faults. The western and W-dipping limb is overprinted by the NNE-trending Nye Bay Anticline and Giblin Syncline (Figure 14). These folds are both S-plunging.

3.2 Early Isoclinal Fold Pattern

The early structure is dominated by isoclines at all scales (Figures 14 and16). Measurements of isocline attitude have been taken from various sources largely field notes by Mike Hall (Nye Bay to Wreck Bay), Ron Berry and Sebastian Meffre (Nye Bay to Mulcahy Bay) and Andrew McNeill (Nye Bay). Other sources include measurements 1) from 1:25,000 Lewis, Elliott, Mulcahy and Propsting Map sheets (Hall and Vicary, 2010a, b, c and d) and 2) in stereonet form from Spry & Baker (1965), McLean and Bowen (1971), and Williams (1982).

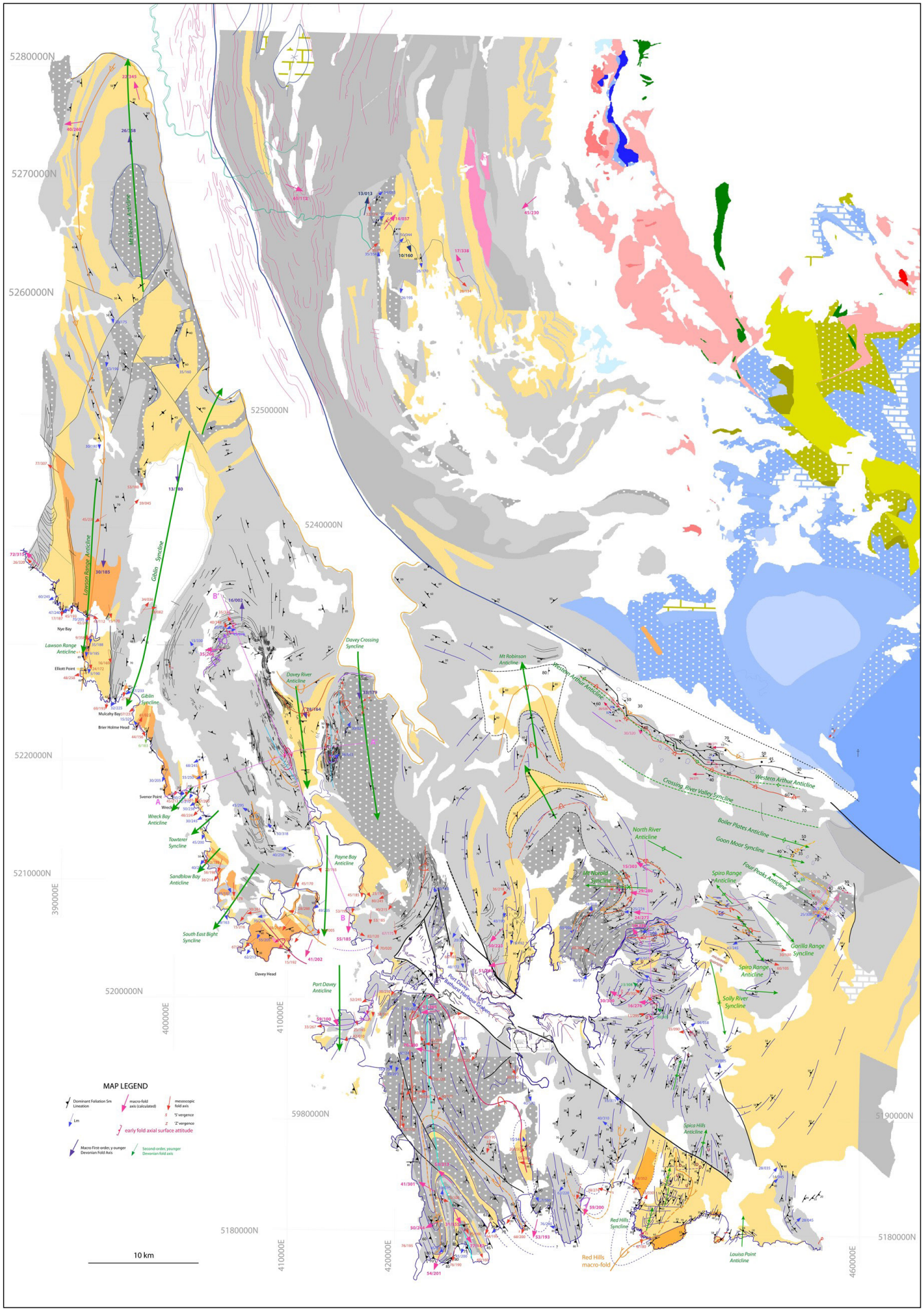

Figure 14. Structure-lithology map of the Southern Tyennan domain. Map base is the 1:25,000 and 1:250,000 digital geological atlas from Mineral Resources Tasmania.

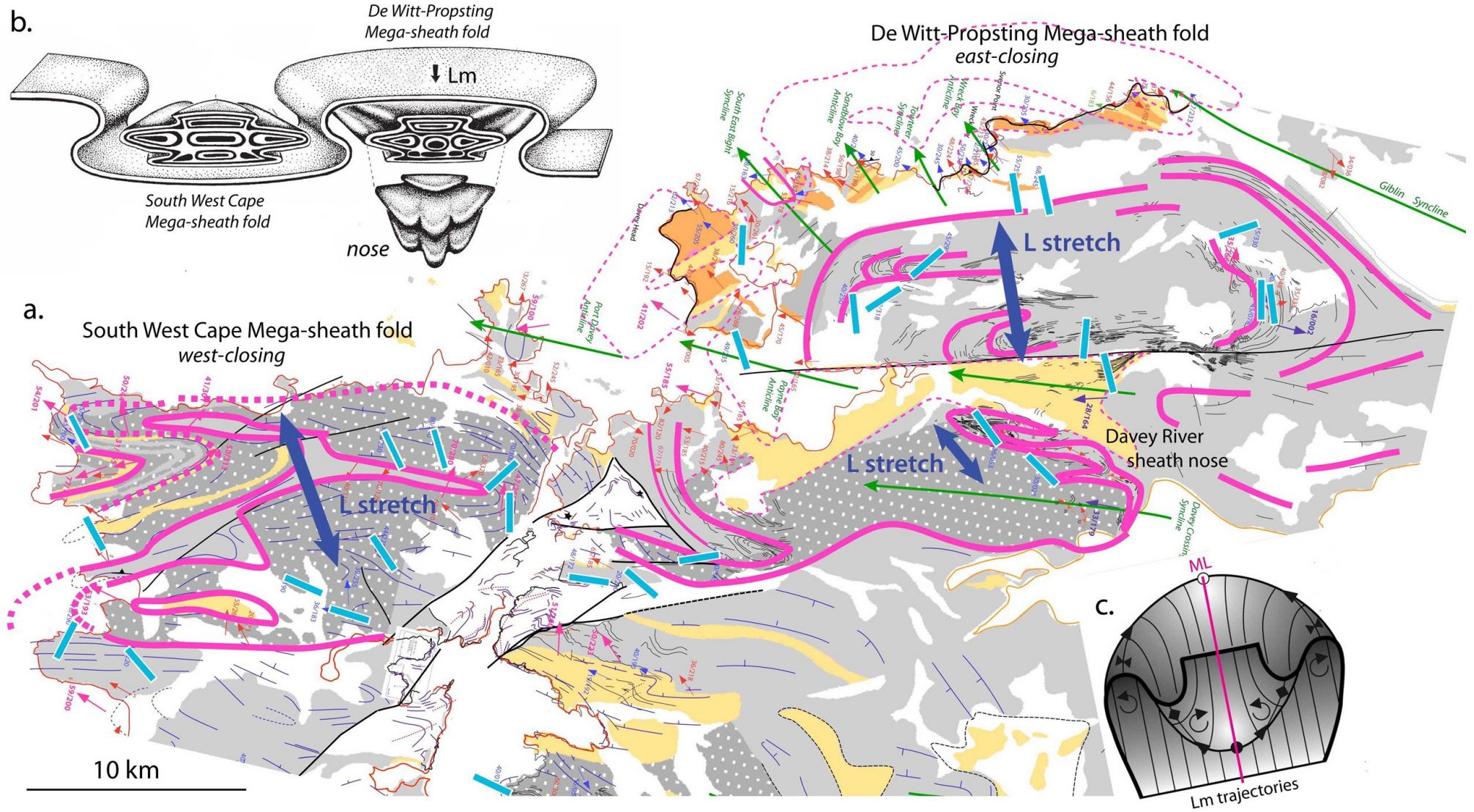

Figure 15. Mega-sheath fold relationships in the central part of the Southern Tyennan domain. a) Simplified structure map of the area showing form lines in So/Sm (pink line traces) defining the outcrop geometry of the mega-folds and structural relationships of the lineation Lm to the mega-folds. b) Schematic 3D diagram of an oppositely-closing sheath-fold pair with sections showing the inferred internal structural geometry after Alsop and Holdsworth (2004, fig.2). c) Diagrammatic top-view of oppositely-closing (antithetic) sheath-fold pair showing hingeline curvature, fold-hingeline vergence (clockwise or anti-clockwise arrows), the sheath-fold median line (ML) and the lineation Lm pattern (after Alsop and Carreras, 2007, fig. 10d).

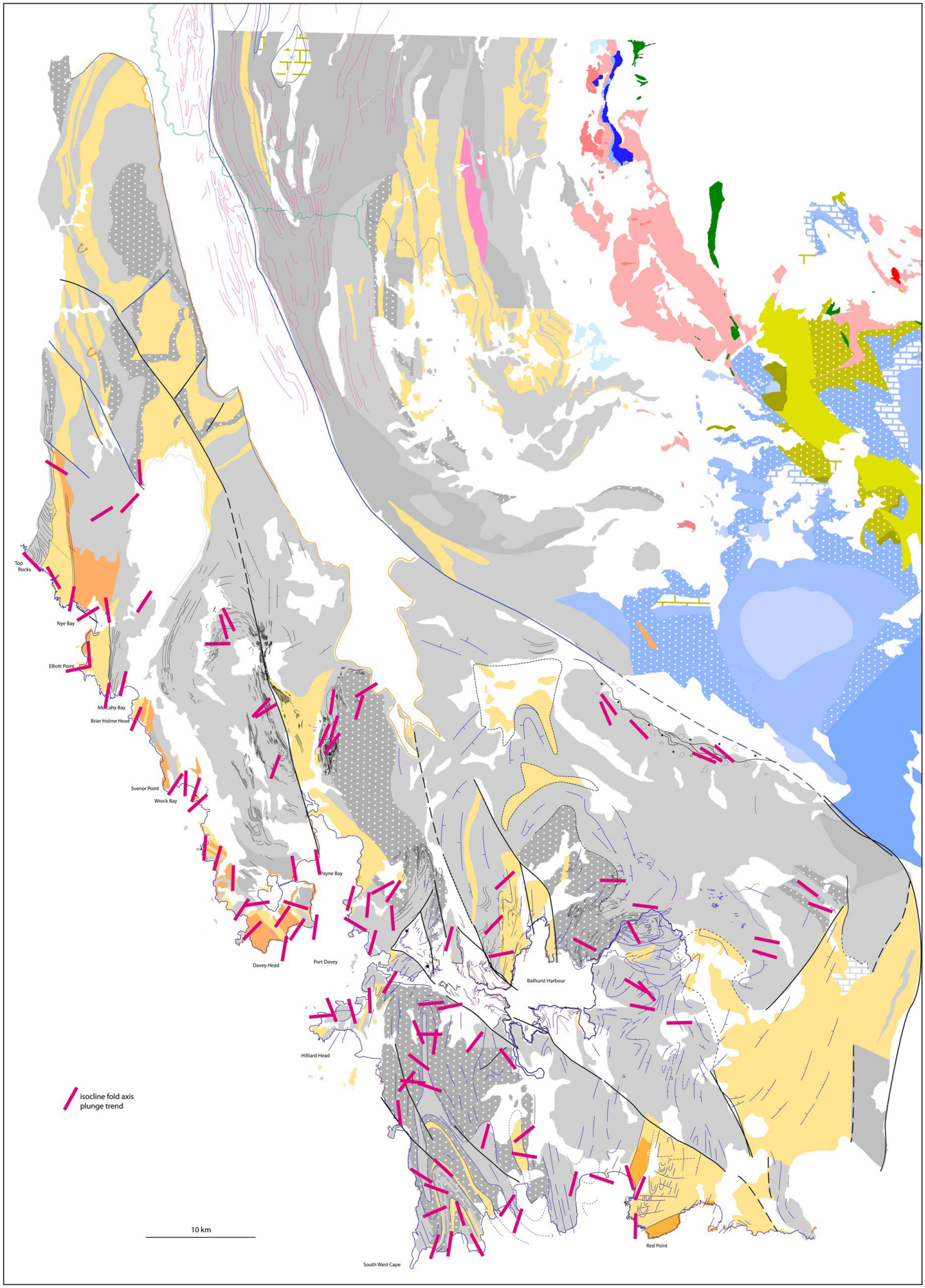

Figure 16. Summary map of mesoscopic isocline fold axis (FA) trends with heavy pink lines showing the regional fold axis plunge direction pattern. Map base is the 1:25,000 and 1:250,000 digital geological atlas from Mineral Resources Tasmania.

The isocline fold axis pattern varies across the Southern Tyennan domain but has an overall east-west trend (Figures 16 and 17). The main features are:

1. South-southwest and south- trends dominate the fold axis pattern of the coastal belt from Mulcahy Bay to Port Davey (Figure 16). This pattern appears coincident with the inferred pinched and attenuated hinges of isoclinal macro-folds in the Mulcahy-Davey Head isoclinal macro-fold stack (Gray et al., 2022);
2. West-northwest- and southwest-trends coincide with the limbs of the Nye Bay fold-nappe, particularly across the Lawson Range (Figure 16);
3. Similar zonation of south-dominant trends within the inferred macro-fold hinges, and northwest-trends on upper limbs versus southwest- and west-southwest on the structurally lower limbs is also broadly consistent across the De Witt-Propsting and South West Cape mega-folds;
4. West of the Spring River Valley-Rugby Range-Ray River Fault the mesoscopic isocline fold axis pattern is broadly east-west trending (Figure 16);
5. The Arthur Range, including the Western Arthur and Eastern Arthur Ranges are northwest-trending (Figure 16).

3.3 Lineation Pattern

The mineral lineation (Lm) summary map of the Southern Tyennan domain (Figure 18) shows:

1. An overall west-southwest to southwest trend for the Southern Tyennan region;
2. But within this there are trend domains of northwest, north-south and northeast trend due to refolding of the pre-folding Lm by both macro- and mesoscopic isoclinal folds (Figure 18a);
3. The northwest Lm trends relate to the upper limbs of the macro-isoclines and northeast trends relate to the lower limbs of the macro-isoclines (Figure 18a);
4. The north-south trends appear to coincide with macro-fold hinge zones and relate to reworking of the mineral lineation during fold-modification (cf. Maclean and Bowen, 1971, p.101). Fold tightening with accompanying hinge rotation can produce younger overprinting mineral lineations within the hinge zones (Figure 18b).

3.4 Early Fold Axis (FA) and Lineation (Lm) Relationships

Rotation sense, either clockwise or counter-clockwise, of the fold axis trend (FA) towards the lineation Lm trend changes from limb to limb for regional-scale inclined plunging to reclined macro-folds. Such changes in the fold axis FA^Lm rotation sense can be used to identify fold hinges in shear-related regional-scale folds (Alsop & Holdsworth, 1999). The approach was also used to both establish and verify the positions of fold axial surface traces (AST) in the Central Tyennan domain (see Gray & Vicary, 2021b).

Originally established for recumbent sheath folds the change from clockwise to counterclockwise fold-hingeline vergence denotes the medial symmetry line of a sheath fold (Alsop and Holdsworth, 2004, fig.13) For inclined plunging to reclined folds with sheath-like form, typical of the macro-folds within the Tasmanian Tyennan nucleus, this change can also be used to delineate the macro-fold hingeline position or axial surface trace position separating upper and lower fold limbs (see circled H positions, Figure 19) .

In general where data is available there is a broad match between inferred and mapping-interpreted macro-fold hinges (circled H positions, Figure 19), particularly for the southwest high-grade coastal belt, the Davey River sheath nose and the South West Cape mega-sheath fold system. In the Southwest High-Grade Coastal Belt changes from clockwise to counter-clockwise sense occur at Nye Bay, Mulcahy Bay and Sandblow Bay (see positions marked by H in Figure 19) confirming the presence of the macro-folds hinges (see hinges 2, 3 and 4 in figure 78, Gray et al., 2022). Further south in the Port Davey area limited Lm data precludes verification of the regional fold hinge-lines there.

For the De Witt-Propsting mega-sheath fold there are limited data for the southern portion of the mega-sheath (Figure 19). In the northern part the upper western limb has anti-clockwise vergence and the structurally lower has clockwise vergence with the approximate hinge position designated by the circled H (Figure 19).

However, non-uniform mapping data and the overall lack of lineation measurements inhibit the overall usefulness of this approach.

3.5 Transport Direction Pattern

The kinematics of emplacement for metamorphic sheets within the Southern Tyennan domain are provided by the following:

1. Movement plane defined by the plane containing the lineation and the perpendicular to the dominant foliation Sm. Shear sense requires other data such as porphyroclast tails and quartz fabric asymmetry
2. Transport direction defined by a plane perpendicular to the intersection line between a shear band (S-C') and the dominant foliation (Sm) with sense given by the deflection of Sm through the shear band.

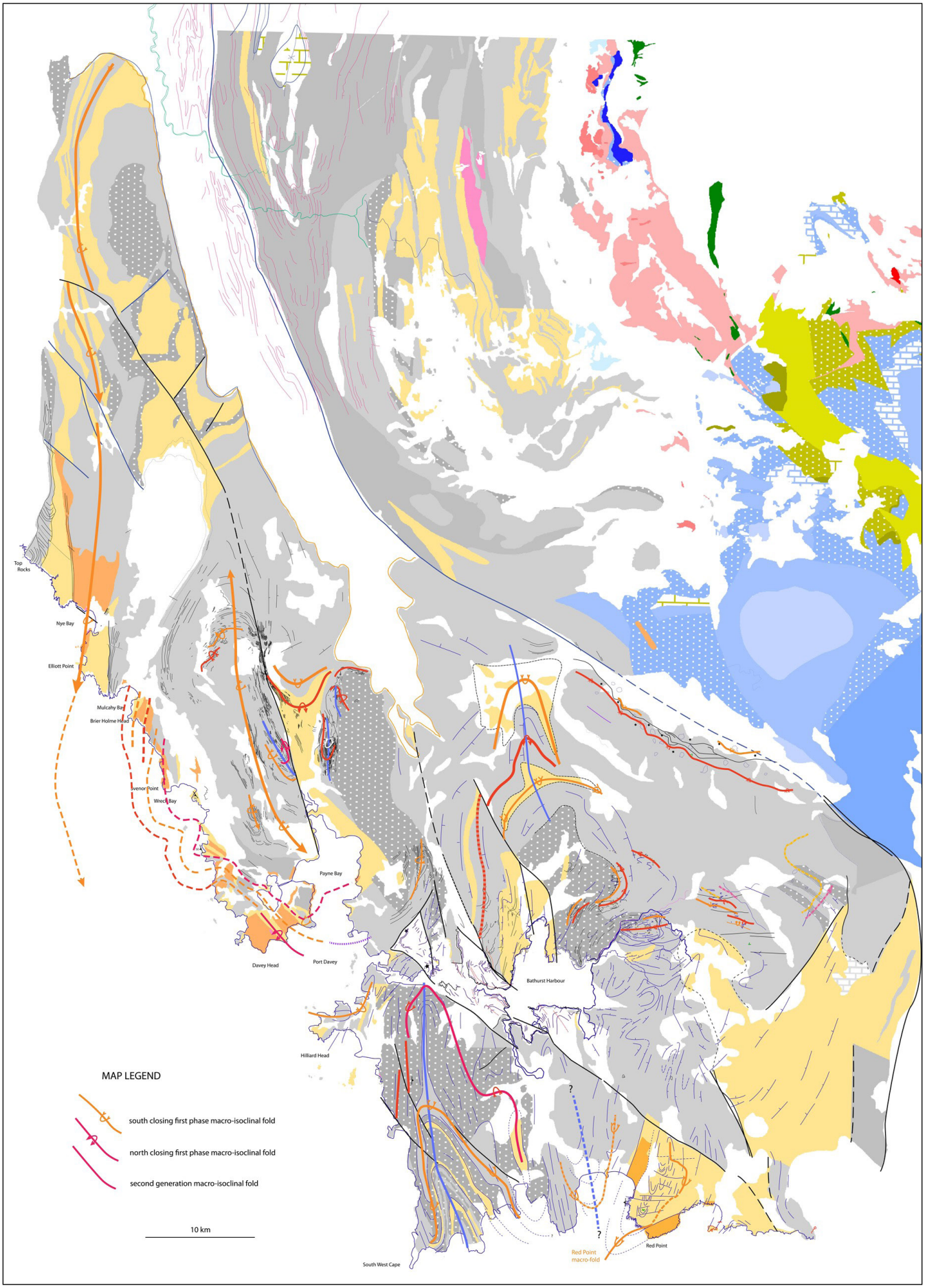

Figure 17. Summary early macro-isocline axial surface trace map. South-closing macro-folds have orange axial surface traces. North-closing macro-folds have red axial surface traces. Dashed lines are interpreted axial surface traces. Map base is the 1:25,000 and 1:250,000 digital geological atlas from Mineral Resources Tasmania.

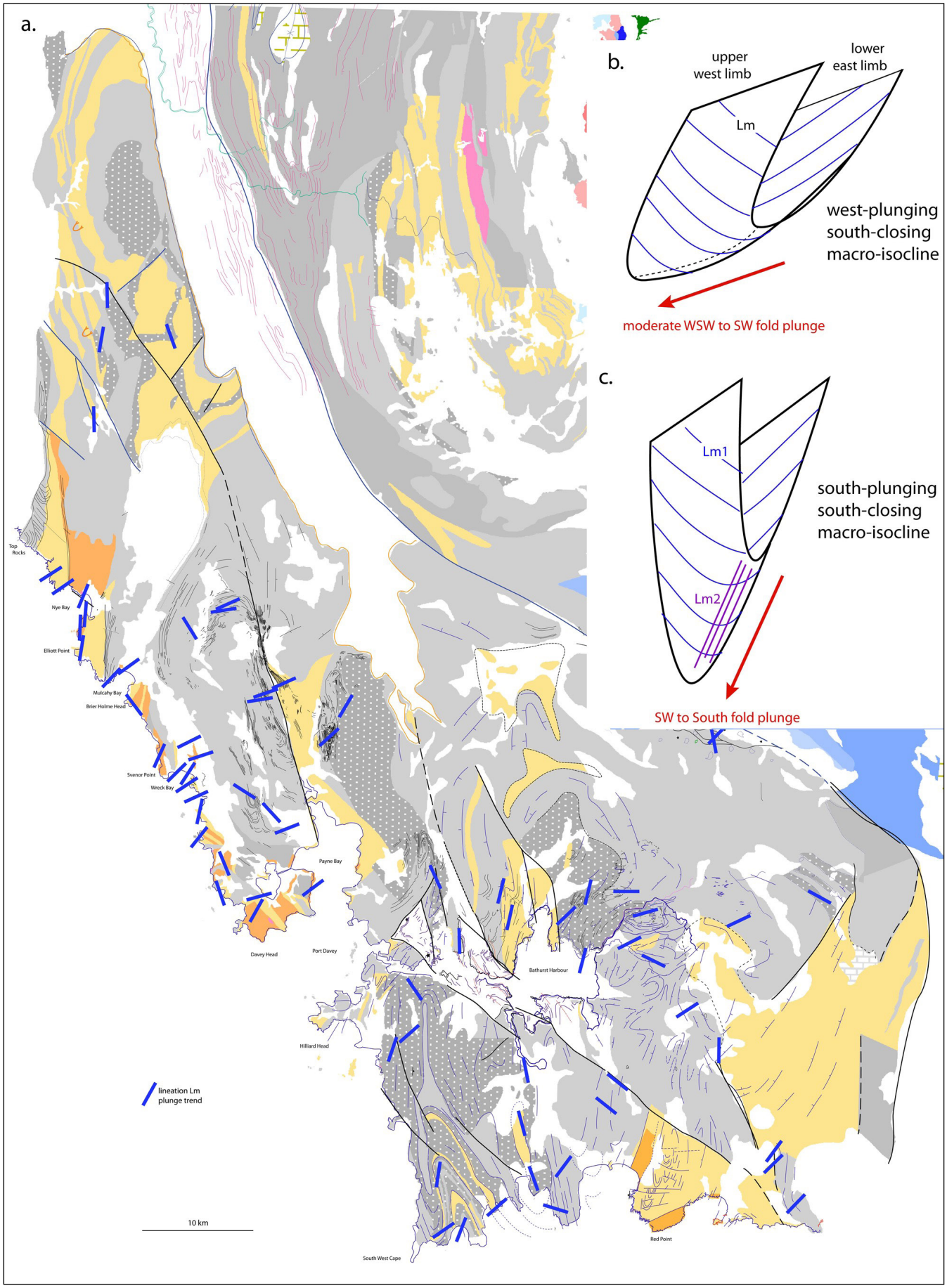

Figure 18. Summary map of mineral lineation (Lm) trends shown by the heavy blue lines (a). Map base is the 1:25,000 and 1:250,000 digital geological atlas from Mineral Resources Tasmania. b) Schematic 3D sketch showing the Lm pattern for an isoclinal fold with inclined plunging approaching reclined geometry. With a southwest plunge on the west-dipping lower limb rotation of the layering about the inferred fold axis will give a northwest plunge on the upper limb. c) Schematic 3D sketch of inclined plunging isoclinal fold with reworked lineation (Lm) within the isoclinal hinge shown by the purple lines.

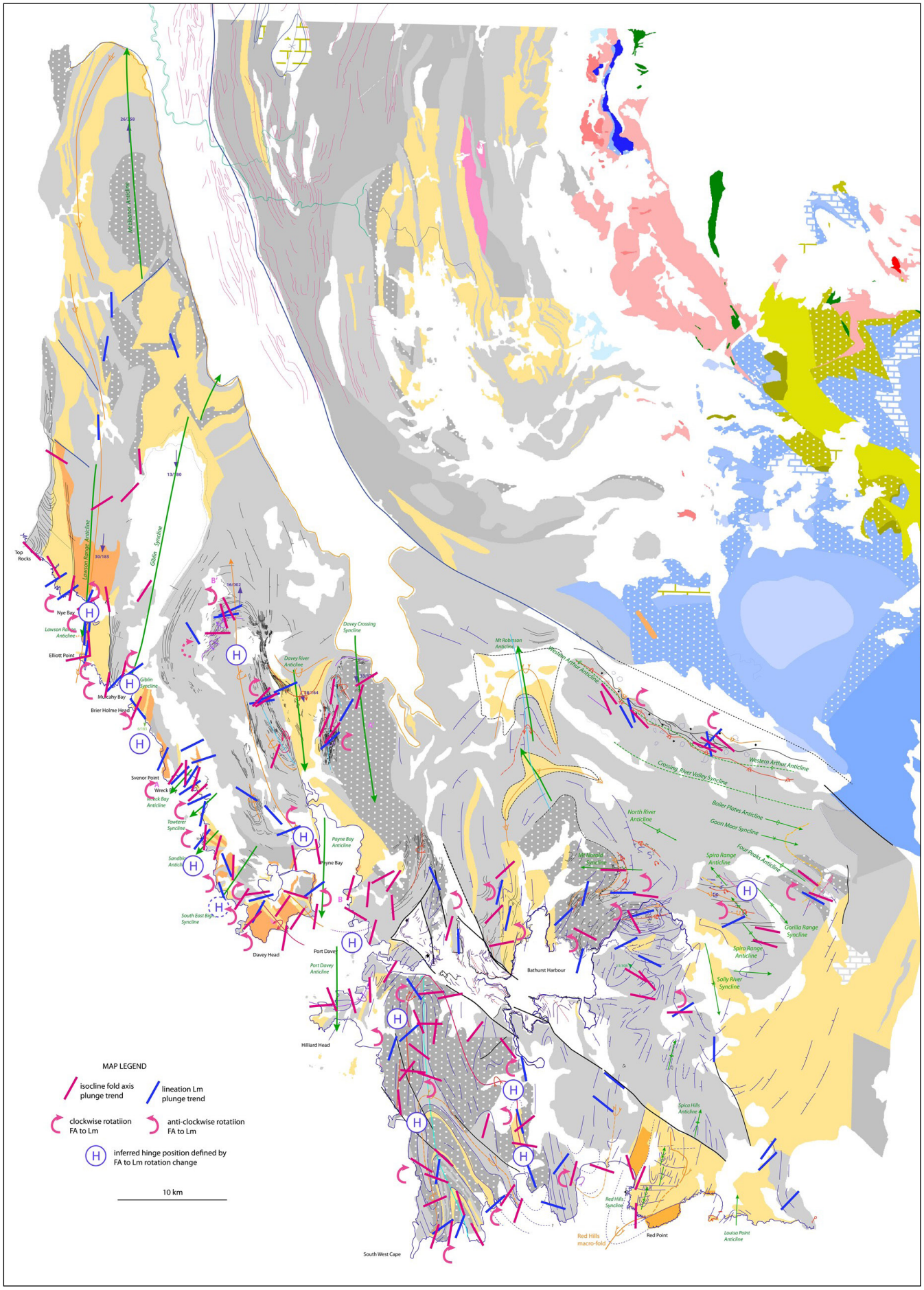

Figure 19. Southern Tyennan domain fold-hingeline-vergence summary map for mesoscopic isoclines (after Alsop and Holdsworth, 2004). The vergence, either clockwise or anti-clockwise, is given by the sense of rotation of the local fold axis trend towards the local mineral lineation Lm closing the acute angle. The fold hingeline-vergence is shown by the red arrows. A change in fold-hingeline vergence indicates the presence of a fold hinge with the hinge positions shown by the circled letter 'H'.

Overprinting fold and fabric analysis indicates:

1. The lineation Lm is folded by the early mesoscopic folds, designated F2 with axial surface crenulation cleavage within the early fabric S1/Sm (Burns, 1964; Maclean and Bowen, 1971; Turner, 1989). Lm therefore predates the F2 mesoscopic folding and the macro-folding;
2. The dominant foliation Sm is a transposition layering that largely postdates the metamorphic peak assemblages within the high-grade schists of the uppermost sheet;
3. The shear bands (S-C') are restricted to the high-strain zones (HSZ) bounding and internal to the metamorphic sheets (Meffre et al., 2001);
4. Upward movement (buoyant expulsion) of sheets bounded above and below essentially "static" (or slower moving) sheets is by translation within shear zones at the contacts. This requires a reversal in shear sense from dextral (west-over-east) at the top to sinistral (east-over west) at the base;
5. The welded and stacked sheets have been folded during emplacement to higher structural levels, requiring folding and possible reactivation of the HSZ and the contained shear bands.

Interpretation of the tectonic emplacement of the Southern Tyennan domain from the movement plane and transport direction data (Figure 20) requires knowledge of 1) the early macro-folding pattern and the positions of individual lineations within the regional structures, and 2) the younger Devonian fold pattern. All movement plane and transport directions have been restored to a common datum by 1) removal of the younger Devonian fold plunges, and 2) rotation of the dominant foliation (Sm) to the horizontal to approximate the pre-isoclinal folding geometry.

The Lm-movement plane summary trend map (thick purple lines and arrows, Figure 20) shows a predominant overall southwest-trending pattern but appears locally complex. Regions of northwest-trending Lm-movement planes occur on the upper limbs of the west-plunging, inclined to reclined macro-folds and zones of approximately north-south trends are coincident with many of the macro-fold hinge zones (Gray et al., 2022, Gray and Vicary, 2022b).

The movement directions are 233° (n=5) for the Southwest High-grade Coastal Belt data (Figure 20c), 223° (n=17) for all data west of the Spring River Valley-Rugby Range-Ray River Fault (Figure 20d) and 293° (n=4) for data east of the Spring River Valley-Rugby Range-Ray River Fault (Figure 20e).

Orientation analysis of the early mesoscopic folds from the Lawson Range give a dominant trend of 250° (Figure 20b) suggesting rotation of these folds towards the bulk stretching direction determined from the Lm-movement plane data. This is typical of sheath fold development (see section 2 in Gray and Vicary, 2022b).

The mid-Cambrian Spring River Valley-Rugby Range-Ray River Fault defines the northeast faulted boundary of the Bathurst Harbour graben (Figure 20a). An apparent rotation of ~70° of the Lm-movement plane trends across this fault suggests a significant rotational component of the east block during middle Cambrian strike-slip graben formation. Geometrically this requires a scissored-fault movement involving anti-clockwise rotation about a pivot-point at the northern fault termination.

This fault boundary is also significant in that it separates a complex shear band-derived transport direction (TD) pattern (Figure 20f) from a uniform northeast-directed pattern within the Arthur Range east of the fault system (Figure 20g). The ~70° rotation inferred from the Lm-movement plane data is not however apparent in the TD data across this fault.

Given that many of the shear sense elements (asymmetric folds, porphyroblast tails and shear bands) form pre-folding (see section 2.5 above) it is important to understand the implications of regional scale isoclinal macro-folding on these elements and their derived shear sense. A schematic diagram (Figure 21) illustrating isoclinal folding by passive limb rotation about the fold hinge-point shows that early-formed shear sense elements maintain the same shear sense from the lower limb to the upper structurally overturned limb. Therefore no change or reversal in shear sense should occur across the mapped or inferred macro-isoclinal folds.

A more detailed discussion of the high-grade coastal belt shear band data is provided in Gray et al. (2022). It is clear that the shear band transport data are complex and at this stage difficult to interpret. Complications relate to 1) the presence of dextral shear bands, and 2) a ~70° change in the bulk movement sense from the early Lm development stage to the later high strain movement welding and emplacement stage (see Gray et al., 2022). One possible scenario is that macro-folding accompanied by shear zone reactivation may lead to flattening components in the attenuated macro-fold hinges and therefore development of both sinistral (synthetic) and dextral (antithetic) shear bands. Clearly the shear sense data and evaluation needs further work.

3.6 Younger Fold Axis (FA) Trends

Younger more open folds refold the early macro-isoclinal folds (Figure 22). As these folds also fold the Ordovician sandstone and conglomerate that sits unconformably on the older quartzite-pelite sequence they are considered mid-Devonian in age related to Tabberabberan deformation (Seymour, 2014). Fold plunges and in part axial surface traces of the younger folds are controlled by the pre-existing architecture of the early-formed macro-isoclines and mega-sheath folds.

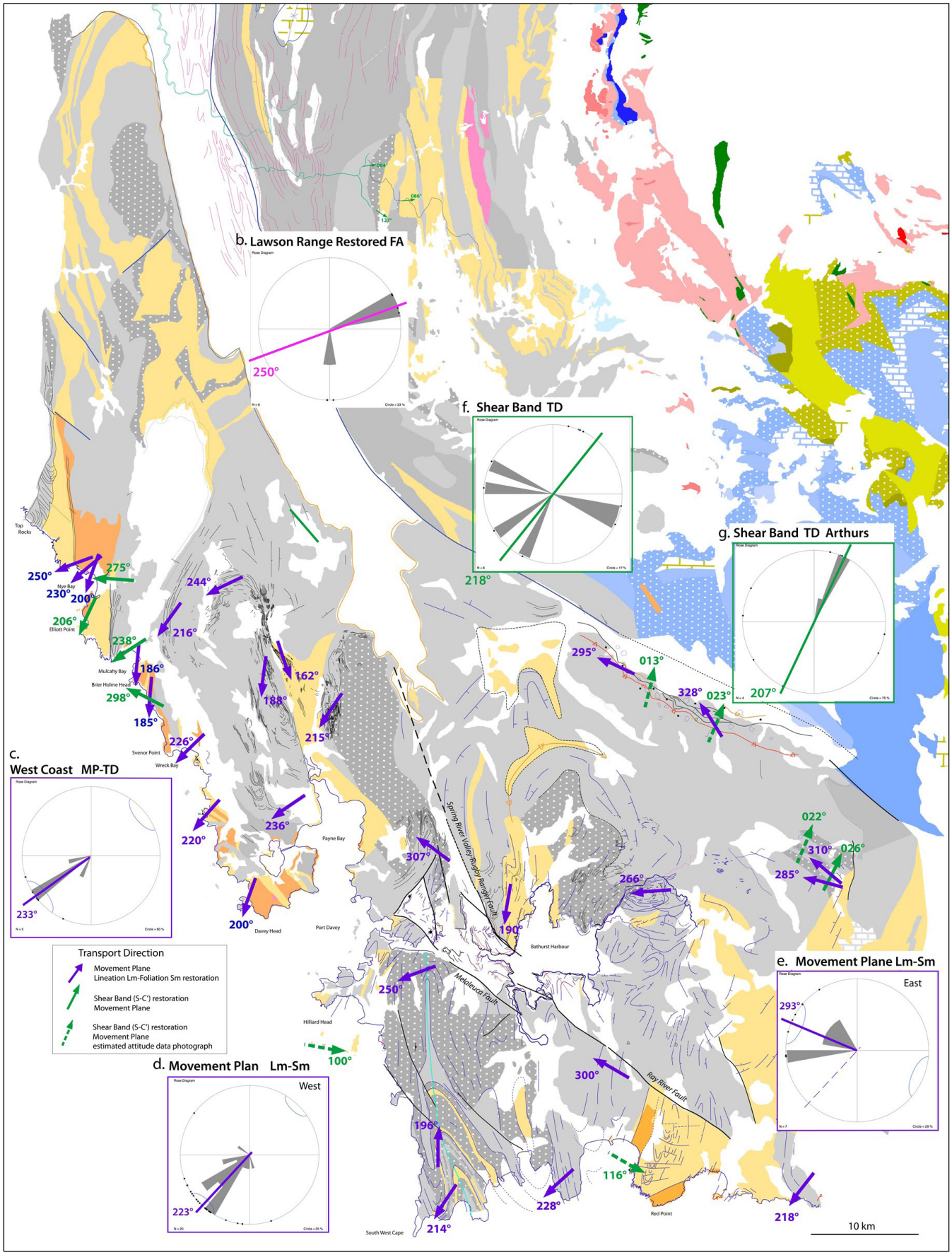

Figure 20. Movement Plane and Transport direction summary map of the Southern Tyennan domain. All data represented by the purple arrow (movement plane strike) and green arrow (shear band transport direction) are restored by removal of the younger Devonian fold plunge and rotation of the contained dominant foliation Sm to the horizontal. a) Summary map with arrows on Mineral Resources Tasmania 1:250,000 digital atlas series map base. b) Rose diagram of the early restored early-isocline axes across the Lawson Range anticline (see Gray et al., 2022, fig. 87b). c) Rose diagram of west coast movement plane strike data (summarised from stereonets Gray et al., 2022, fig. 87). d) Rose diagram of total restored Sm-Lm movement plane data west of the combined Spring River Valley-Rugby Range-Ray River Fault. e) Rose diagram of total restored Sm-Lm movement plane data east of the combined Spring River Valley-Rugby Range-Ray River Fault. f) Shear Band transport data (TD) for the western Southern Tyennan domain. g) Shear Band transport data (TD) for the Arthur Range in the northeastern Southern Tyennan domain. Refer to Appendix 1 for further information.

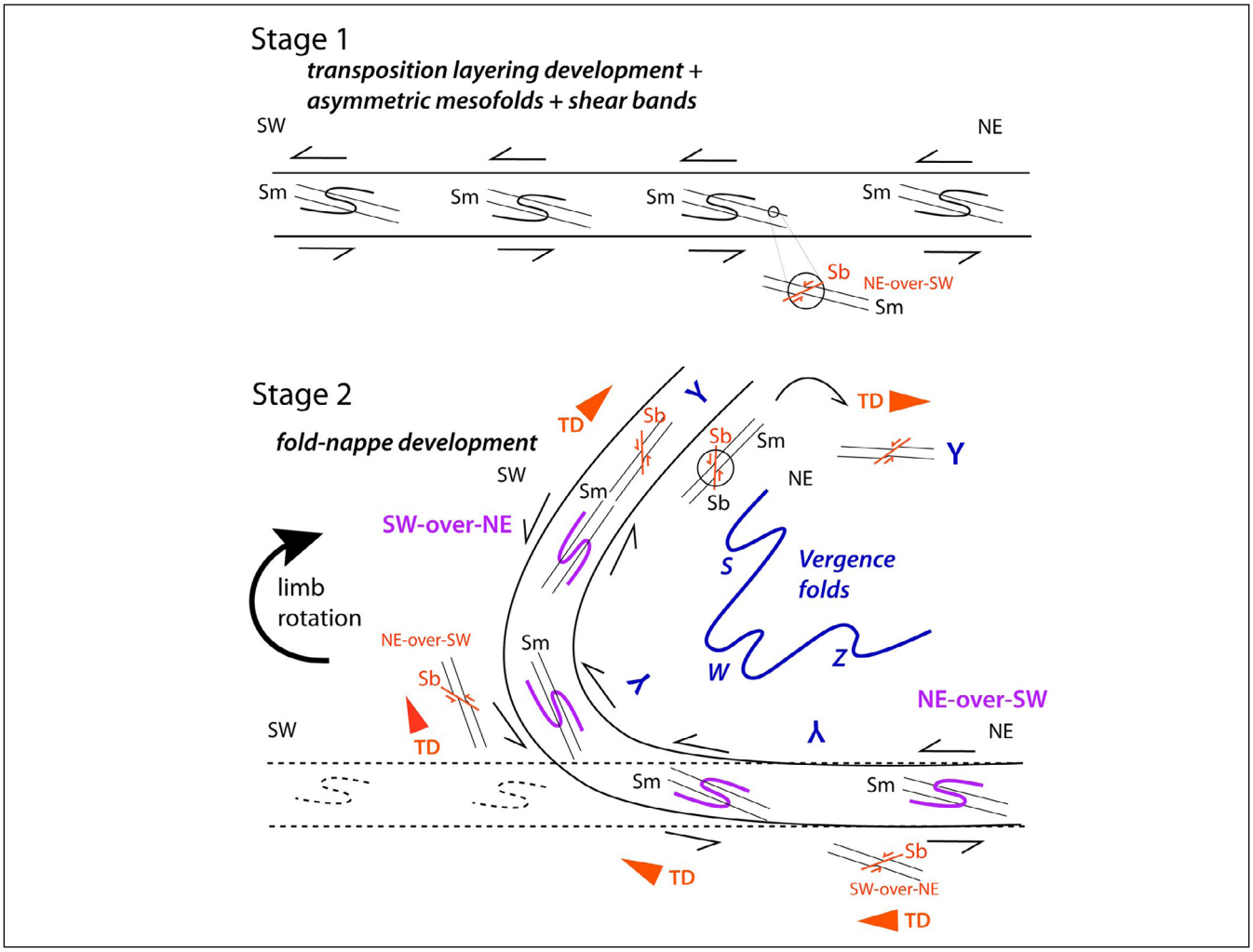

Figure 21. Schematic profile diagram illustrating folding of early-formed (pre-folding) NE-over-SW shear sense elements through the nose of a tight to isoclinal macro-fold. These include S-vergent asymmetric folds and sinistral NE-over-SW shear bands (Sb). The lower limb represents the Stage 1 undeformed position shown in (a) with Stage 2 folding by clockwise limb rotation about the fold-hinge shown in (b).

Much of the western part of the Southern Tyennan domain is refolded by north-south trending folds that are sub-parallel and co-planar with the mega-sheath folds (Figure 22). The coastal belt from Wreck Bay to South East Bight is refolded by southwest plunging, north-east-southwest trending folds (Figure 22). In the vicinity of the Arthur Range northwest-trending folds are dominant and define the northern margin of the Southern Tyennan domain. East-west trending folds occur in the central "core" of the eastern fold domain in the Mt Norold-Harrys Bluff-High Round Mountain ridgelines.

The main younger folds that affect the coastal belt (Gray et al., 2022) are listed below with their fold axis attitudes. These are:

Lawson Range Anticline:	*25°/202°*
Giblin Syncline:	*25°/178°*
Wreck Bay Anticline:	*49°/217°*
Towterer Syncline:	*49°/212°*
Sandblow Bay Anticline:	*44°/207°*
South East Bight Syncline:	*36°/217°*
Port Davey Anticline:	*41°/215°*

In the central part of the Southern Tyennan domain major Devonian age folds (Gray and Vicary, 2022c) include the:

Davey River Anticline	*28°/164°*
Davey Crossing Syncline	*33°/179°*
Mt Robinson Anticline	*23°/356°*
Mt Braddon Anticline	*08°/337°*

In the northeast Devonian folds of the Western and Eastern Arthur Ranges (Gray and Vicary 2022a) include the:

Arthur Range Anticline (east end)	*04°/285°*
Crossing River Valley Syncline	*04°/288°*
Boiler Plates Anticline	*04°/097°*
Goon Moor Syncline	*10°110°*
Four Peaks Anticline	*04°/299°*
Federation Peak Anticline	*18°/316°*

In the southeast major Devonian folds (Gray and Vicary, 2022d) include the:

Red Hills Syncline	*08°/011°*
Louisa Point Anticline	*25°/007°*

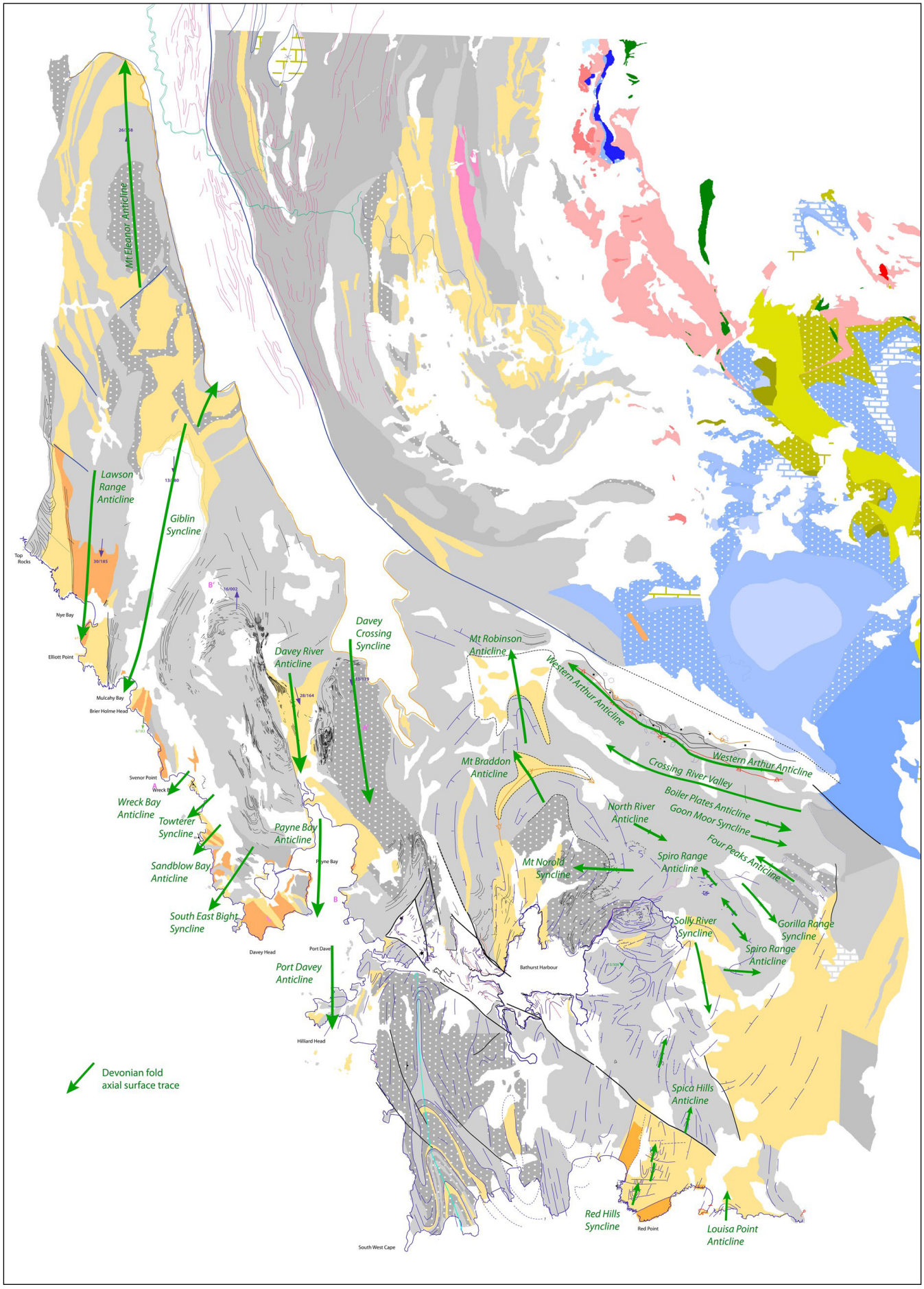

Figure 22. Younger Devonian major fold axial surface trace map. Fold axial surface traces are shown as green lines with the barb/arrow denoting the direction of plunge. Map base is from the Mineral Resources Tasmania 1:250,000 digital atlas series.

3.7 Fault Pattern

Major faults include 1) the ~50 km long, north-northwest trending Giblin Valley-Payne Bay fault in the east that transects the De Witt-Propsting mega-sheath fold, 2) the major northwest-trending fault network associated with the Bathurst Harbour graben in the south-central part, and 3) the major domain-bounding Orange River fault along the Orange River valley with segments along the northern Davey River valley and the Huon Valley (Figure 23).

All of these faults are steeply dipping to sub-vertical with straight to curved outcrop traces and apparent oblique slip movements. They are interpreted here as mid-Cambrian extensional faults that were reactivated and inverted in the middle Devonian deformation (cf. Seymour, 2014). Many have been an apparent locus of sedimentation with remnants of the Ordovician sedimentary succession preserved along the footwall of the fault.

The Port Davey-Bathurst Graben (Figure 23) is a mid-Cambrian fault-controlled basin (Williams, 1982) constructed from a dominant northwest-trending fault set bounded laterally by smaller northeast-trending faults that close the basin (see Section 5). The northern boundary is the major, ~40 km long composite Spring River Valley-Rugby Range-Ray River fault that potentially extends northwards along part of the Crossing River valley to join the northern domain-bounding fault as a splay fault.

In the South West Cape region (Figure 23) a series of isolated, ~10-15 km long, northwest-trending faults that are sub-parallel with the Port Davey-Bathurst Graben bounding faults include the Hannat, New Harbour and Window Pane Bay Faults (Hall, 1965).

In the Lawson-Charles Ranges of the northwest (Figure 23) a conjugate fault set consists of northeast- and northwest-trending faults truncate and offset the northern continuation of the Nye Bay fold-nappe and the Mt Eleanor Anticline.

3.8 Constructed Structural Profiles and Cross-sections

The positions of structural profiles and cross sections across the Southern Tyennan domain are show in Figure 24. These are designated P1 through P10 with cross-referencing to the figure numbers in this publication.

4.0 SOUTHERN TYENNAN DOMAIN STRUCTURAL ELEMENTS

This section summarises the structural elements that make up the structural architecture of the Southern Tyennan domain (Figure 3). The overall geometry, attitude, structural character and the definitions of the elements are presented. More detailed descriptions down to the outcrop scale are provided in the previously published supplementary papers that treat each element individually (see end of Section 1).

4.1. The Nye Bay Fold-nappe

The Nye Bay fold-nappe (element 1, Figures 2 and 3) is a major south-closing, west-plunging, reclined to recumbent macro-isoclinal fold cored by high-grade schist and flanked by phyllite and low-grade quartzite (Figures 25, 26 and 27). The upper, overturned western limb has a map width of ~7 km and extends from Top Rocks to Nye Bay (Figures 25 and 26). The lower eastern limb of the fold-nappe crops out from Elliott Point to Mulcahy Bay and is juxtaposed against structurally lower high-grade schist along an interpreted high strain zone coincident with the mouth of the Mulcahy River (Figures 25 and 26). Southwards the high-grade schist is part of a series of second-order, structurally lower, isoclinal macro-folds with in-folds of low-grade pelite and quartzite (Mulcahy Bay-Port Davey Isoclinal Fold Stack).

The litho-structural map (Figure 25) shows key elements including:

1. A southwards tapering or thinning of the high-grade schist (Ptpg) towards Elliott Point.
2. A loss of high-grade schist (Ptpg) north of the Lawson Range, across a northwest-trending cross-fault.
3. Thinning northwards of the low-grade pelite (Ptp) units that enclose the high-grade schists away from the inferred macro-fold hinge at Elliott Point (i.e. layer thickening within the inferred hinge and layer thinning and attenuation along the fold limbs).
4. A pinch out of low-grade pelite (Ptp) north of the Giblin River along the eastern flank of the high-grade schist, such that north of Nye Bay the high-grade schists sit directly on quartzite.
5. A re-appearance of low-grade pelite north of the Giblin Syncline closure.
6. High-strain, mylonitic, platy schistose quartzite is more common along the eastern contacts of the quartzite unit.
7. A northwest-trending dextral-oblique slip fault set and a northeast-trending sinistral-oblique fault set.
8. Folding of the Nye Bay fold-nappe by the Mt Lawson Anticline and Giblin Syncline (Figures 25 and 26).

Due to the overall west-dip of the West Coast succession the northern and most western part at Top Rocks is structurally higher than the macro-fold sets at Port Davey. The fold-nappe in the north is therefore at the highest structural level. It has an overturned western limb, is south-closing, west-plunging and approaching reclined geometry, and has a high-grade schist core (hinge zone). All these relationships are identical to those of the Franklin Fold-nappe that dominates the structurally highest part of the Central Tyennan domain to the north. The Franklin fold-nappe has been mapped to Mt McCall, some 75 km to the north (Gray & Vicary,

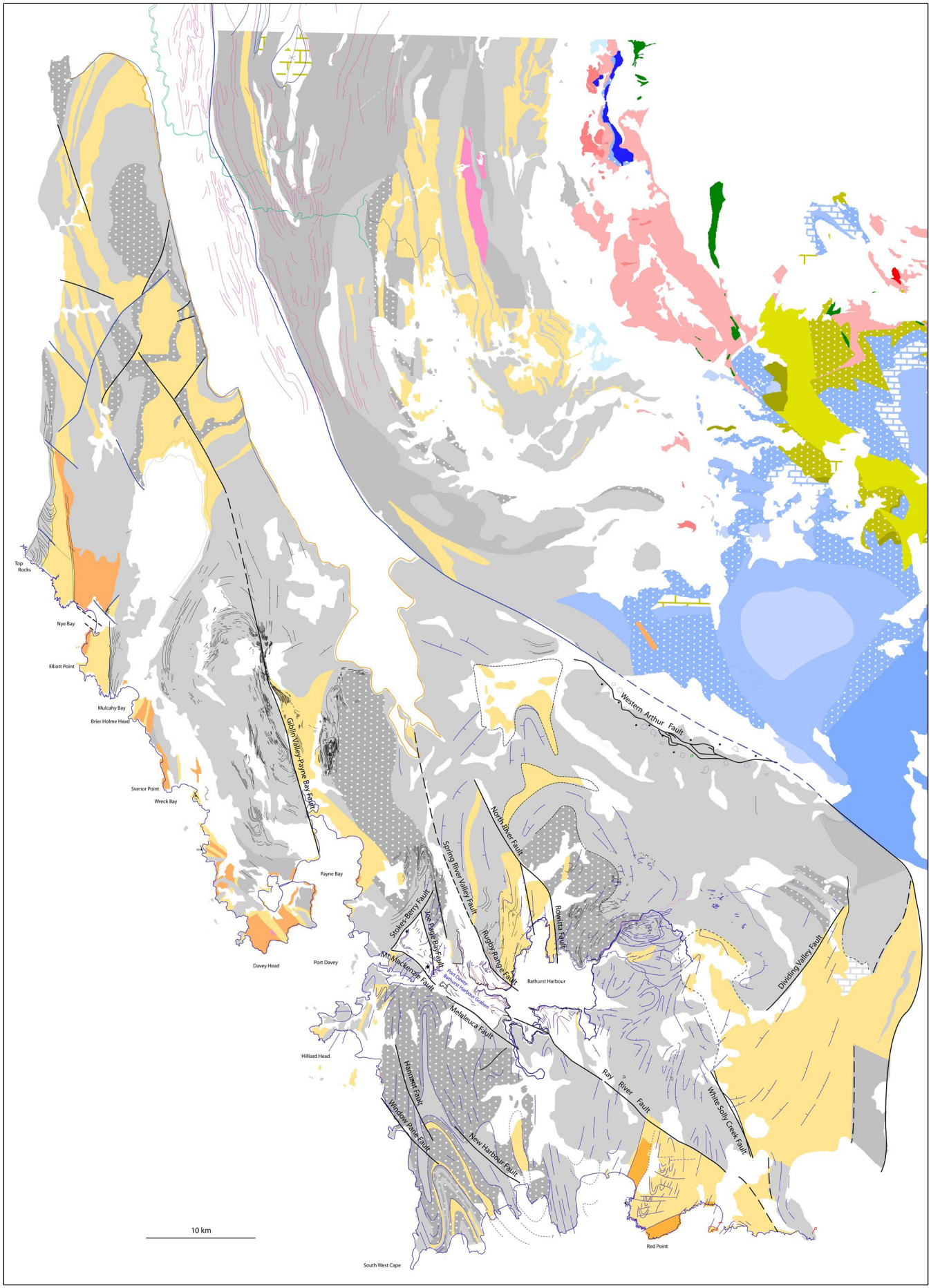

Figure 23. Southern Tyennan domain fault summary map. Fault traces are shown as heavy black lines. Fault names in the South West Cape area are after Hall (1965).

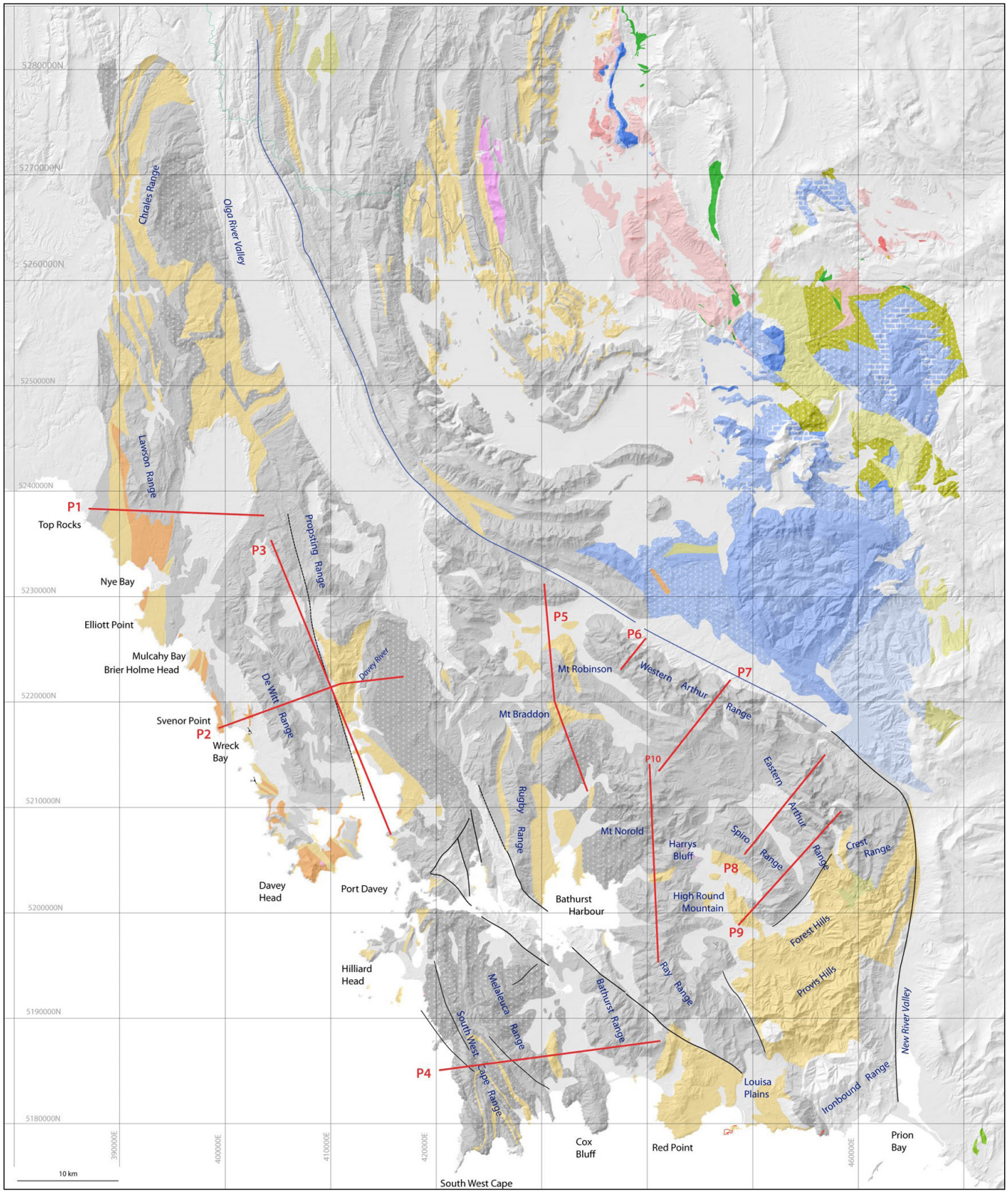

Figure 24. Location map of structural profiles and cross-sections across the Southern Tyennan domain.

Section P1 is Figure 26

Section P2 is Figure 36

Section P3 is Figure 37

Section P4 is Figure 48

Section P5 is Figure 51b

Section P6 is Figure 55

Section P7 is Figure 57 section C-D

Section P8 is Figure 57 section E-F

Section P9 is Figure 57 section G-H

Section P10 is Figure 57 section A-B

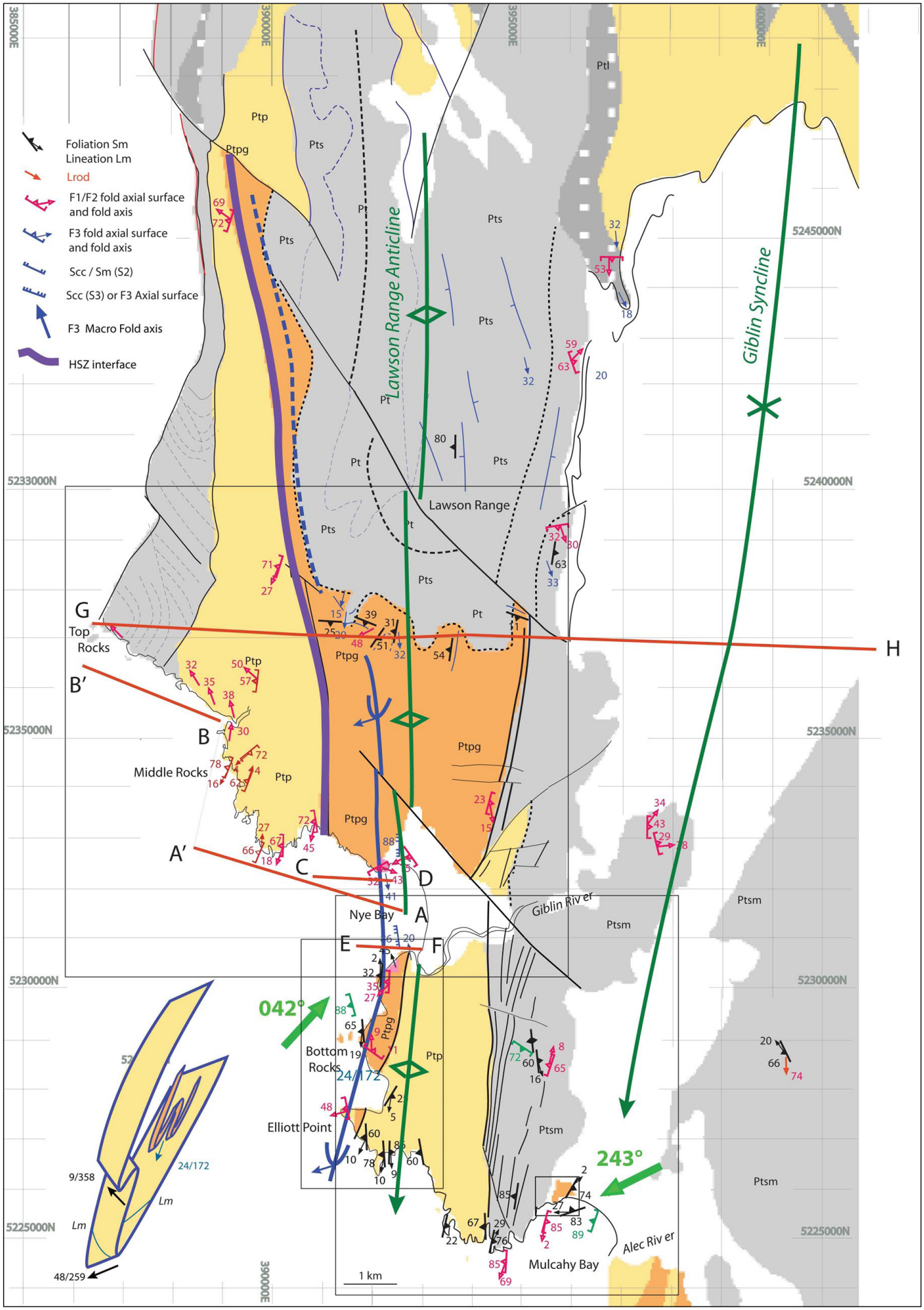

Figure 25. Lithological and structural relationships in the Nye-Mulcahy Bay area. Base map is the Mineral Resources Tasmania digital geological atlas Lewis, Elliott, and Mulcahy 1:25,000 map sheets. Positions of section lines A-A', B-B', C-D, E-F and G-H are shown by the thick red lines.

2021b), and now with potential continuation beneath the Cambro-Ordovician of the Elliot Range suggests that the highest levels of the Tyennan structural unit has an markedly asymmetric over-fold (fold-nappe) that extends the entire western margin of the Tyennan massif on the order of 200 km.

The inferred closure, based on extrapolation of contacts southwards into the Southern Ocean assuming a flattened similar-fold form, gives length scales of ~30 km for the hinge within low-grade pelite and almost ~45 km for the hinge in quartzite (Figures 28 and 29). Unfolding the inferred fold geometry requires a stacking sequence of high-grade schists underlain by low-grade phyllite, underlain by quartzite.

4.2 Mulcahy Bay-Port Davey Isoclinal Fold Stack

The Mulcahy Bay-Port Davey Isoclinal Fold Stack (element 2, Figures 2 and 3) sits below the Nye Bay Fold-nappe (Gray et al., 2022). From Mulcahy Bay southwards a series of second-order, structurally lower, isoclinal macro-folds are defined by alternating high-grade and low-grade layers (Figures 28, 29, 30 and 31). The macro-folds have axial trace length of ~26 km and extend from Mulcahy Bay to Port Davey (Figures 29 and 31). In the southern part, from Alfhild Bay to Port Davey the map pattern is dominated by a complex "mushroom" fold interference pattern where early, northwest-trending, reclined isoclinal macro-folds are refolded by younger, open Devonian northeast-trending, southwest-plunging folds. These change to open, more north-south trending, south-plunging folds at Port Davey (Figures 28 and 31).

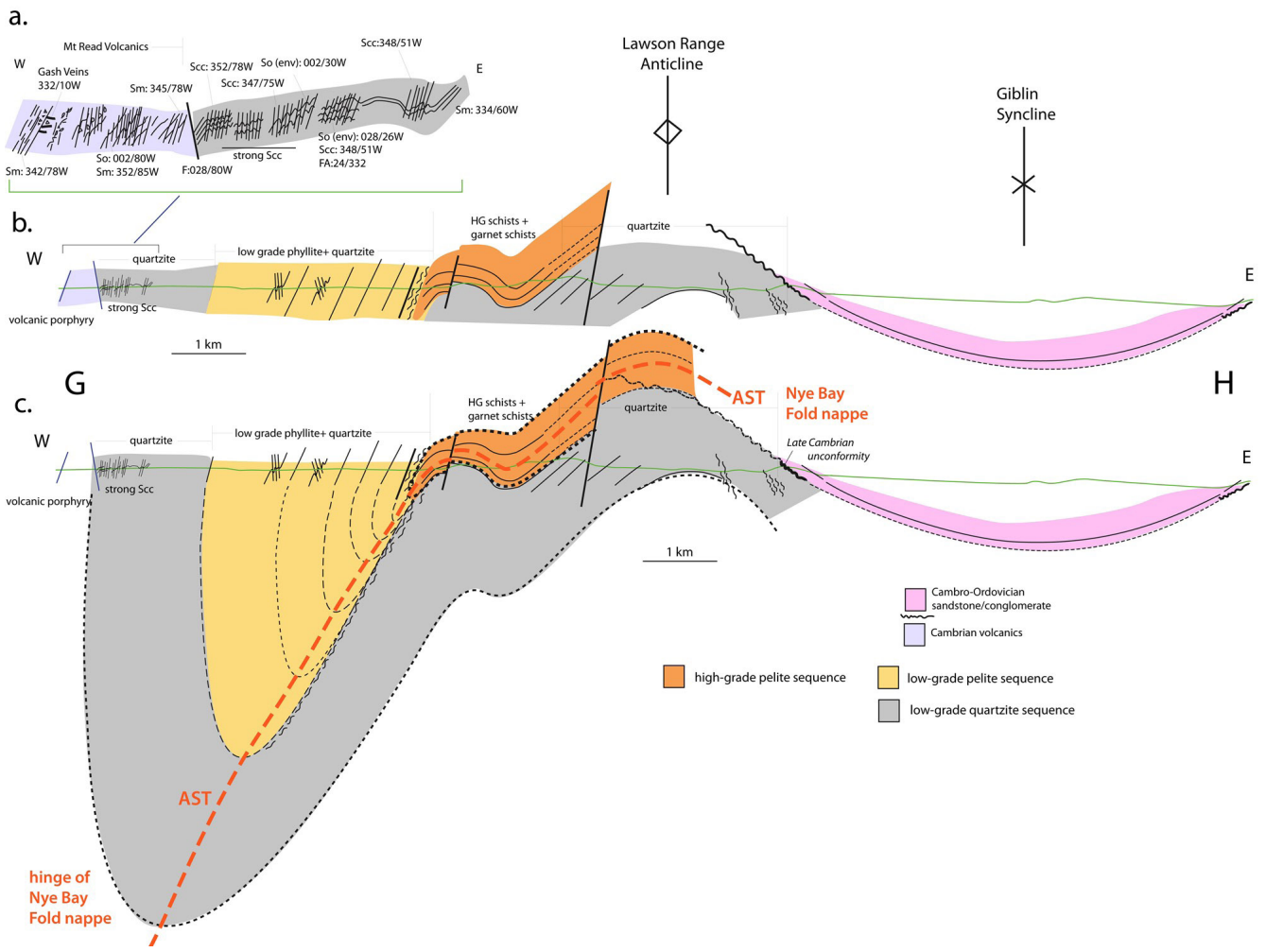

Figure 26. Structural profile from Top Rocks across the Lawson Range to the Giblin River Valley. This is regional structural profile P1 shown in Figure 24. a) Schematic structural profile at Top Rocks across the Cambrian-Proterozoic contact (from Miller, 2004). b) Structural profile G-H from Top Rocks to the Giblin Valley across the Lawson Range. c) Fold interpretation of the profile in (b) with wedge-out of the low-grade phyllite along the western flank of Nye Bay fold-nappe (see Gray et al., 2022). AST: recumbent fold axial surface trace. Younger, upright, open Devonian folds include the Lawson Range Anticline and the Giblin Syncline.

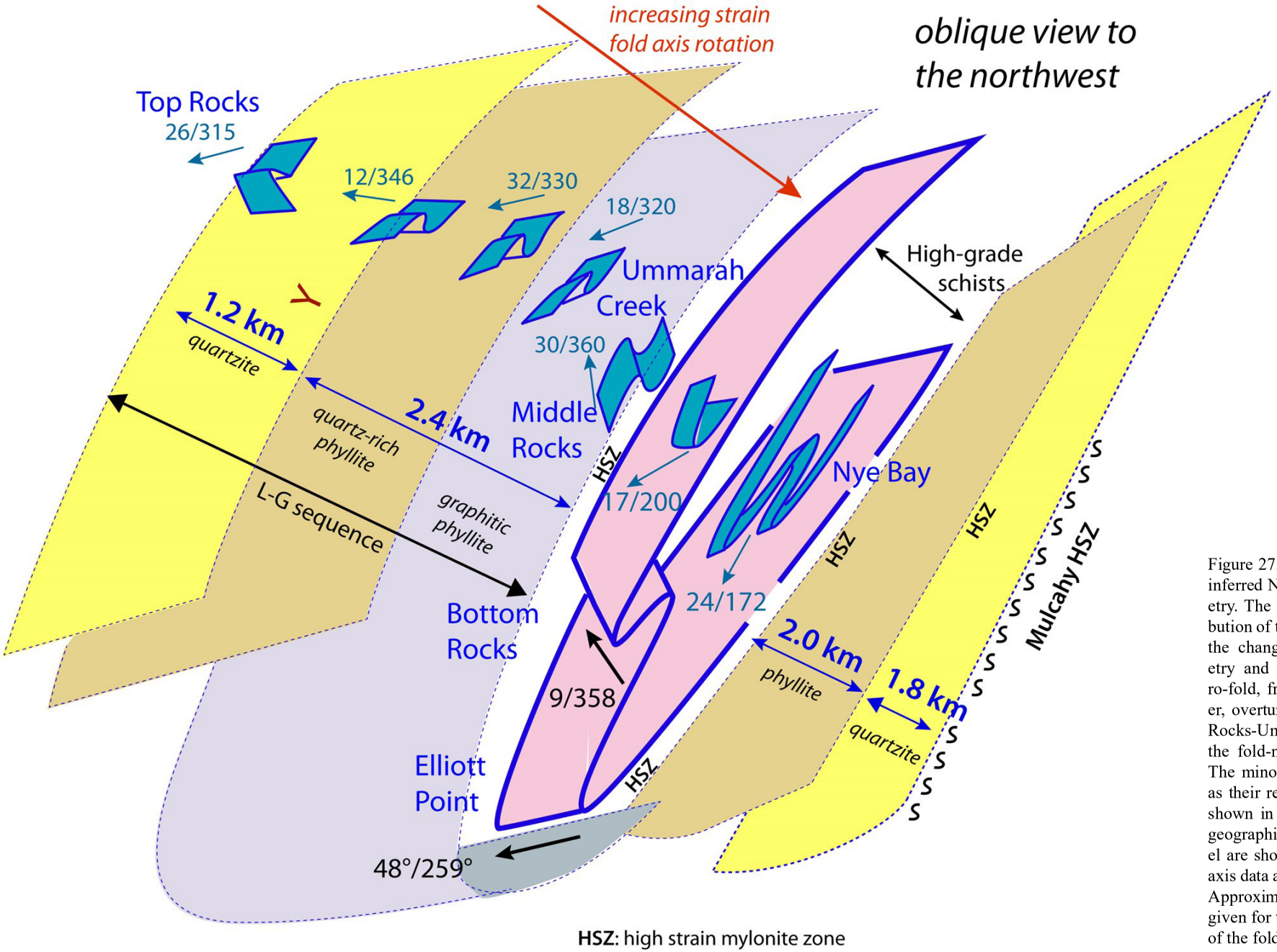

Figure 27. 3D oblique model of the inferred Nye Bay fold-nappe geometry. The diagram shows the distribution of the litho-tectonic layering, the changes in minor fold geometry and attitude across the macro-fold, from the structurally higher, overturned western limb at Top Rocks-Ummarah Creek through to the fold-nappe hinge at Nye Bay. The minor fold geometries as well as their respective fold plunges are shown in aquamarine. Positions of geographic locations in the 3D model are shown in blue text. The fold axis data are presented in Figure 25. Approximate unit thicknesses are given for the upper and lower limbs of the fold-nappe.

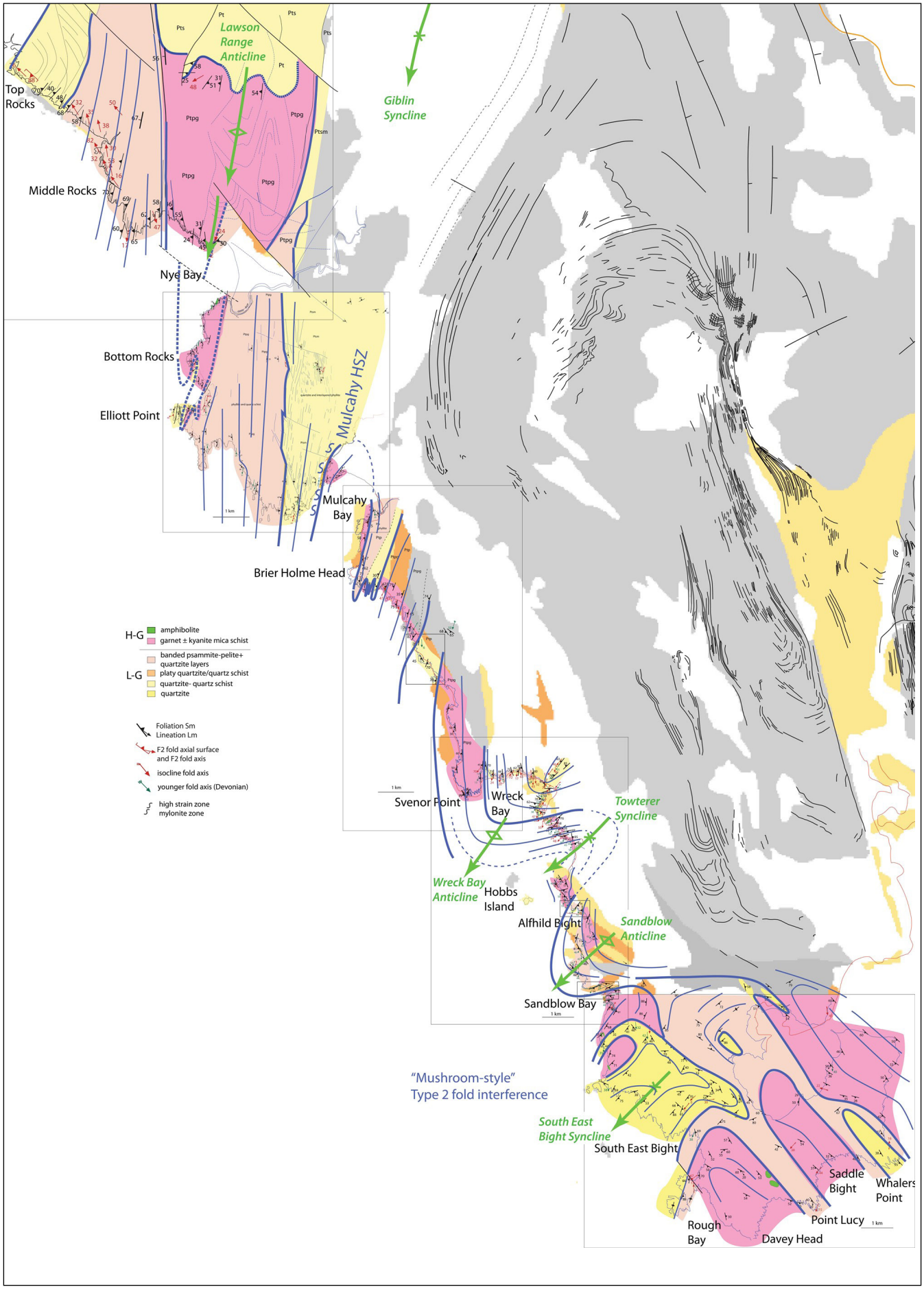

Figure 28. Structural interpretation map utilising Sm and So/Sm form lines to extrapolate the mapped distribution of lithologies and establish a macro-structural geometry for the southwest high-grade coastal belt (see Gray et al., 2022).

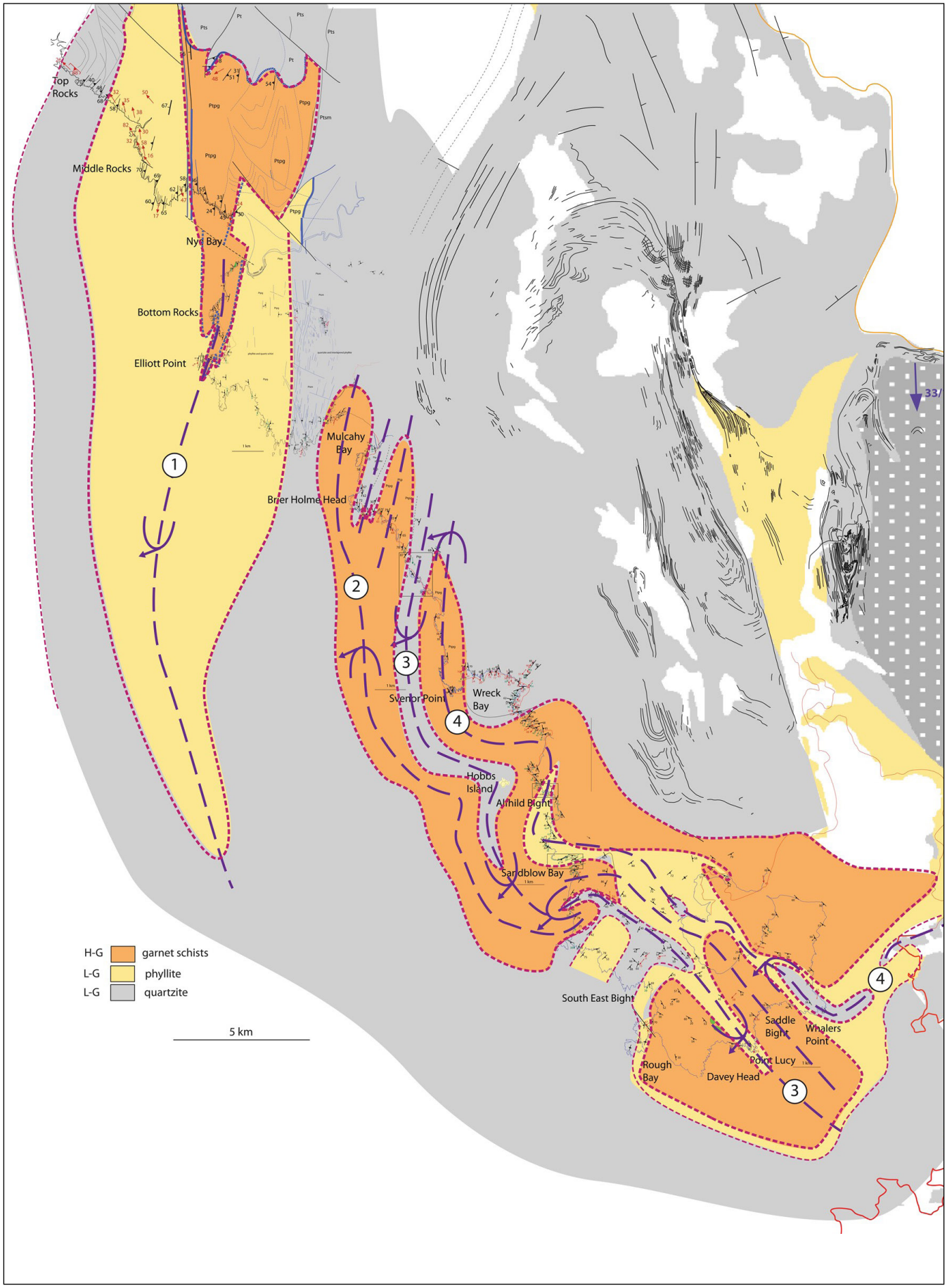

Figure 29. Axial trace map of inferred recumbent fold closures based on outcrop structural data and lithological distribution presented in Gray et al. (2022). Macro-folds include: 1) Nye Bay south-closing fold-nappe. 2) doubly-plunging, north-closing Mulcahy Bay fold. 3) south-closing in-fold in low-grade quartzite.4) north-closing Svenor Point fold cored by high-grade schist.

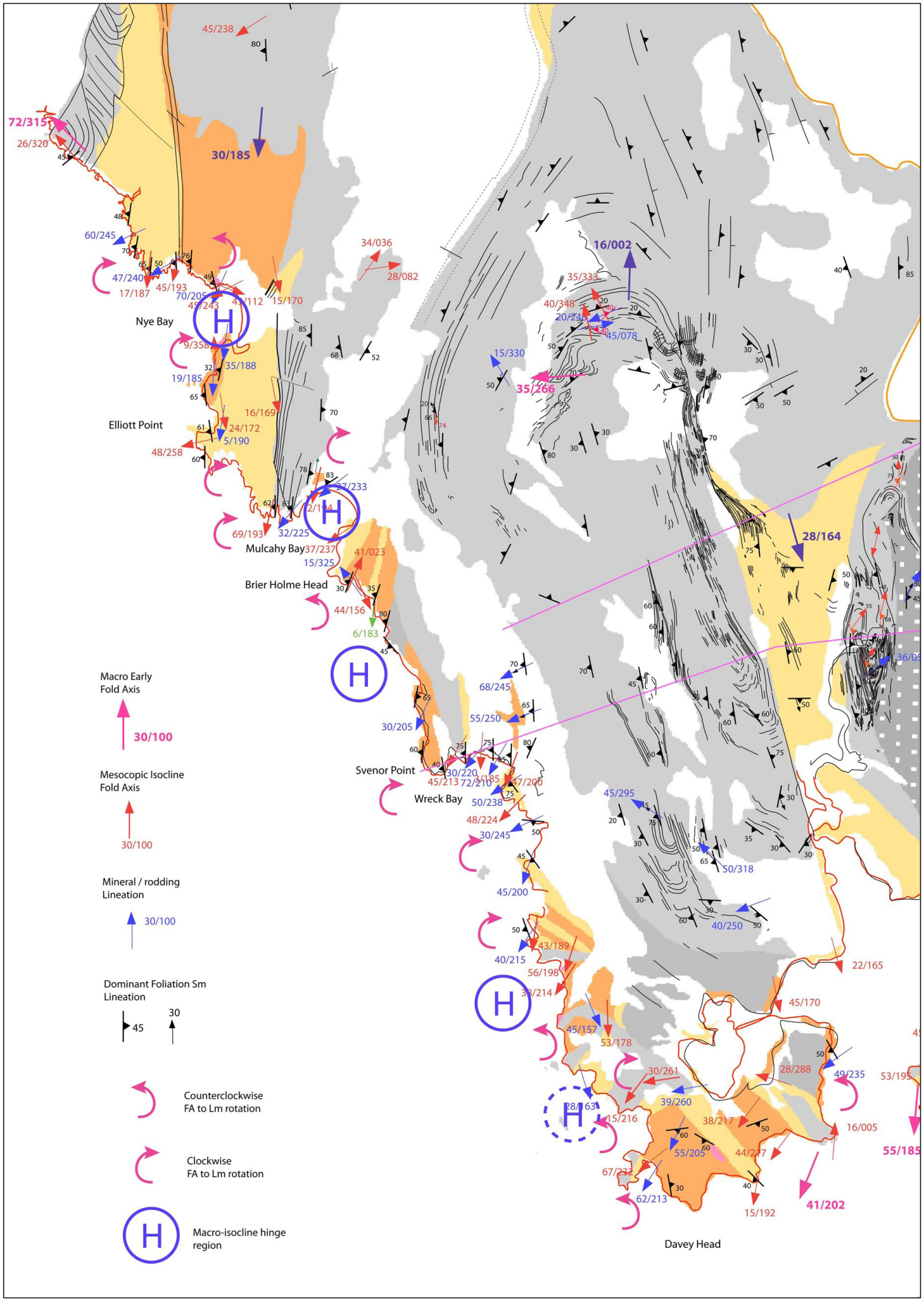

Figure 30. Map of Fold hinge-line vergence (after Alsop and Holdsworth, 2004) for the southwest high-grade coastal belt. The red arrows show the rotation direction of the early F1/F2 fold axis towards the mineral-stretching lineation (Lm) by closing the acute angle. A change from clockwise to counterclockwise rotation indicates a regional scale, macro-fold hinge position (H).

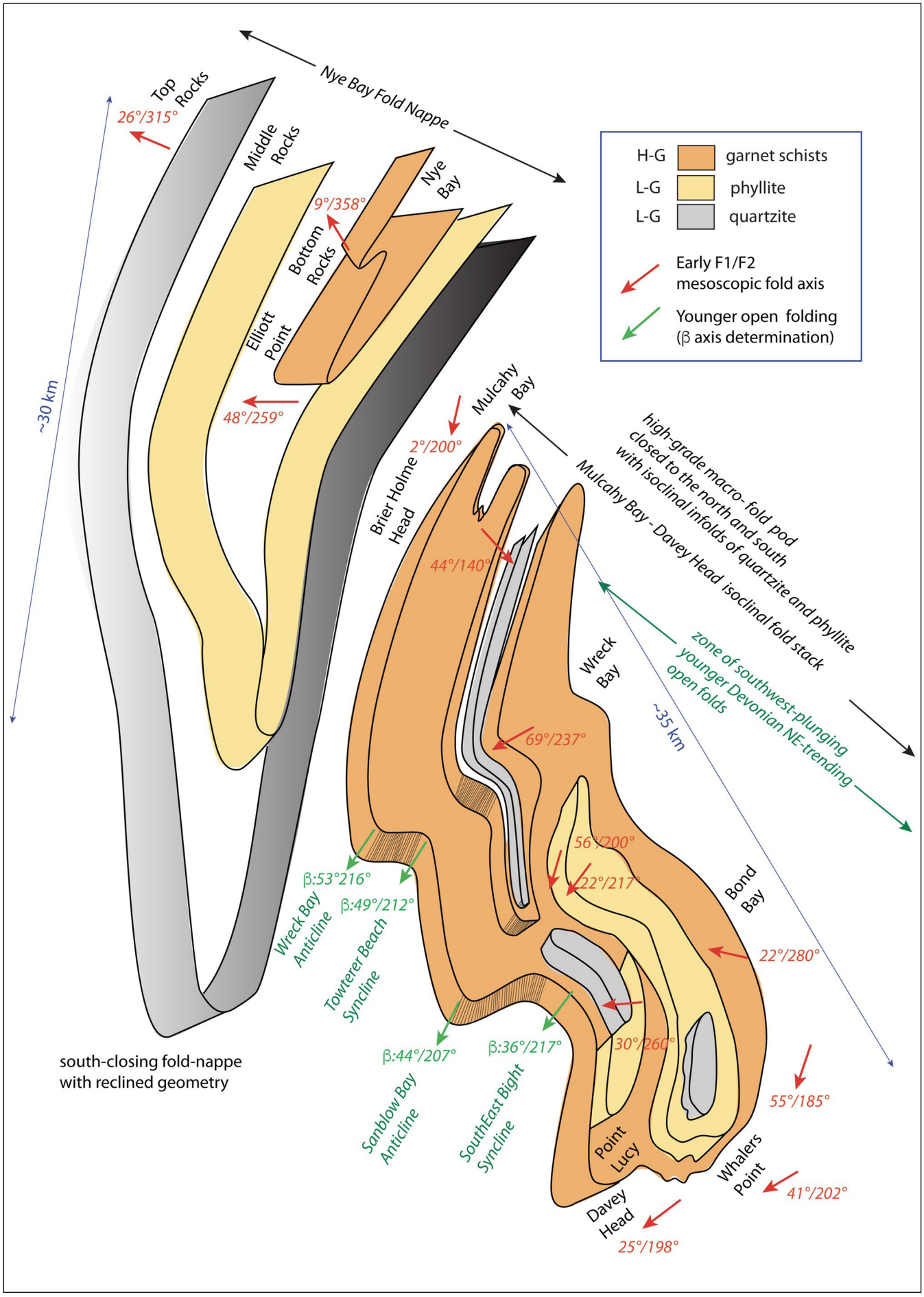

Figure 31. 3D schematic diagram of the Nye Bay Fold nappe and the Mulcahy Bay-Davey Head isoclinal fold stack.

The current macro-structure and regional structural geometry was established from form lines in the dominant foliation Sm and So/Sm (Figure 28), the mapped distribution of lithologies (Figure 29), and early isocline (F1/F2) fold axis and lineation Lm attitude data. Changes from clockwise to counter-clockwise rotation of early isocline axes towards the mineral lineation Lm occur at Nye Bay, Mulcahy Bay, Brier Holme Head-Svenor Point, and Sandblow Bay (Figure 30). These changes define the axial surface trace positions of major folds and match the positions of the axial surface traces of the inferred macro-folds (compare Figures 29 and 30).

4.3 De Witt-Propsting Mega Sheath Fold

The De Witt-Propsting mega-sheath fold (element 3, Figures 2 and 3) is the dominant fold structure in the Southern Tyennan domain (Gray and Vicary, 2022b). It has a distinct, elongated, ovate form in quartzite ridgelines expressed in the topography (Figure 32) and structural form lines (Figures 33 and 34). The shape is modified by later younger folds, 1) tightened by open, co-planar north-south trending Devonian folding that is superimposed on the north- and south-closing sheath shoulders (Figure 34), and 2) open southwest plunging and trending Devonian folds that fold the southwest corner of the sheath carapace in high-grade schists (Figure 34). The core of the mega-sheath is cut by the sub-vertical Payne Bay-Giblin Valley Fault (Figures 34 and 35).

A simplified DeWitt-Propsting sheath form is shown by the heavy blue form lines in Figure 35a with axial (Figure 36) and longitudinal (Figure 37) profiles providing the sectional geometry of the mega-sheath fold (compare with Figure 35b). The mega-sheath fold has two outcrop parts due to refolding and tilting on the limbs of the younger anticline (Figure 36), thus providing two oblique sections in map view. The largest profile section occurs on the western, west-dipping anticlinal limb (Figure 37), whereas the eastern limb provides the Davey River profile as the nose or eastern termination of the mega-sheath fold (see Section 4.4 following).

The De Witt-Propsting mega-sheath fold consists of three shells (Figure 38), an outer 1.5 km thick shell of alternating intensely banded So/Sm and platy to mylonitic quartzite with Sm dominant, a middle shell ~3.5 km in thickness constituting a folded domain of asymmetric isoclinal fold pairs in compositional layering So/Sm, and an inner shell or core of ~1.7 km thickness consisting of refolded isoclinal folds and multiple fabrics reflecting successive overprinting in progressive deformation. The inner shell projects across the younger anticline as the complexly deformed Davey River nose to the mega-sheath fold. The outer and middle shells do not have uniform character and thickness around the mega-sheath and appear discontinuous southwards along the De Witt Range (Figures 33 and 37). They show transitions from banded So/Sm to zones of platy quartzite due to braided development of high-strain zones. The outer quartzite is isoclinally in-folded with, and therefore interdigitates with, the overlying low-grade pelite and high-grade schist to form an isoclinal fold-stack as carapace to the mega-fold (Gray et al., 2022).

The De Witt-Propsting mega-sheath fold has cats-eye-fold sheath geometry with 1) an ellipticity ratio (R') of the outer ellipse (Ryz) to the inner ellipse (Ry'z') of 0.81 (i.e. R'<1) where 2) Ryz=2.57 and Ry'z'=2.97 such that Ry'z'>Ryz, and 3) the shell thickness ratio (Tyz=Ty/Tz) varies from 2 to 2.6. The cats-eye sheath form is indicative of folding within a simple or general shear deformation (Alsop and Holdsworth, 2006).

Unfolding or removing the effects of the younger anticlinal fold (Figure 39) enables reconstruction of the mega-sheath fold to give a projected sheath length ('x' dimension) of ~20 km, a maximum width ('y' dimension) of ~29 km, an apical angle of 50° and an interlimb angle of 10° (Figure 40).

4.4 Davey River Sheath Nose

The Davey River elongated, S-shaped, sinuous quartzite ridgeline (Figure 41a) has closed loop form with lateral pinched, fold-nose terminations typical of a sheath-like 'tectonic fish' (Figure 41b). It is defined by two sets of isoclinal macro-folds that are coaxially refolded about a northeast plunging fold axis (Figure 41c). The Davey River fold system is the interpreted east-plunging nose of the De Witt-Propsting mega-sheath fold folded across the Davey Creek Anticline (Figure 39) (Gray and Vicary, 2022b). The "nose" has an unfolded length ('y' dimension) of ~12.5 km, a maximum map width of 1.7 km and therefore a true thickness ('z' dimension) of ~1.4 km (Figure 40).

The macro-geometry consists of two major, north-south trending, inclined plunging F2 folds that coaxially refold isoclinal F1 macro-folds (Figures 41b, 42 and 43). The closed formline patterns suggest the early isoclines (AST1) have doubly plunging sheath-like form refolded with a banana-like outcrop pattern by the north-south-trending macro-isocline set (Figures 42 and 43). Curved hingelines and intersection lineations at the outcrop scale (Figure 7 after Maclean and Bowen, 1971) reflect sheath-fold initiation at the meso-scale (Gray and Vicary, 2022b). The two defined early F1 macro-hinge zones contain F1 mesoscopic isoclinal folds within So/Sm (Figure 44) that are enveloped by zones of intense Sm (profile A-A', Figure 44h). Zones of platy to mylonitic quartzite (Figure 44d) also appear to envelope the broader early macro-hinges to constrain the pinched, lateral noses of these early folds (Figure 42).

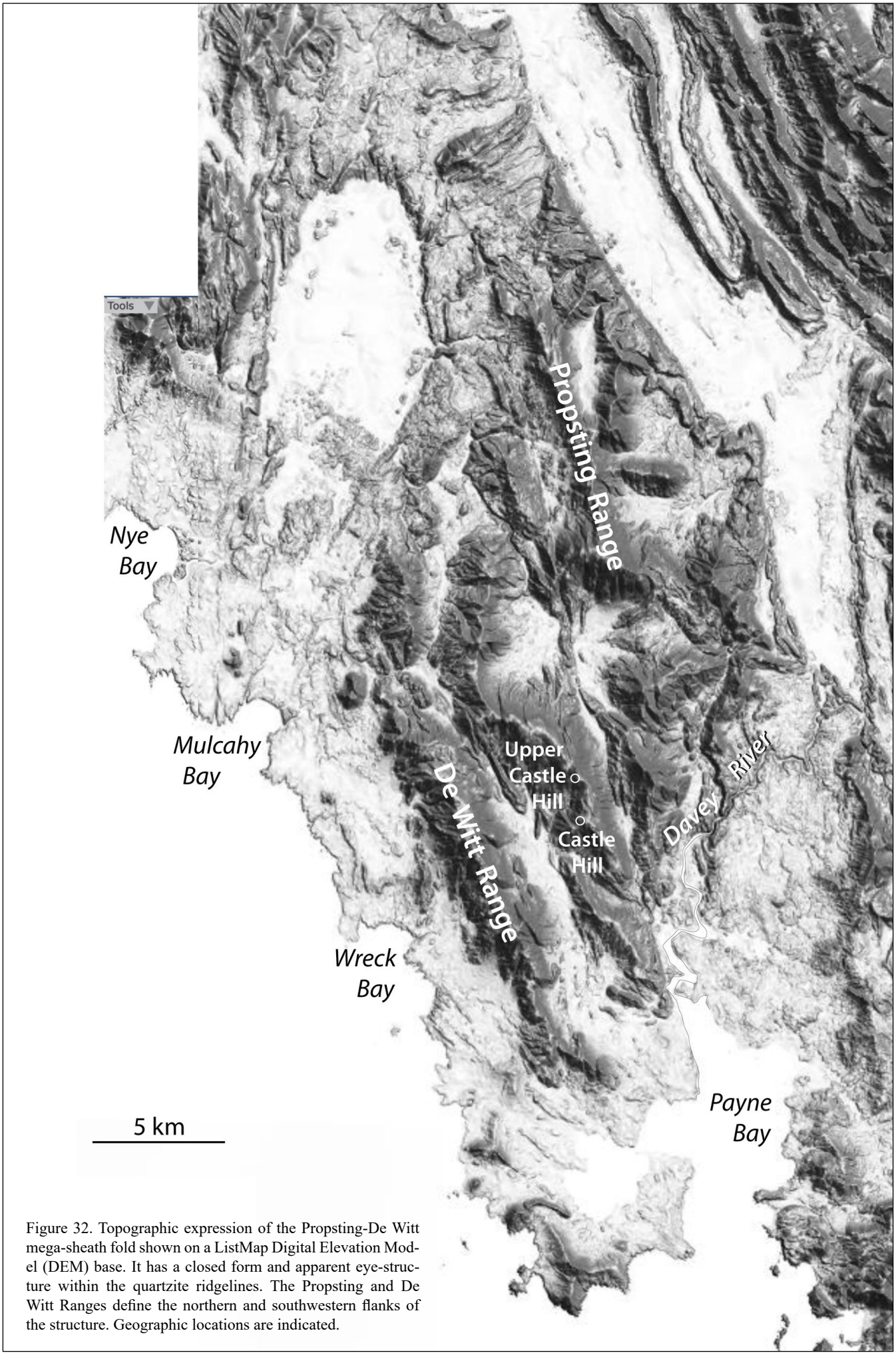

Figure 32. Topographic expression of the Propsting-De Witt mega-sheath fold shown on a ListMap Digital Elevation Model (DEM) base. It has a closed form and apparent eye-structure within the quartzite ridgelines. The Propsting and De Witt Ranges define the northern and southwestern flanks of the structure. Geographic locations are indicated.

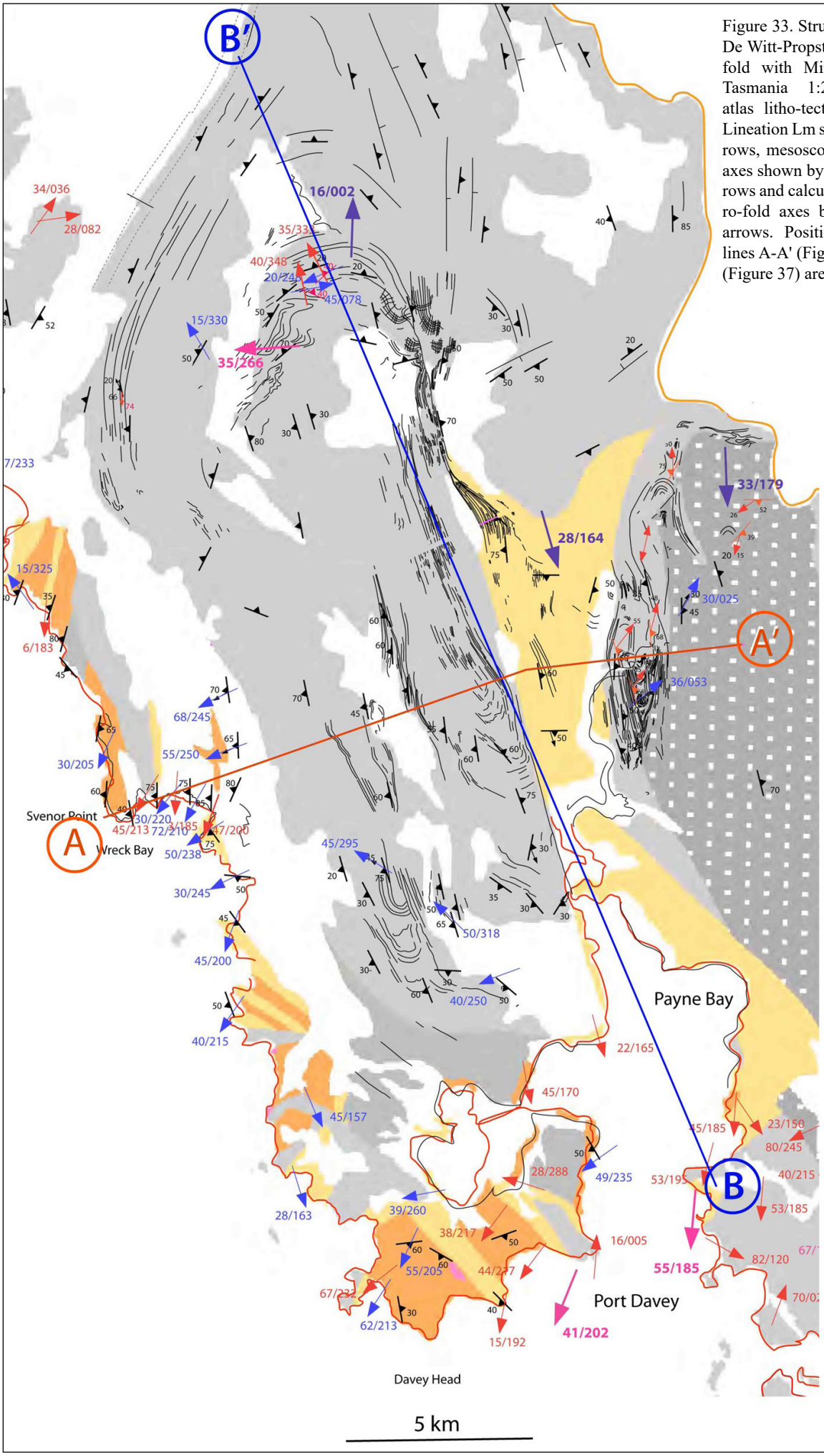

Figure 33. Structure map of the De Witt-Propsting mega-sheath fold with Mineral Resources Tasmania 1:250,000 digital atlas litho-tectonic map base. Lineation Lm shown by blue arrows, mesoscopic isocline fold axes shown by the red small arrows and calculated β axis macro-fold axes by the large red arrows. Positions of asection lines A-A' (Figure 36) and B-B' (Figure 37) are shown.

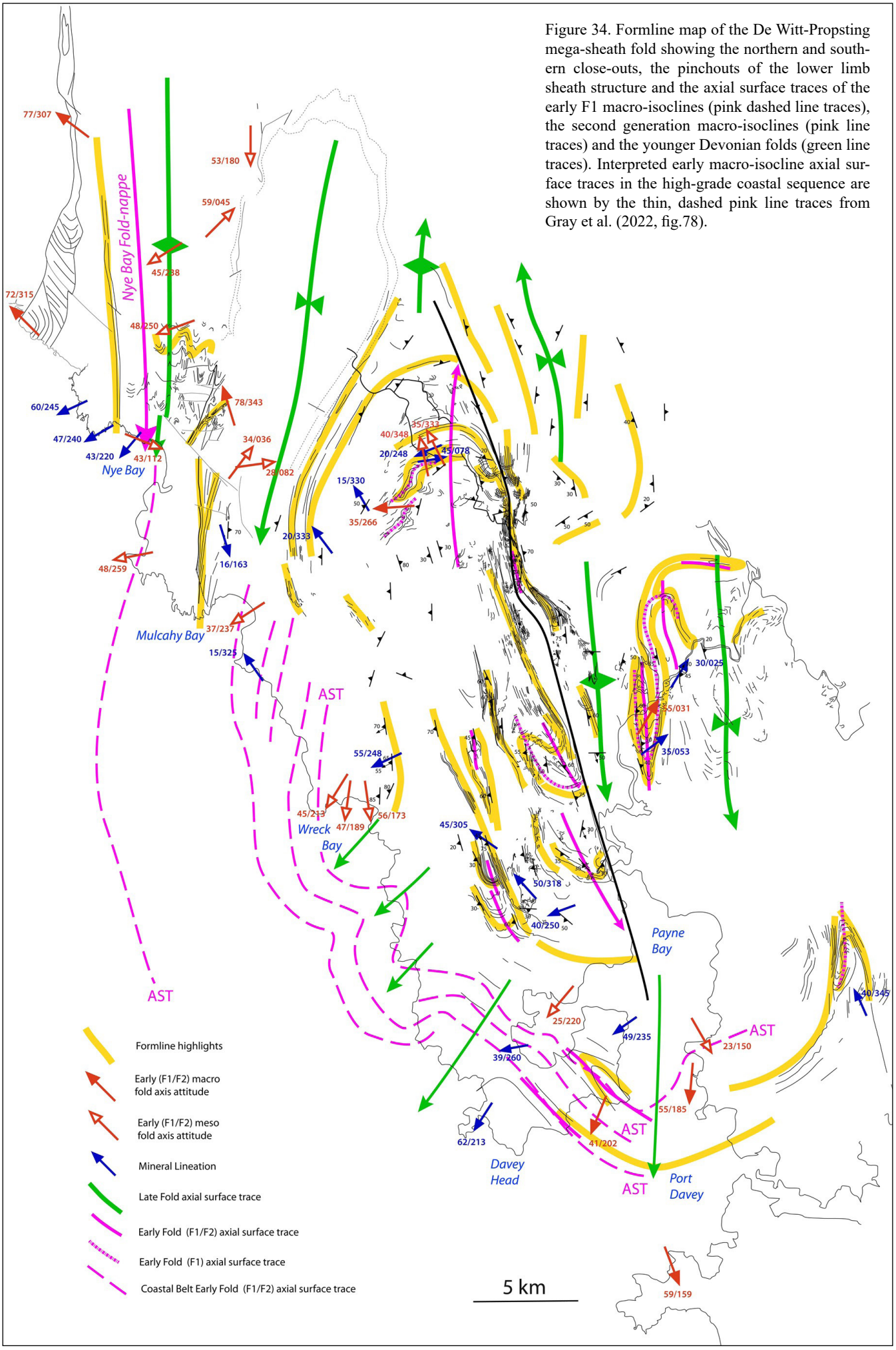

Figure 34. Formline map of the De Witt-Propsting mega-sheath fold showing the northern and southern close-outs, the pinchouts of the lower limb sheath structure and the axial surface traces of the early F1 macro-isoclines (pink dashed line traces), the second generation macro-isoclines (pink line traces) and the younger Devonian folds (green line traces). Interpreted early macro-isocline axial surface traces in the high-grade coastal sequence are shown by the thin, dashed pink line traces from Gray et al. (2022, fig.78).

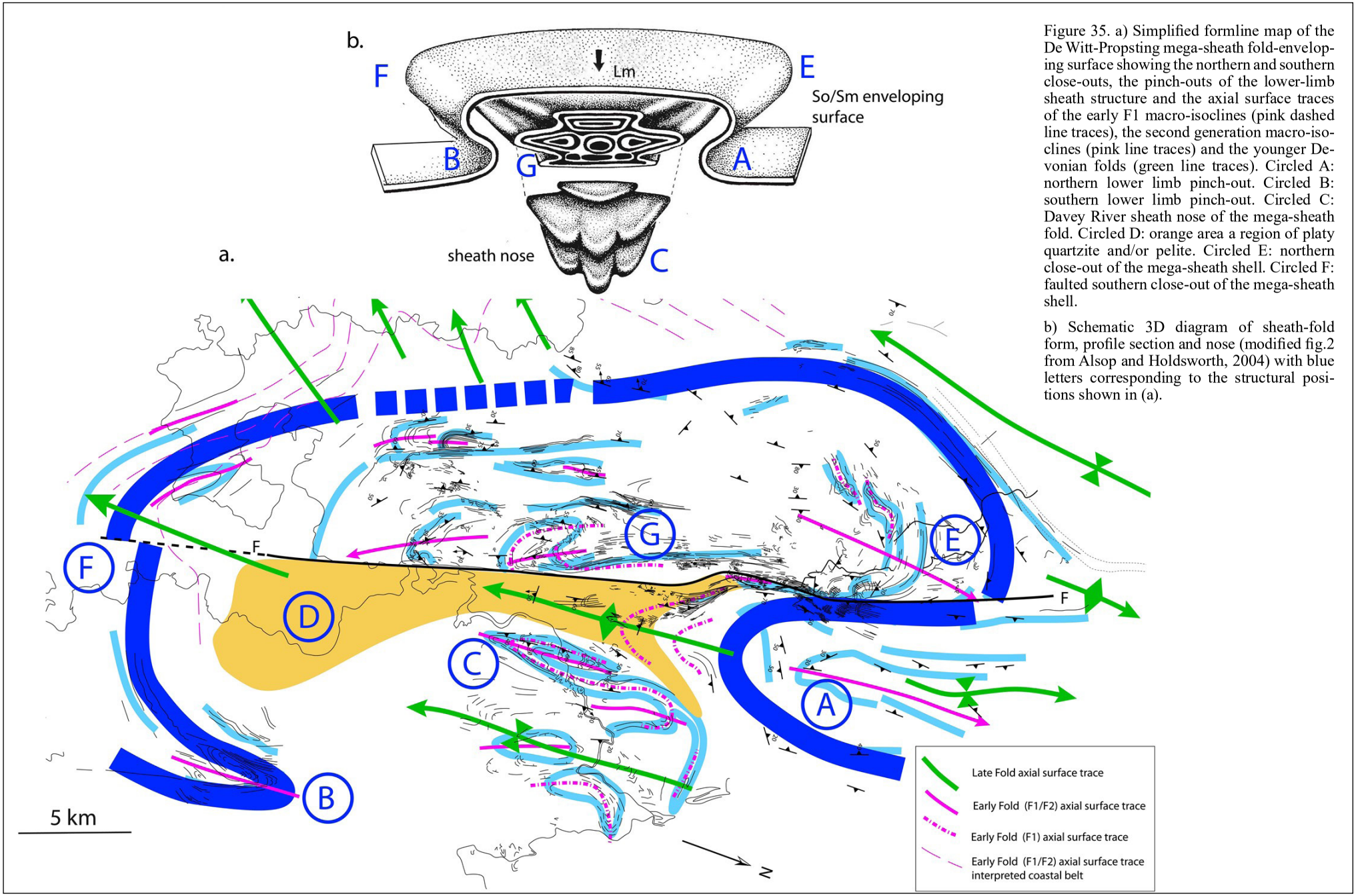

Figure 35. a) Simplified formline map of the De Witt-Propsting mega-sheath fold-enveloping surface showing the northern and southern close-outs, the pinch-outs of the lower-limb sheath structure and the axial surface traces of the early F1 macro-isoclines (pink dashed line traces), the second generation macro-isoclines (pink line traces) and the younger Devonian folds (green line traces). Circled A: northern lower limb pinch-out. Circled B: southern lower limb pinch-out. Circled C: Davey River sheath nose of the mega-sheath fold. Circled D: orange area a region of platy quartzite and/or pelite. Circled E: northern close-out of the mega-sheath shell. Circled F: faulted southern close-out of the mega-sheath shell.

b) Schematic 3D diagram of sheath-fold form, profile section and nose (modified fig.2 from Alsop and Holdsworth, 2004) with blue letters corresponding to the structural positions shown in (a).

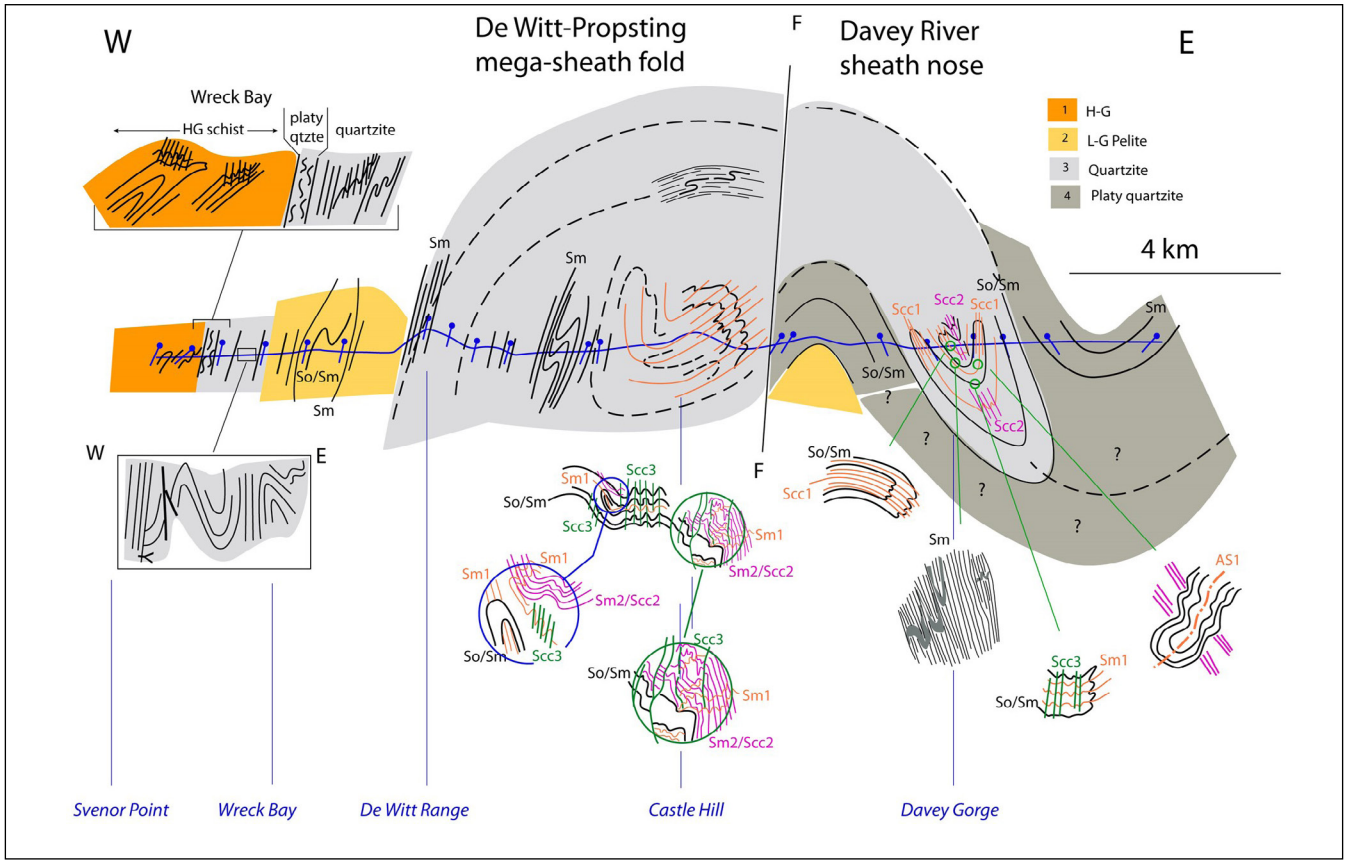

Figure 36. East-west structural section (section line A-A' shown in Figure 33) across the De Witt-Propsting mega-sheath fold. This is regional structural profile P2 shown in Figure 24. It approximates the x-z plane of the sheath fold. The diagram also shows local structural/fabric relationships within the quartzite containing the mega-sheath fold (grey unit) and the structural relationships for the western, homoclinally west-dipping carapace to the mega-sheath fold. bright orange: H-G schist. grey: L-G quartzite. yellow-orange: L-G pelite; dark grey: schistose quartzite.

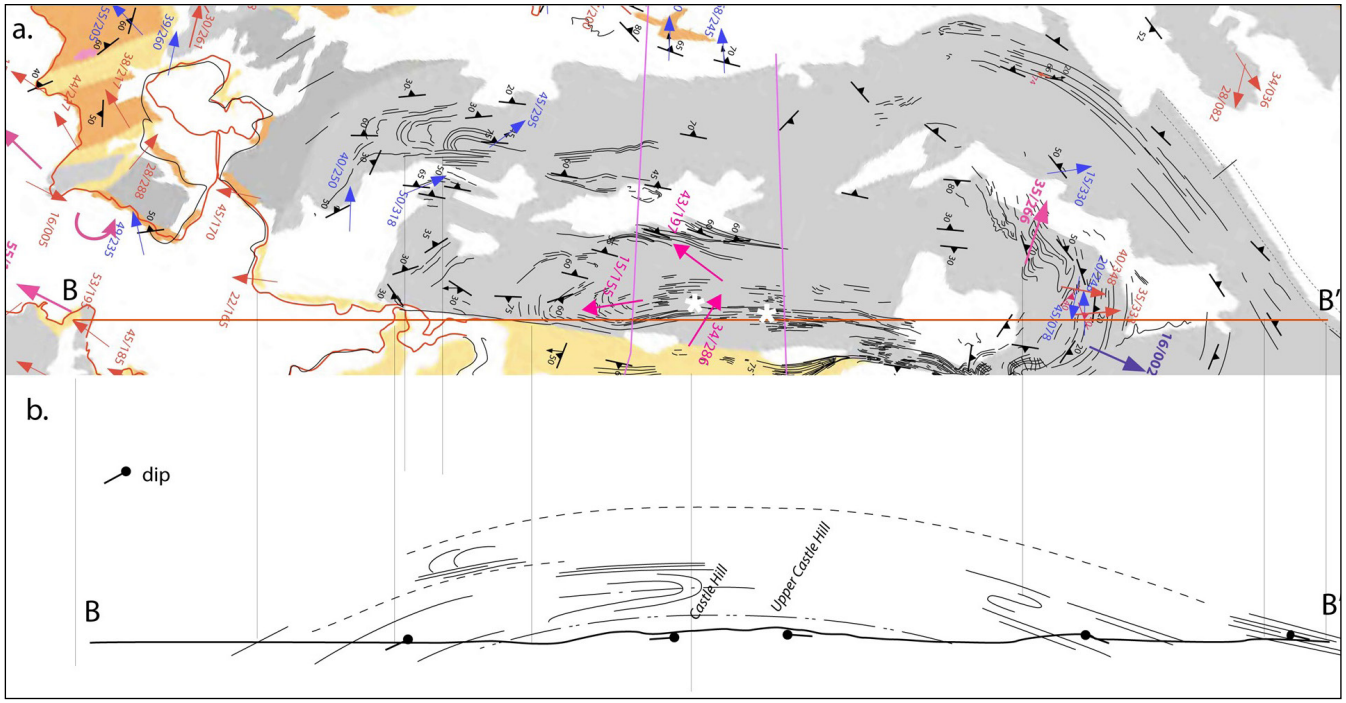

Figure 37. North-south long structural section B-B' (looking east) from Port Davey to the Giblin River Valley (340° profile alignment) across the De Witt-Propsting mega-sheath fold. a) Structure map segment showing form lines, structural data and position of the section line (see also Figure 33). is regional structural profile P3 shown in Figure 24 Structure map with structural data showing foliation Sm (black strike/dip symbol), lineation Lm (blue arrows), fold axis (red arrows) attitudes. Bright orange: H-G schist. Grey: L-G quartzite. Yellow-orange: L-G pelite.

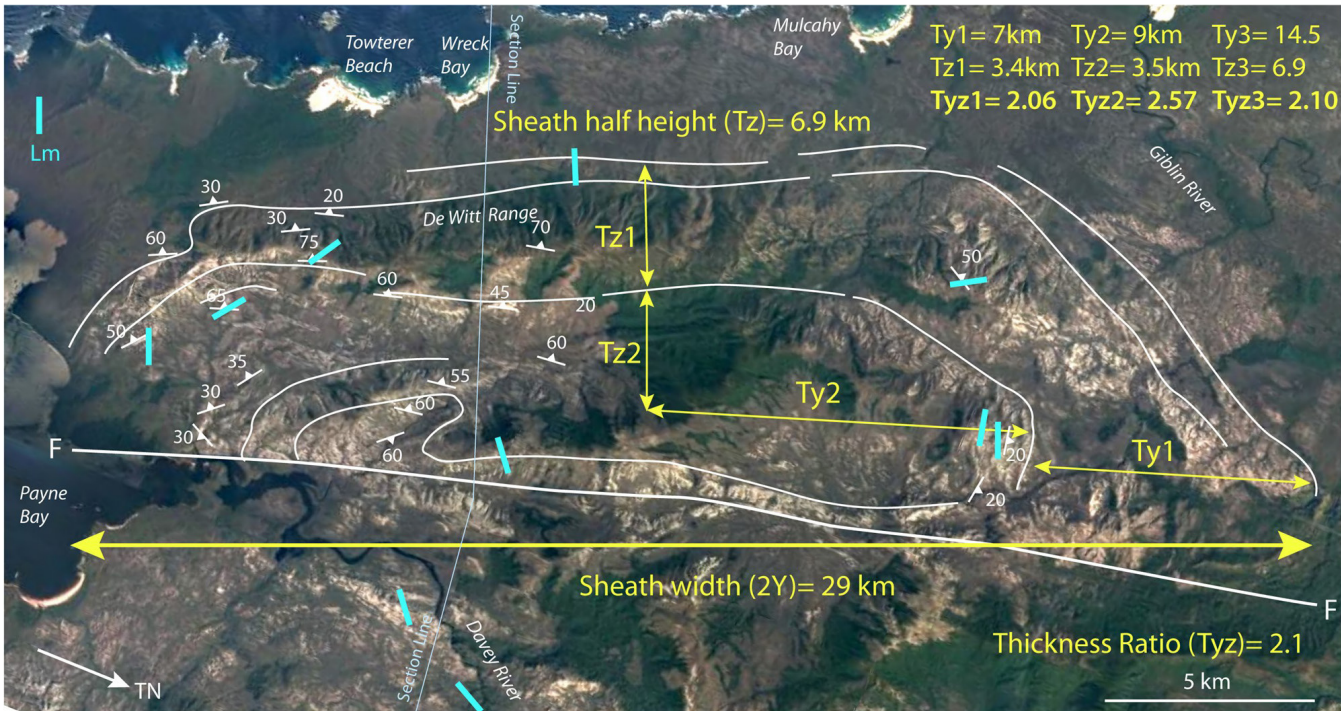

Figure 38. Approximate down-plunge profile view of the De Witt-Propsting mega-sheath fold on a Google Earth image base. Form lines in So/Sm (white line traces) define the shape, sheath geometry and the inner and outer ellipses of the mega-sheath fold. Thickness measurements Ty and Tz are shown for the outer (designated 1) and inner ellipses (designated 2). Note the sheath is cut by a sub-vertical fault on the eastern side (lower part of the Google image) shown by the white line trace near the yellow arrowed length dimension line. Note the Google image has been rotated 105° clockwise to view the sheath in an approximate profile plane. The coast is at the top of the image with beach areas of Mulcahy Bay (top centre right), Wreck Bay and the dunes of Towterer Beach (top centre left) visible.

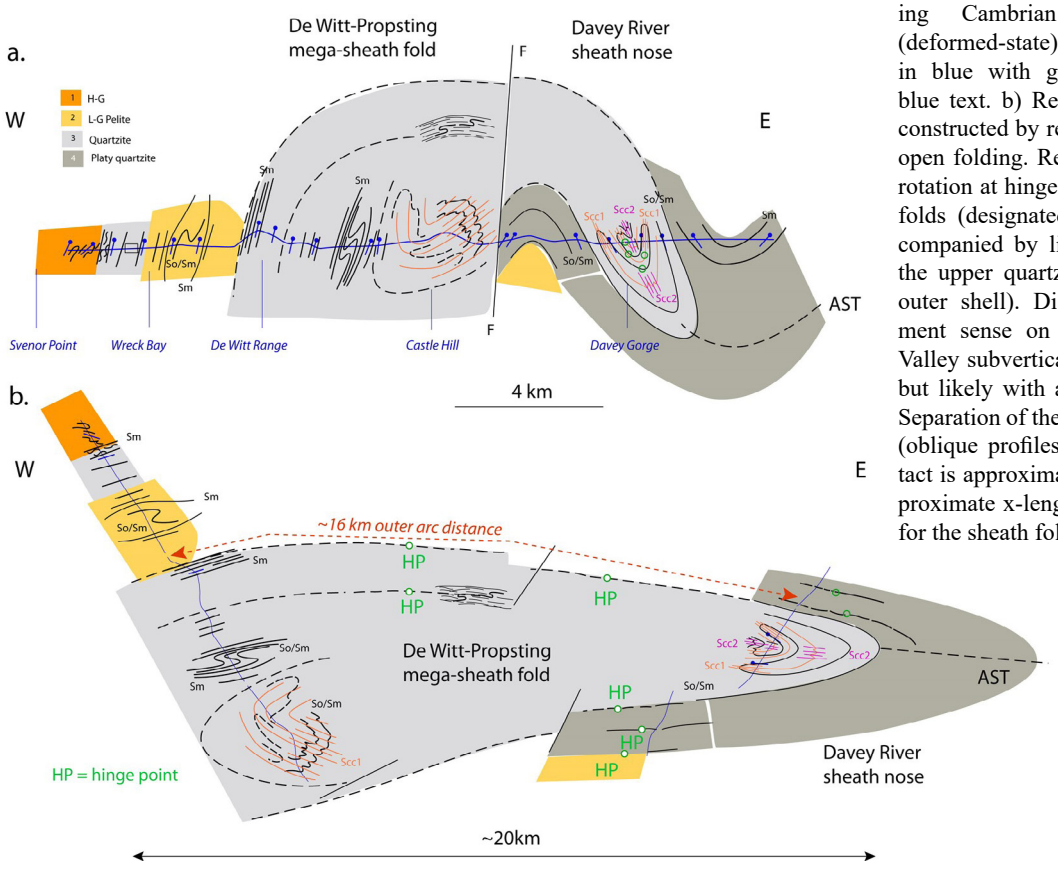

Figure 39. De Witt-Propsting mega-sheath longitudinal (x-z plane) profile restoration. a) East-west cross-section showing the folded and faulted, east-closing Cambrian sheath fold-nappe (deformed-state). Topographic surface in blue with geographic locations in blue text. b) Restored fold-nappe form constructed by removal of the Devonian open folding. Restoration was by hinge rotation at hinge points of the Devonian folds (designated by the green H) accompanied by line-length balancing of the upper quartzite contact (uppermost outer shell). Displacement and movement sense on the Payne Bay-Giblin Valley subvertical fault (F) is unknown, but likely with a west-side component. Separation of the now rotated map views (oblique profiles) along the upper contact is approximately 16 km with an approximate x-length dimension of 20 km for the sheath fold-nappe.

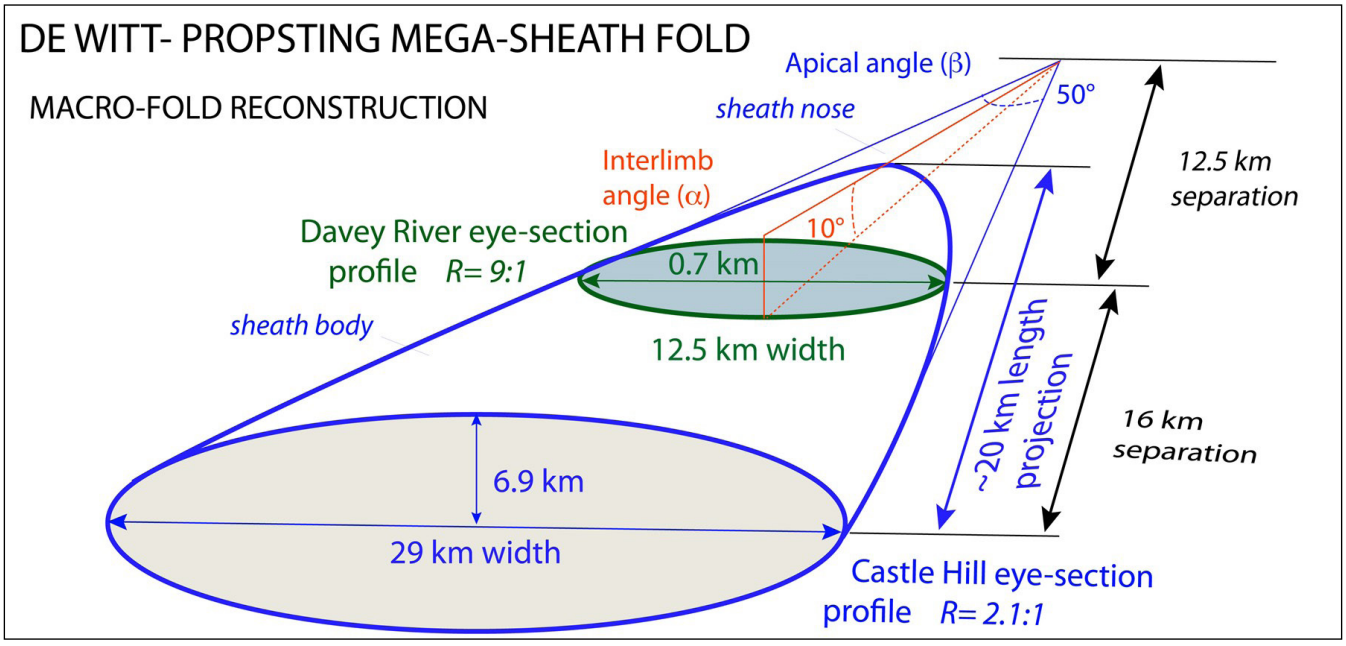

Figure 40. Reconstruction of the shape of the De Witt-Propsting mega-sheath form using 1) the outer shell dimensions from the Castle Hill eye-section (khaki ellipse) and the Davey River "eye"-section (green ellipse), and 2) the section spacing of ~16 km based on the unfolded longitudinal x-z section in Figure 21. These give a projected length (x direction) of ~20 km, an apical angle of 50° and an interlimb angle of 10° for the proposed mega-sheath fold.

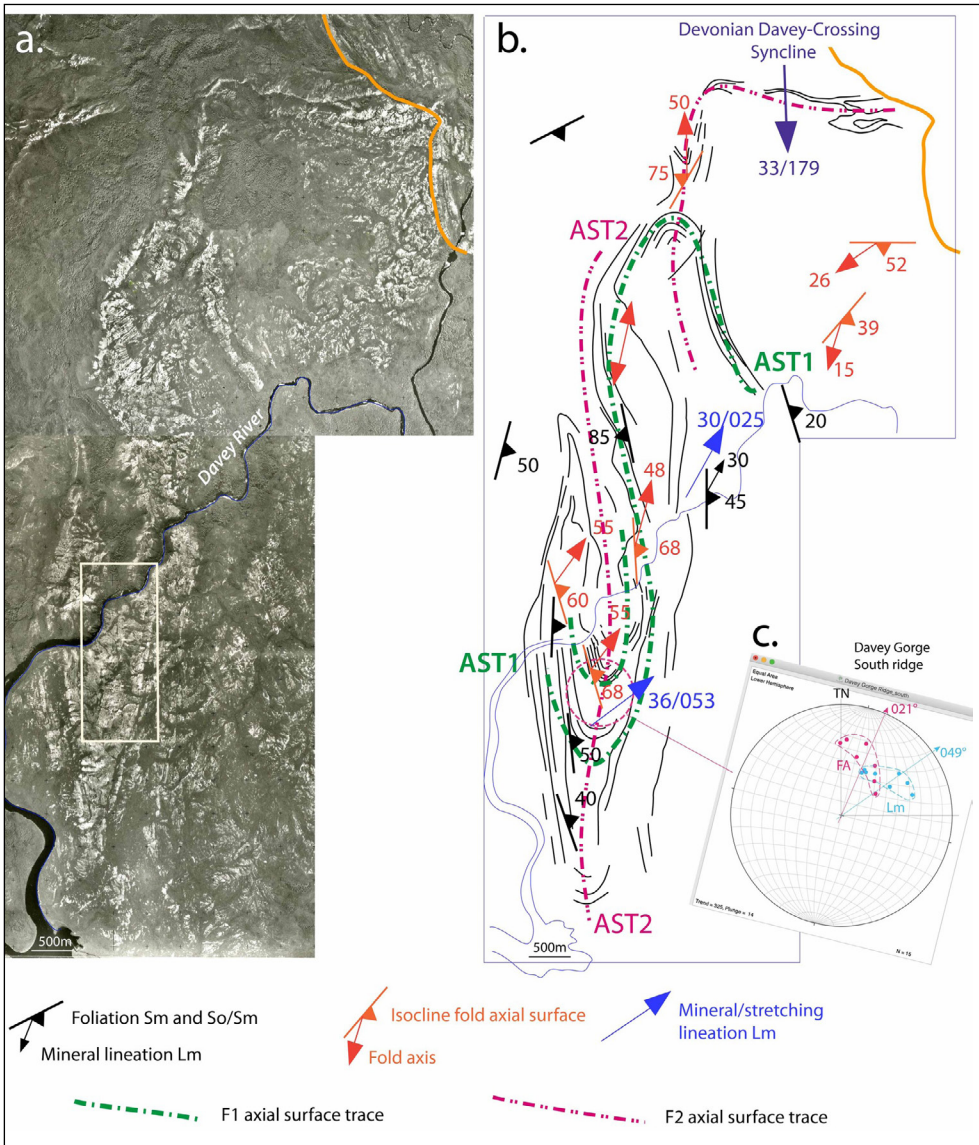

Figure 41. The Davey River fold system as the interpreted nose of the De Witt-Propsting mega-sheath fold.

a) Aerial photograph-mosaic of the showing tapered fold-closure terminations and apparent closed loop form suggestive of curved sheath-like hinges. The fold system is transected by the Davey River and extends from Brooks Reach in the south to Davey Creek in the north. The position of Davey Gorge is within the white rectangle (See Figure 42).

b) Structure map with So/Sm formline traces (black lines), structural data and F1 and F2 fold axial traces.

c) Stereonet showing plotted meso-isocline fold axis FA (pink dots) and lineation data Lm (blue dots) collected by the authors on the ridgeline south of Davey Gorge. The vector mean azimuths are shown for the fold axis (pink arrow) and lineation (blue arrow) data requiring clockwise fold-hingeline vergence (see Section 2, Gray and Vicary, 2022b).

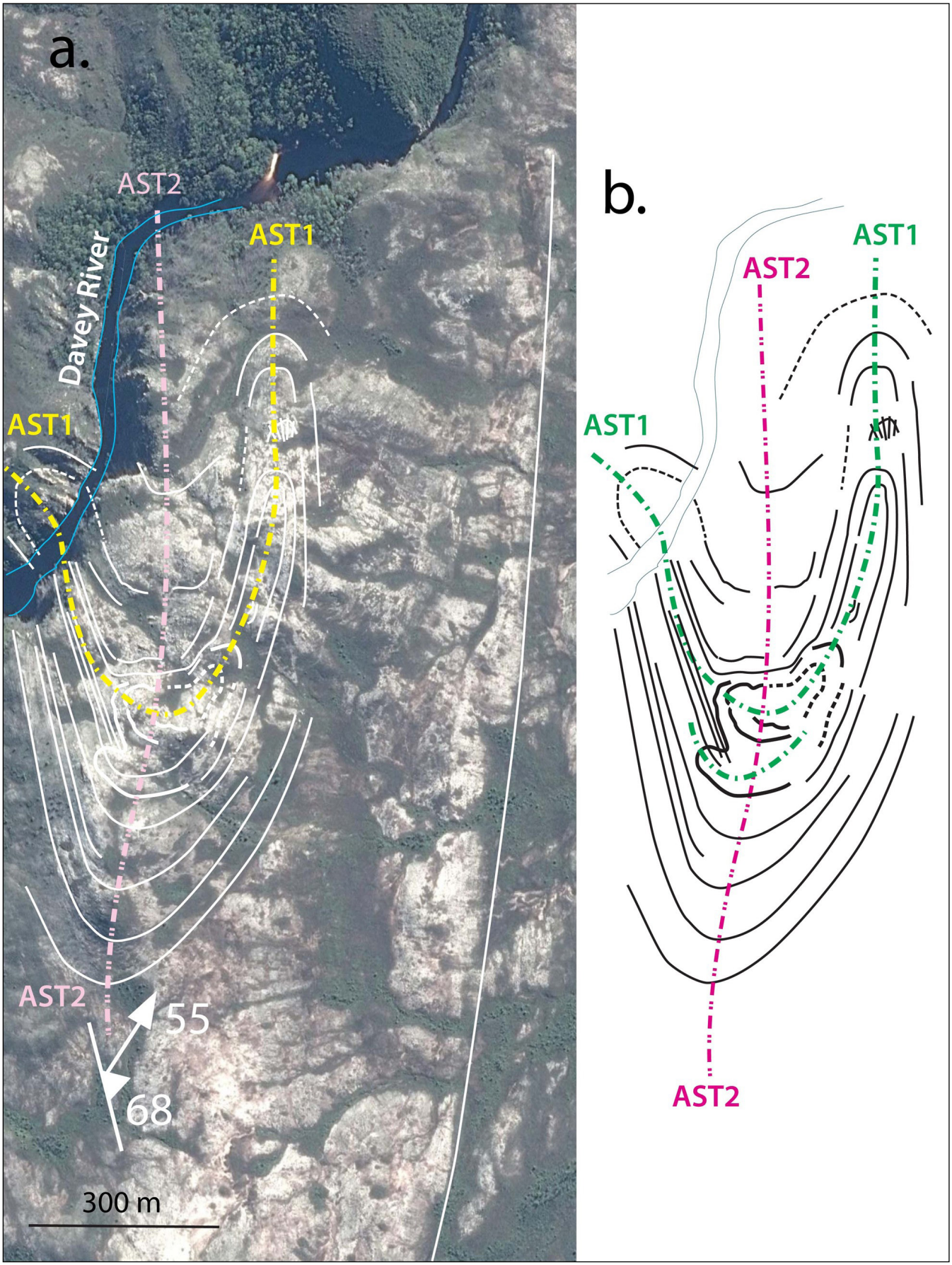

Figure 42. Detailed structural So/Sm and Sm formline interpretation of the northern part of the ridgeline south of Davey Gorge. Google satellite image as base. b) F1 and F2 fold interference pattern with axial surface traces shown as AST1 (green dashed trace) and as AST2 (pink dashed trace). Outcrop traces suggest the early isocline (AST1) has doubly plunging sheath-like form refolded with a banana-like outcrop pattern by the north-south-trending macro-isocline set. The location of the map is shown by the white rectangle in Figure 41.

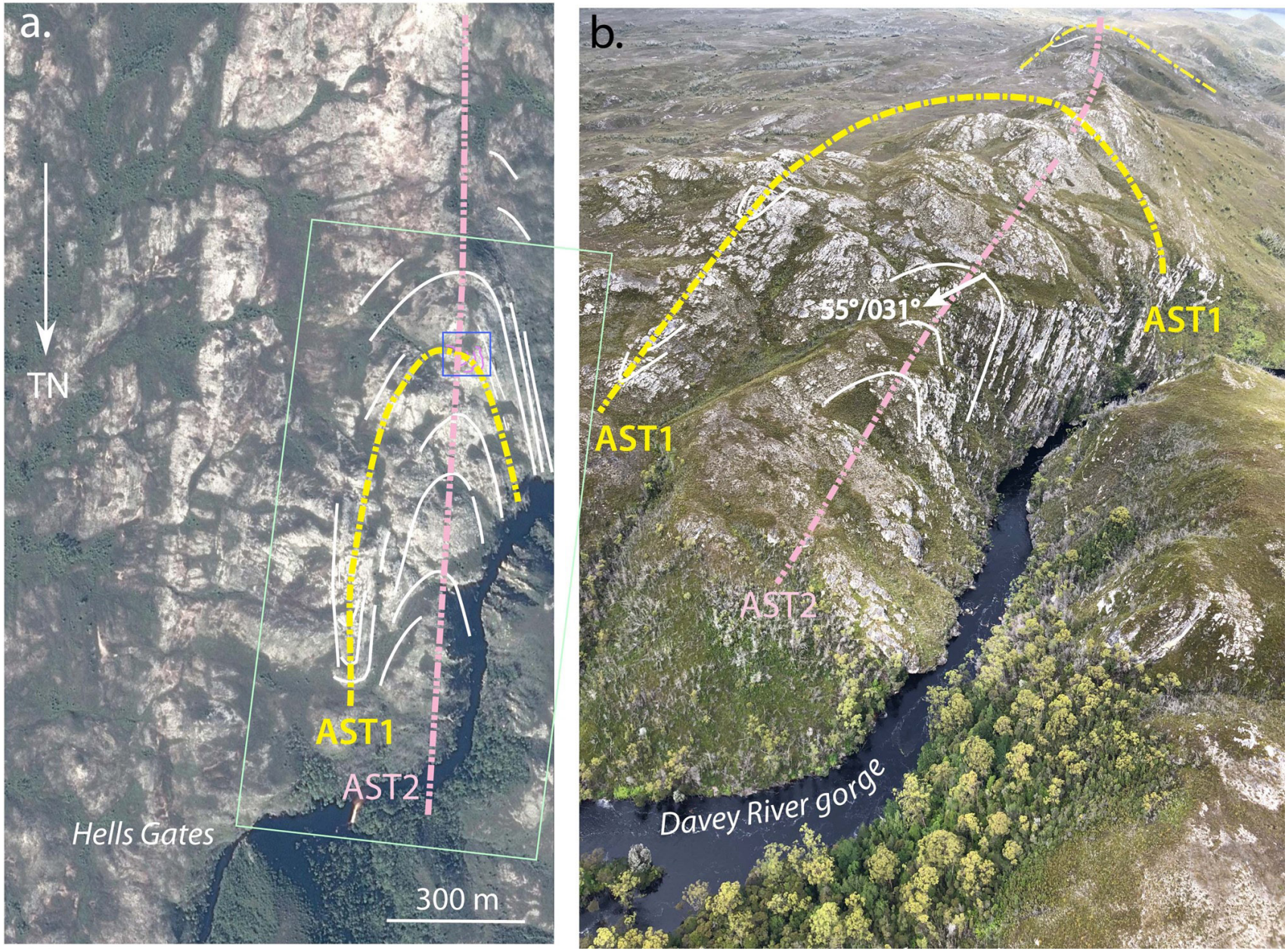

Figure 43. Structural interpretation of ridgeline south of Davey Gorge. a) Google image oriented to match the photo in (b). b) Photo of ridgeline south of Davey Gorge from helicopter. View is looking to the south. The photo location is given by PP3 on Figure 56 in Gray and Vicary (2022b). Fold plunge is 55°/031°. Formline interpretation shows compositional banding So/Sm and Sm (white line traces) and axial surface traces of inferred two sets of isoclinal macro-folds. AST1 trace: yellow dashed line. AST2 trace: pink dashed line.

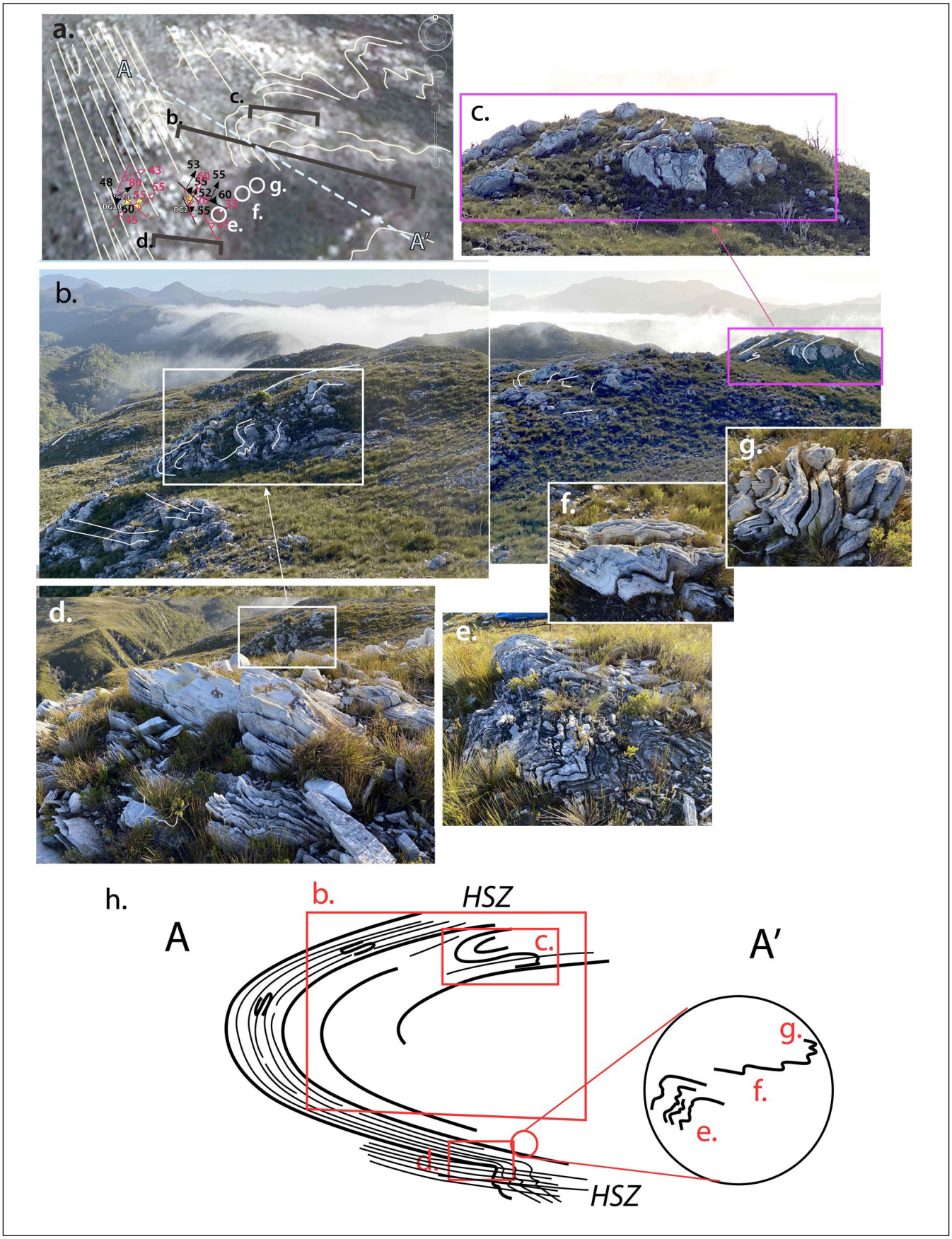

Figure 44. Composite Photo profile of north-closing, earliest-phase (F1) isoclinal macro-fold on ridge above Davey Gorge. The photo-stitch profile location is given by PP4 on Figure 56 in Gray and Vicary, 2022b) . a) Formline interpretation structure map on Google image base. Positions of photos and the photo profile in (b) are shown. b) Photo-stitch profile of hillside providing an oblique view of the early macro-fold hinge, with a third-order recumbent fold in hillside (upper right). c) Enlargement of recumbent fold shown in (b). d) Platy quartzite typical of the high-strain zone bounding the hinge zone on the recumbent fold lower limb. e), f) and g) are photos of mesoscopic folds transitional from the hinge into the lower limb. h) Sketch profile A-A' show the approximate form of the early fold closure with red outlines indicating the positions of the photos and photo-profile above.

The revised geometry of the Davey River fold system as the interpreted sheath nose of the De Witt-Propsting mega-sheath fold is presented in a schematic 3D diagram (Figure 45). It shows the northeast-plunging, bulbous form with pinched north and south lateral terminations that give the pod-like, tectonic "fish" (MacLean and Bowen, 1971) or augen geometry. Inset sketches show the fabric and refolding relationships at various positions through the macro-fold system. These support the presence of early F1 recumbent folded zones that are refolded by the north-south trending isoclinal folds. The F2 macro-isoclines are dominant and control the sigmoidal outcrop pattern.

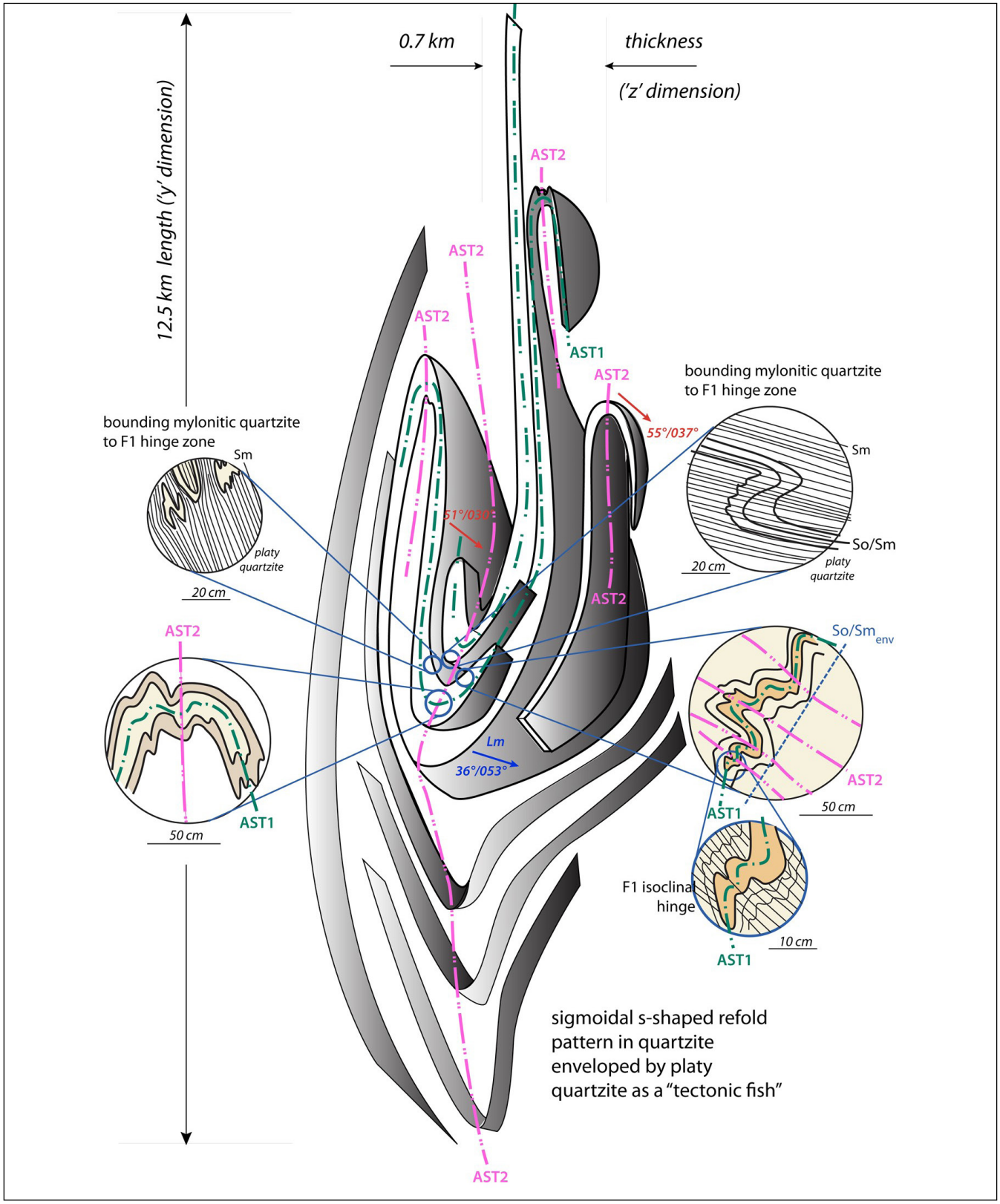

Figure 45. Schematic 3D diagram illustrating the internal structure of the tectonic "fish" or augen that defines the nose of the De Witt-Propsting mega-sheath fold. Inset circled diagrams are schematic sketches of key fabric elements and relationships used to refine the geometry of the mega-sheath fold nose (see Gray and Vicary, 2022b). Green dashed-dot lines are F12 axial surface traces (AST). Pink dashed-double dot lines are F2 axial surface traces (AST).

4.5 South West Cape Mega-Sheath Fold

The South West Cape mega-sheath fold (element 5, Figures 2 and 3) is en echelon with the De Witt-Propsting mega-sheath fold as part of a regional-scale oppositely closing fold-pair (Gray and Vicary, 2022b). It has a minimum length ('y' sheath dimension) of 25 km and a half-width ('z' sheath dimension) of 8 km (Figure 46). By closing out a possible oval or eye-shaped form of the inner shell it is likely that half of the mega-fold is offshore. Map geometry is typical of a regional-scale mushroom-style Type 2 fold interference pattern where F1 macro-isoclinal folds are coaxially refolded by upright, north-south trending, isoclinal F2 macro-folds (Figure 47). These are the same geometrical relationships seen in the inner shell of the De-Witt-Propsting fold and the Davey River sheath nose. Component folds in the South West Cape mega-fold have inclined plunging to reclined geometry with west-plunge (Figure 47) in contrast to the northeast plunge in the Davey sheath nose, a plunge-change related to the younger Devonian refolding.

The lower limb of the South West Cape mega-sheath fold transitions structurally into a recumbent, isoclinal fold pair consisting of an upper southwest-closing recumbent macro-fold overlying a northeast closing macro-fold. This recumbent fold pair relationship holds for the entire region east of Bathurst Harbour to the Arthur Range, including the Ray Range, Mt Norold and the Spiro Range with an areal extent of 450-500 square kilometres.

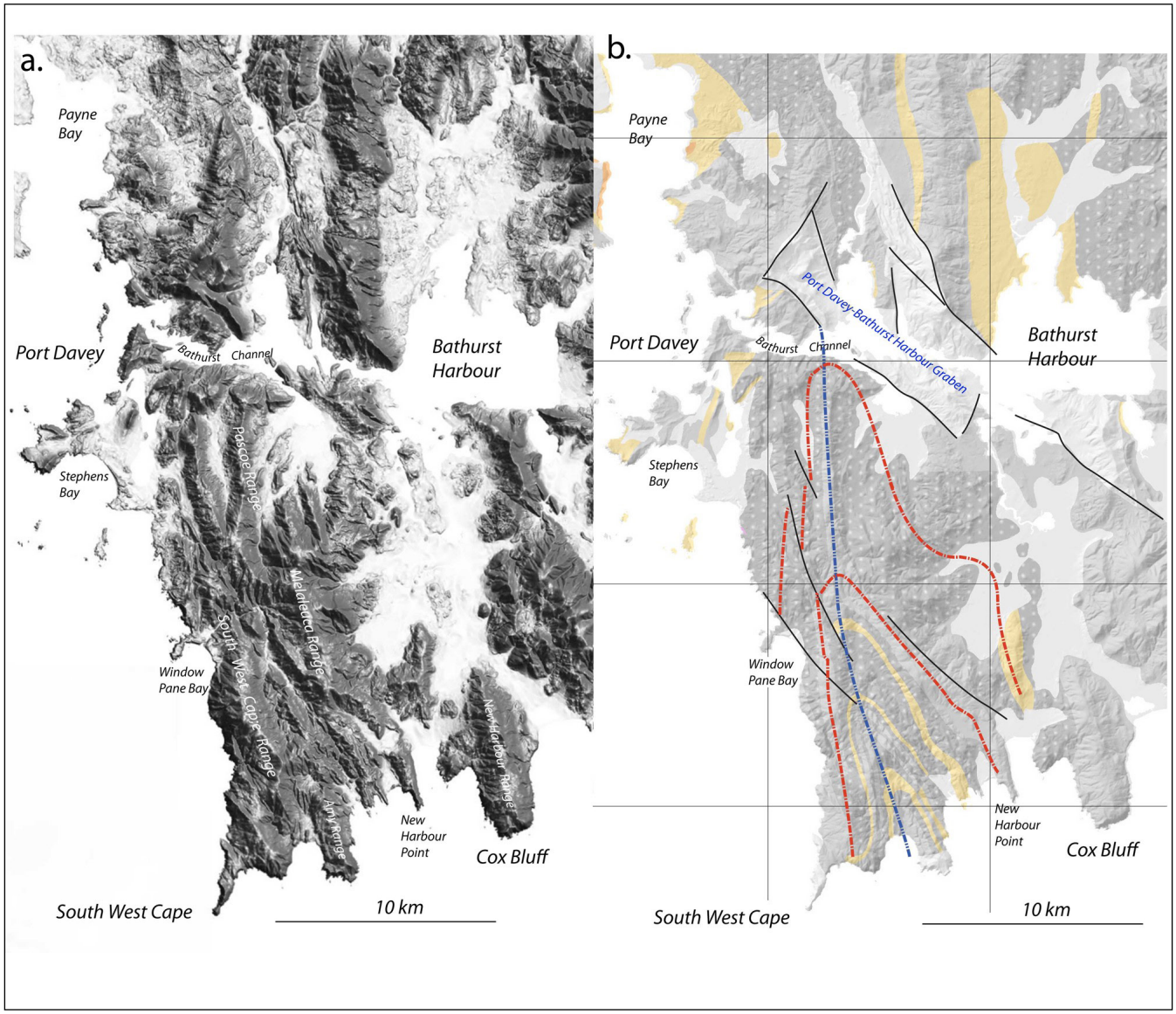

Figure 46. Digital Elevation Model (DEM) of the South West Cape area. a) Tasmanian ListMap greyscale DEM showing the southwest topography with ranges and coastline, extending north to Payne Bay and east to Cox Bluff and Bathurst Harbour. b) Litho-tectonic map units draped on the DEM showing a regional-scale, macro-fold centred on Amy Range and Wilson Bight. The litho-tectonic map base is from the Mineral Resources Tasmania 1:250,000 digital atlas. The map units are: 1) pale orange: low-grade pelite, 2) grey: low-grade quartzite, 3) dark grey with white stipple: low-grade platy and/or schistose quartzite, and 4) light grey: younger sequence of turbidites and conglomerate. Red dashed-dot line traces: F1 macro-isocline axial surface traces. Blue double dot dashed line trace: F2 macro-isocline axial surface trace.

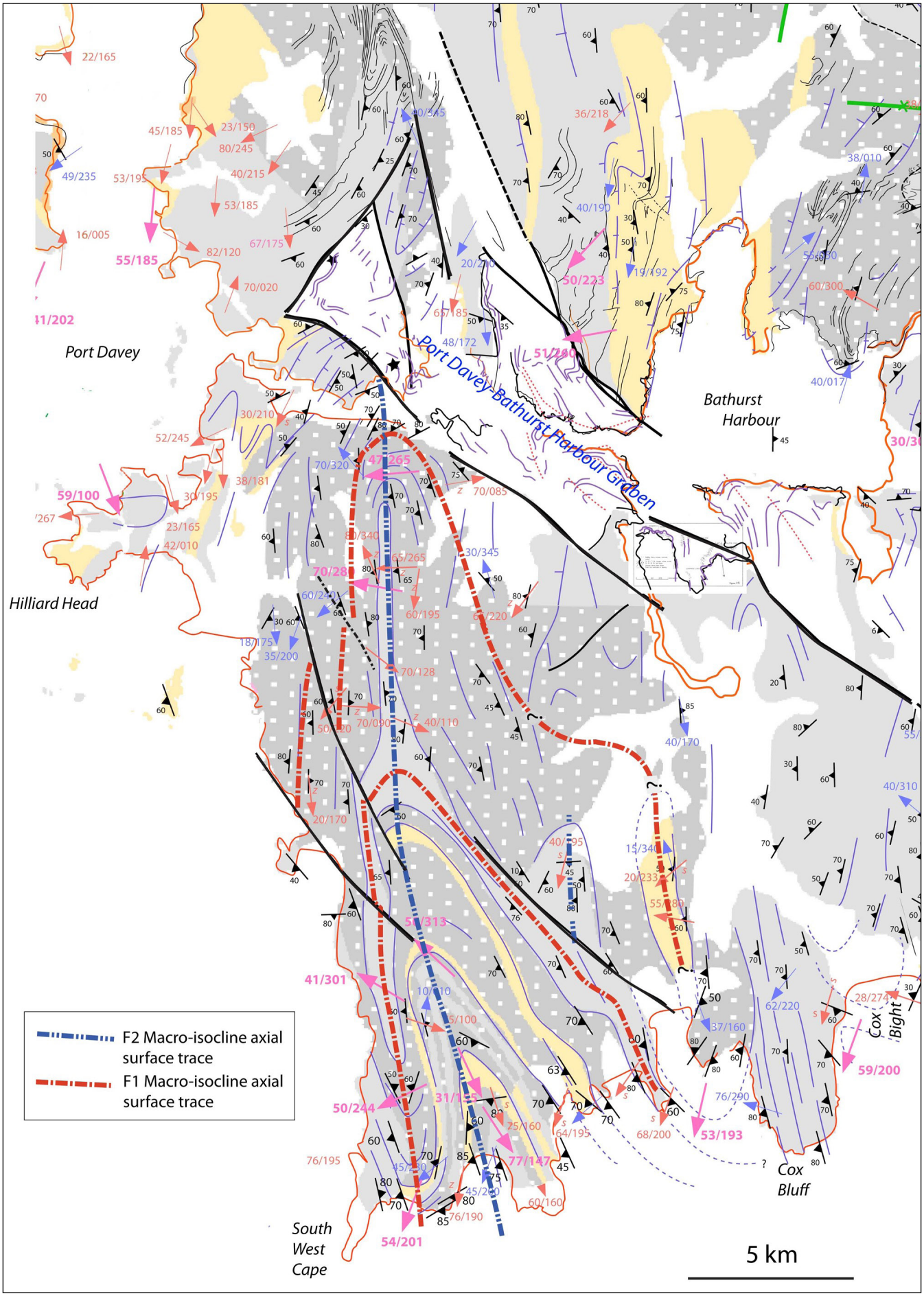

Figure 47. Detailed structure map of the South West Cape mega-fold system showing black strike and dip attitudes for the So/Sm and Sm foliation. Blue arrows are plunges and plunge directions of the mineral lineation Lm. The small red arrows are measured mesoscopic isocline fold axis data. Larger pink arrows are calculated macro-fold axis data. The axial surface traces for the large regional scale early (F1) isoclinal folds are shown by the red dot-dashed lines and the F2 macro-isocline axial surface trace by the blue dot-dashed line. Faults are shown by the thick black line traces.

Section construction (Figure 48) involved 1) control by the So/Sm attitudes close to the section line plotted as dip markers with either true dip or apparent dips (Figure 48a), combined with 2) the map pattern with plunge projections (Figure 48b), and 3) the litho-tectonic unit distribution. Plunge reversals along with marked changes in plunge, as well as steep plunges in places made the section construction difficult. Plunge changes from end to end of the macro-fold closeouts (Figure 49) supports the sheath-like character but with fold segments approaching reclined geometry with west plunge.

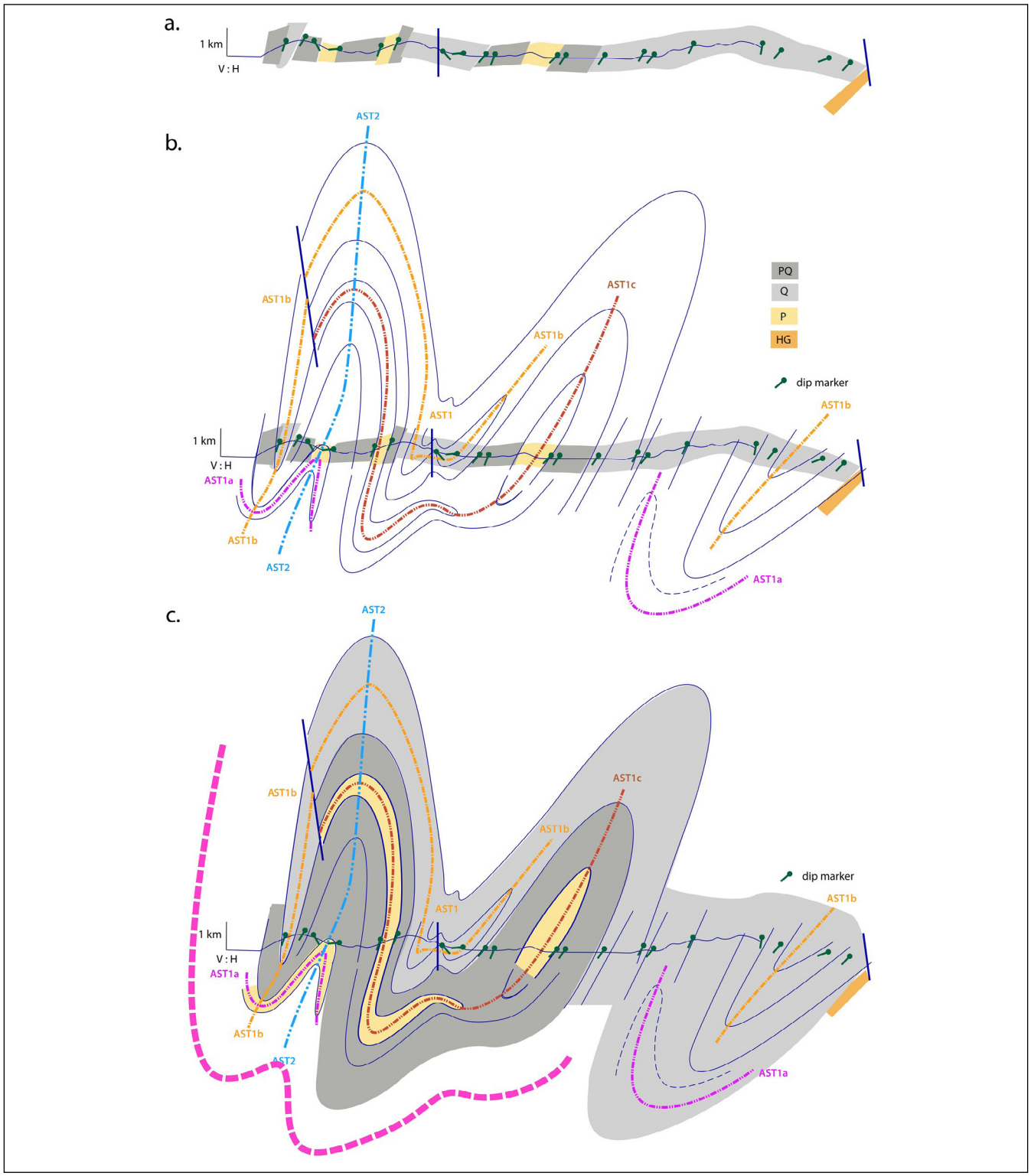

Figure 48. Interpretive structural cross-section across the South West Cape mega-sheath fold system (Profile P4, Figure 24). The section is problematical in that the fold plunges are in and out of the section (see map view, Figure 47). Mesoscopic folds and the interpreted hinges also show marked plunge variations. As a consequence this is a first pass profile where some artistic license has been used. The gross form of isoclinal folds refolded by isoclinal folds is the character of the core of the mega-sheath fold. a) Topographic profile with dip trace markers in So/Sm. b) Interpretative profile based on the map interpretation in Figure 47 and the profile in (a). c) Interpretative structural section showing isoclinally refolded isoclinal macro-folds (orange and red dashed axial surface traces AST). The blue dashed trace is the second phase isoclinal fold axial surface trace (AST2). The heavy pink dashed line trace represents the generalised So/Sm form of the mega-sheath fold outer shell.

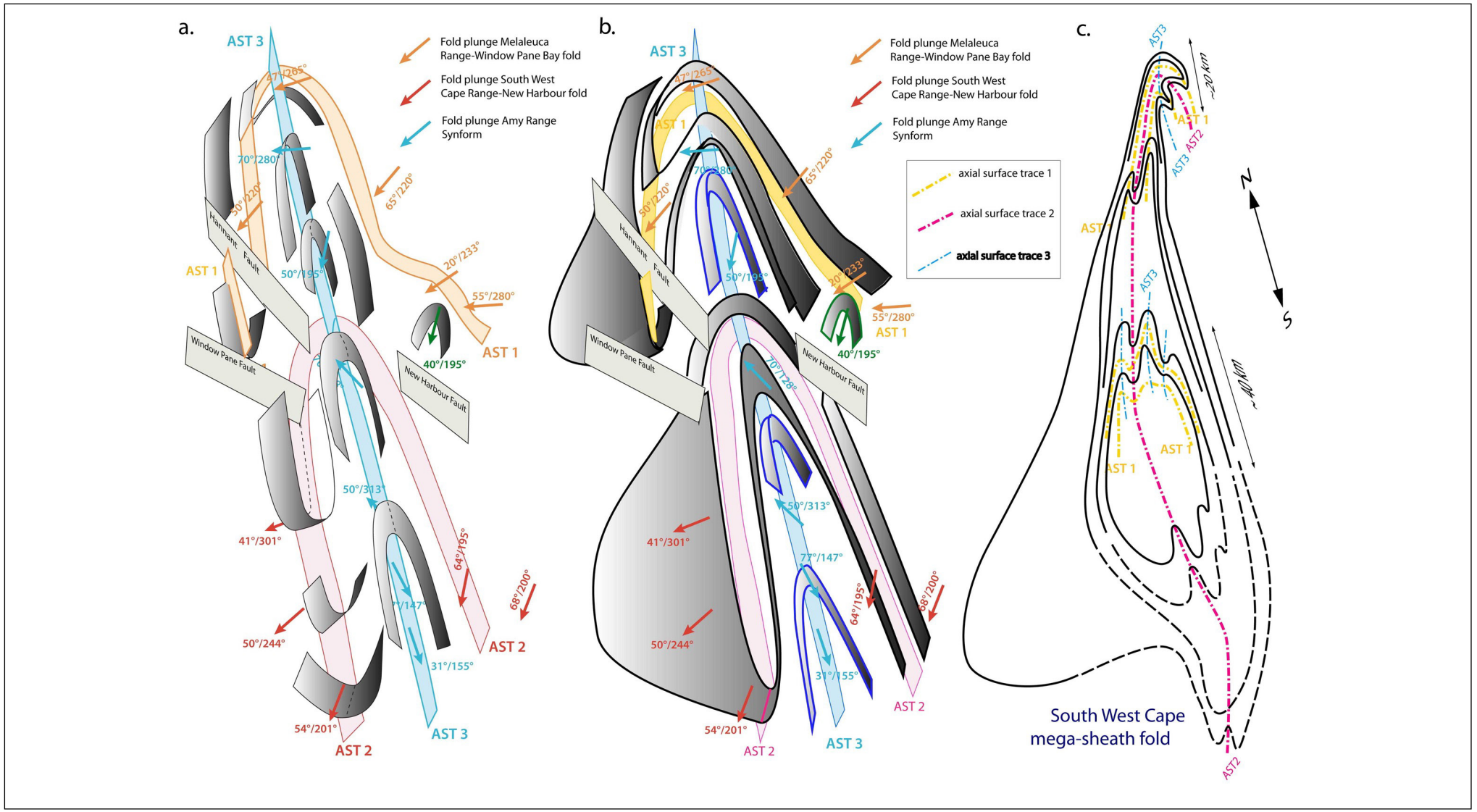

Figure 49. South West Cape mega-sheath fold reconstructions looking north-northeast. a) Schematic 3D diagram showing the geometry of individual fold-hinge segments of each macro-fold within the mega-sheath fold system. Fold plunges are shown by the respective arrows denoting plunge and plunge direction. b) Schematic 3D diagram showing the interpreted complete form of each of the macro-folds, where:

AST1 (orange surface): axial surface trace for the Melaleuca Range-Window Pane Bay fold.

AST2 (pink surface): axial surface trace for the South West Cape Range-New Harbour fold

AST3 (blue surface): axial surface trace for the Amy Range synform.

The earlier folds with AST1 and AST2 generally have west-plunge but also plunge to the southwest and northwest. The younger macro-isocline AST3 has more south-plunge.

c) Schematic 3D form of the outer shell of the South West Cape west-closing mega-sheath fold. AST1, AST2 and AST3 refer to the different generations of isoclinal folding (refer AST1a, AST1b, AST1c and AST2 in Figure 48).

4.6 Eastern Fold Domain

Structurally the eastern Southern Tyennan domain (Figure 50) consists of three orders of macro-isoclinal folds (Gray and Vicary, 2022c) including 1) northern termination of the South West Cape mega-fold system as a refolded 1st order downward-closing fold-nappe with an approximate axial surface length of 30 km, 2) 2nd order macro-folds that fold quartzite-pelite units within the hinge of the 1st order fold-nappe (Figure 51) and the Red Point macro-fold (Figure 52) folding high-grade schist and pelite with wavelengths of ~5 km, and 3) 3rd order macro-fold pairs with wavelengths of ~400-500 m that define a regional "wave train" above a high-strain lower bounding zone (Figures 53, 54 and 55).

4.6.1 Second Order Folds

The 2nd order macro-folds include the Mt Robinson, Mt Braddon and Red Point macro-folds (Figures 50 and 51).

4.6.1.1 Mt Braddon and Crossing Plains macro-folds

The downward-closing Mt Robinson and Mt Braddon folds (Gray and Vicary, 2022c) are approximately symmetrical, downward-closing, W-shaped folds within the plunging nose of the South West Cape mega-sheath fold system (Figures 50 and 51a). The fold-nappe nose shows a reversal in unit stacking from the upper limb to the lower limb (Figure 51b). This refolded hinge zone (Figure 51c) represents the northern close-out of the South West Cape mega-sheath fold beneath the De Witt-Propsting mega-sheath fold. In map view it is attenuated, northern close-out with a plunging fold-nappe geometry (Figures 51b and d).

4.6.1.2 Red Point Macro-fold

The Red Point macro-fold (Gray and Vicary, 2022d) is a south-closing, west-plunging, tight to isoclinal fold cored by low-grade pelite flanked by high-grade schist (Figure 52). The hinge is projected offshore with the western limb represented by the north-northeast trending schist belt along the Black Cliff Hills, the NMGS of Mulder et al (2015), and the eastern limb along the southern coastline from Red Point to Louisa Bay as the SMGS of Mulder et al. (2015). The macro-fold has an inclined plunging form approaching reclined geometry with a calculated fold axis is 41°/254° (Figures 52 and 53a).

Younging data suggest the western structurally higher limb is structurally overturned but right-way-up whereas the southeastern structurally lower limb is up-side down. The axial surface trace (orange dot-dashed line in Figure 52) separates regions of right-way-up (U) versus upside down (D) younging.

The Red Point macro-fold has been obliquely refolded by a series of open, north-plunging, north-south trending folds through the low grade pelite of the Red Hills and that of the hinge area exposed along the coastline from Black Cliff to Contact Cove (Figures 52 and 53b). A series of sub-parallel, sub-vertical, east-west-trending faults with dextral sense also offset the macro-fold (Figure 52).

4.6.2 Isoclinal Fold Pair "Wave Train"

The lowest structural level of the Southern Tyennan domain is dominated by a wave train of S-vergent asymmetric fold pairs (Gray and Vicary, 2022c). These 3rd order folds, with examples shown in Figures 54 and 55, define the inferred fold "wave train" (Figure 56). The wave train occurs in the low-grade quartzite dominant sequence extending eastwards some 60 km from Bathurst Harbour to the Arthur Range, occupying an area of approximately 1200 square kilometres (Figure 50). A series of structural profiles of the "wave train" across the region (Figure 57) demonstrate the continuity of the asymmetric fold pair and their apparent occurrence at the same structural level. The fold-pair system 1) sits structurally below the South West Cape mega-sheath fold system but appears a lateral transition away from the plunging nose with the Crossing Plains and Mt Braddon macro-isoclinal folds, and 2) occurs within the mega-sheath fold lower limb in the quartzite-dominated sequences (Figure 50).

This quartzite sequence sits above low-grade dolomitic pelite of the far eastern part of the Southern Tyennan domain exposed in the Forest Hills and upper reaches of the New River (Dixon and Sharples, 1986), and in the Solly River Valley and Provis Hills (Figure 50). Observations from Harrys Bluff and the flanks of Mt Pollux indicate development of intensely foliated quartzite and micaceous quartzite towards this contact (Gray and Vicary, 2022c), suggestive of a high-strain zone contact.

Measured or calculated dimensions of the asymmetric isoclinal fold pair are a ~430 m limb separation distance (LSD) distance, and a hinge separation distance (HSD) of ~400-450 m. Estimates from the Harrys Bluff cliff exposure suggest the quartzite has a deformed thickness of ~700 m (Gray and Vicary, 2022c). Although the fold-pair is dominantly preserved in cliffs and hillsides of quartzite, the Federation Peak-Geeves Bluff ridgeline (Figure 58) shows quartzite with intercalations of pelite and intercalated quartzite-pelite.

Development of such an asymmetrical fold-pair with the form shown in Figure 59b and c is geometrically suggestive of a regional-scale shear lozenge cored by asymmetric folds (Figure 59d). The evolution of this basal "shear lozenge" on the lower limb of the South West Cape mega-sheath fold requires 1) initial imbricate stacking of the lithotectonic units in this basal zone with unit repetition (Figure 59c), and 2) large shear strains across the extent of the eastern Southern Tyennan domain (Figure 59d).

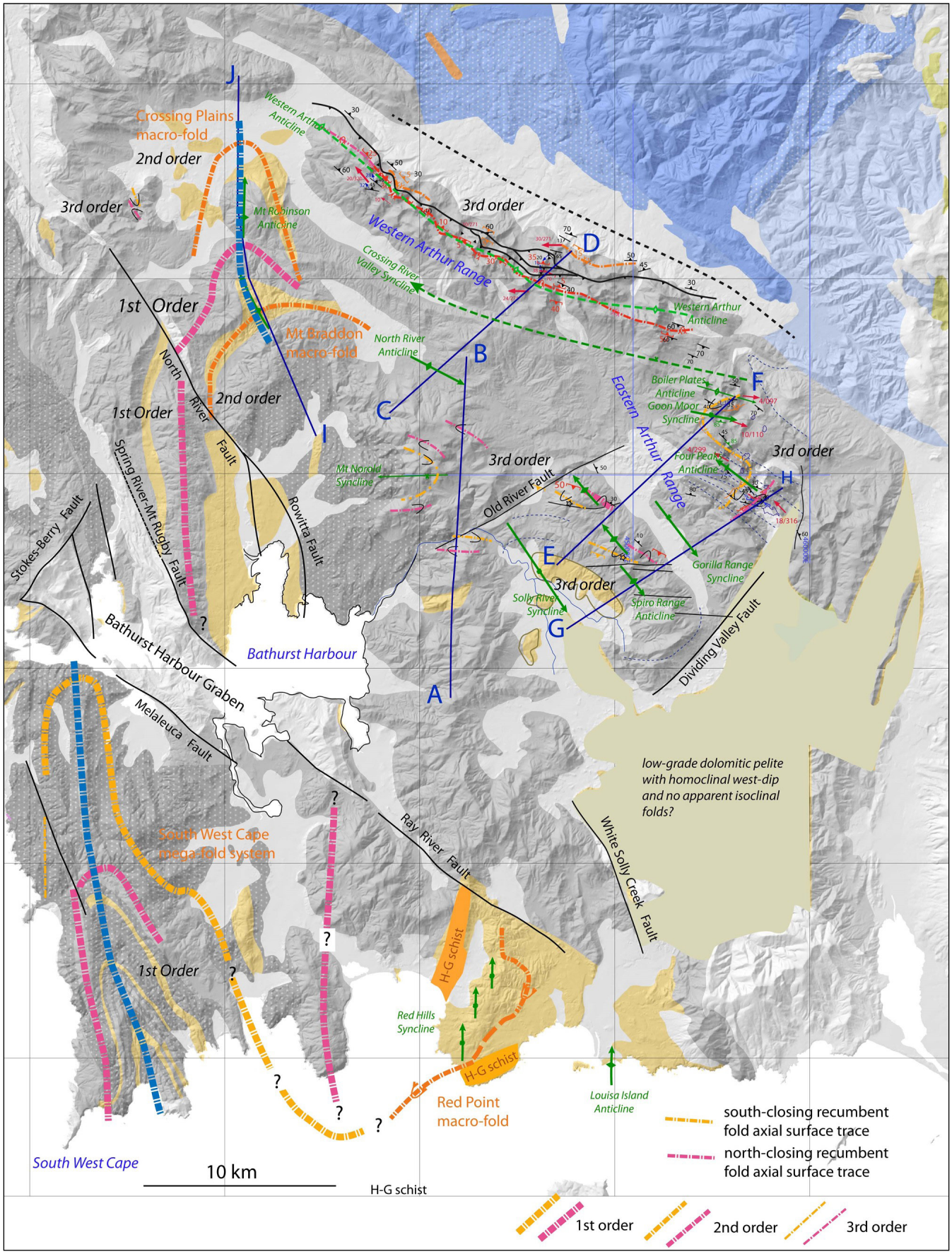

Figure 50. Fold axial surface trace (AST) map showing south-closing (orange dashed line trace) and north-closing (pink dashed line trace) isoclinal axial surface traces. Fold order is differentiated by the axial surface (AST) line thickness. Younger Devonian fold traces are shown by the green line traces. Faults are shown by black line traces. Section lines A-B (P10), C-D (P7), E-F (P8), G-H (P9) and I-J (P5) are shown by the dark blue lines (see Figure 24). Map base is the Mineral Resources Tasmania 1:250,000 digital atlas draped over DEM. For the Mt Robinson and Mt Braddon areas the main axial surface trace AST (pink dashed line) lies within quartzite (grey) and splits the pelite (orange) bands. The heavy blue dashed lines are second generation isoclinal macro-folds that isoclinally refold the early macro-folds.

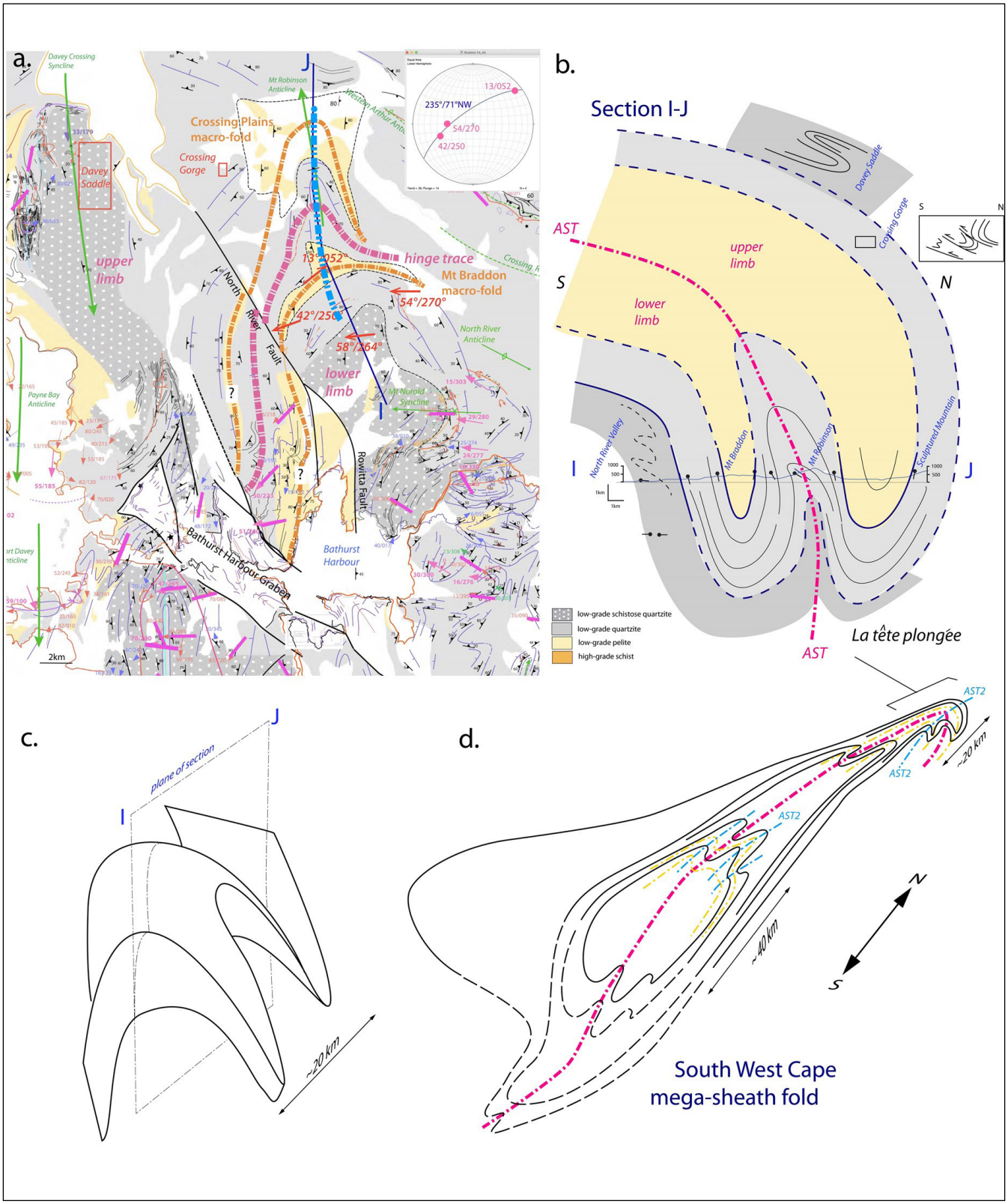

Figure 51. 2nd order folds and the northern termination of the South West Cape mega-sheath fold. This is regional structural profile P5 shown in Figure 24. a) Axial surface trace map of the northern sheath-fold termination incorporating the Crossing Plains and Mt Braddon macro-fold hinges (orange dashed axial surface traces). The main axial surface trace is shown by the pink dashed line. The base map is from the Mineral Resources 1:250,000 digital atlas. The red arrows show calculated (β determination) fold plunges for parts of the Braddon macro-fold. Inset stereonet shows best-fit great circle (235°/71°NW) to the calculated fold axes. The location of the section line I-J is shown (blue line trace). b) Section I-J along the hingeline of the Mt Robinson anticline. The profile extends from the Rowitta Plains to Sculptured Mountain. c) 3D schematic diagram illustrating the geometry of the Type 2 fold interference at Mt Robinson and Mt Braddon. d) Schematic 3D interpretation of the west-closing South West Cape mega-sheath fold. The sectional view is an oblique map projection used to construct the sheath form aided by mesoscopic fold axis plunges. The northern prolongation of the sheath-fold represents the attenuated and refolded fold-nappe geometry shown in (b). First phase isoclinal fold axial surface traces are shown as pink and orange dashed lines. Second phase isoclinal fold axial surface traces are shown by the blue dashed lines (AST2).

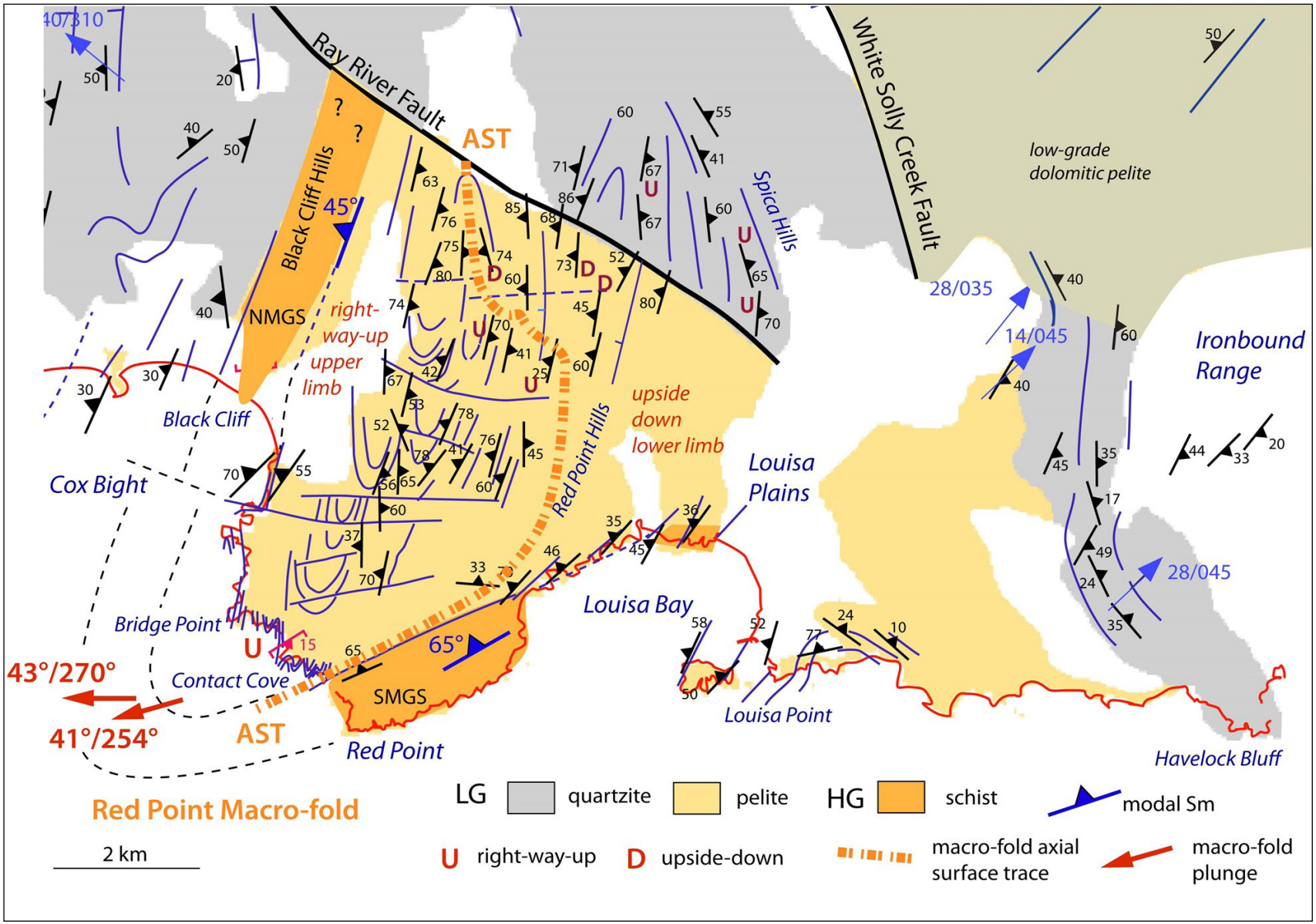

Figure 52. Structure map of the Red Point macro-isoclinal fold. Structural data from 1) Lennox (2013) based on mapping in January-February of 1980, and 2) Mulder (2013) Honours thesis mapping. Younging data from Lennox (2013) plotted as D: upside down compositional layering; U: right-way-up compositional layering. Blue arrows: lineation Lm attitude data. Lithological map base is from Mineral Resources Tasmania 1:250,000 digital atlas series. Thin dashed black lines depict the macro-fold closure. The thick orange dashed line is the macro-fold axial surface trace (AST). NMGS: Northern medium grade sequence; SMGS: southern medium-grade sequence.

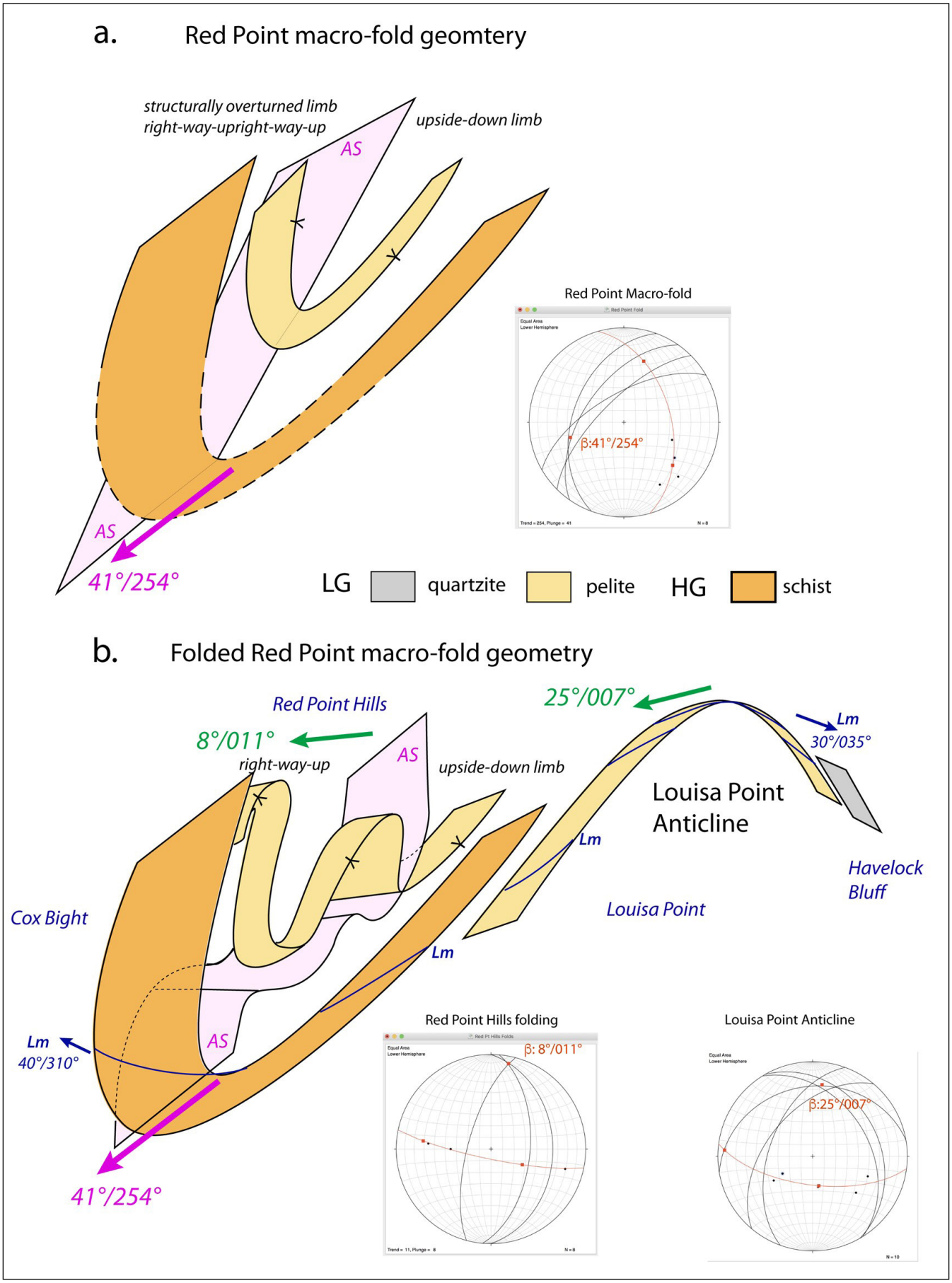

Figure 53. Interpretative 3D structural geometry of the Red Point Hills-Red Point area.

a) Macro-fold form by connecting the northern and southern HG belts by an inclined plunging closure with a β axis of 41°/254°. b) 3D schematic geometrical diagram of a refolded Red Point macro-fold by younger north-south folding in the Red Point Hills and the Louisa Bay-Louisa Point area. The east-west-trending, right lateral strike slip-faults have been removed in 3D diagram. Stereonet insets show the β fold axis determinations for the Red Point Hills folding (β: 8°/011°) and the Louisa Point Anticline (β: 25°/007°).

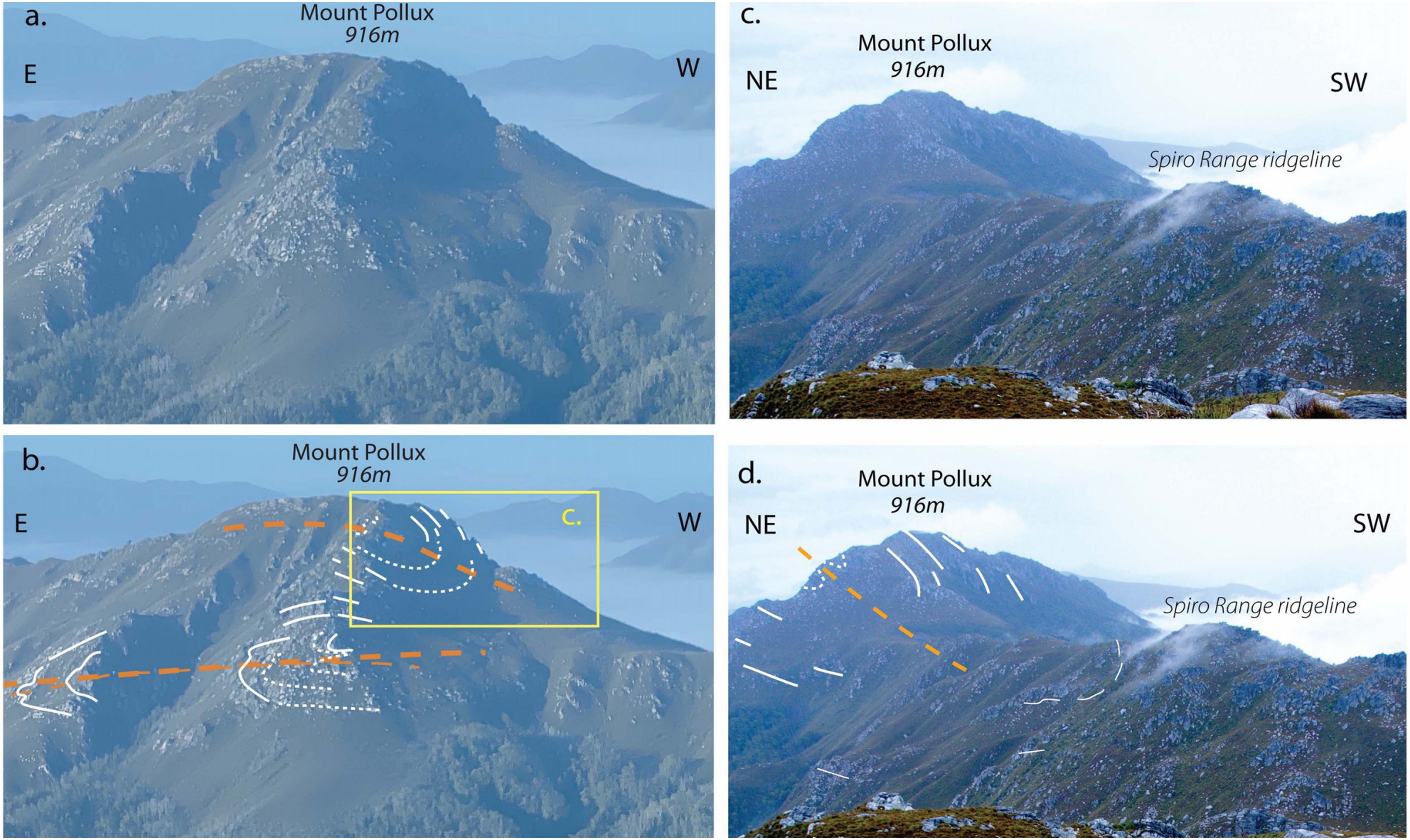

Figure 54. Helicopter and bush walker photographs of Mount Pollux (916 m) showing recumbent fold closures. These are examples of how the regional structures were interpreted across the eastern part of the Southern Tyennan domain. a) and b) annotated and non-annotated helicopter photograph of Mount Pollux looking south. The helicopter flight path was southwest along the Old River valley. An asymmetric fold pair intersects the northwest face of Mount Pollux . The southwest-closing fold hinge in shadow is structurally higher than the northeast-closing fold hinge. There is broad arching of the axial surface traces due to the younger, Devonian Spiro Range Anticline. c) and d) Annotated and non-annotated photographs of Mount Pollux looking southeast from Mount Castor. The photographs provide better definition of the structurally higher, southwest-closing macro-isocline that is in shadow in (a). Form lines in So/Sm: white and white dashed lines. Macro-fold axial surface traces: orange dashed lines.

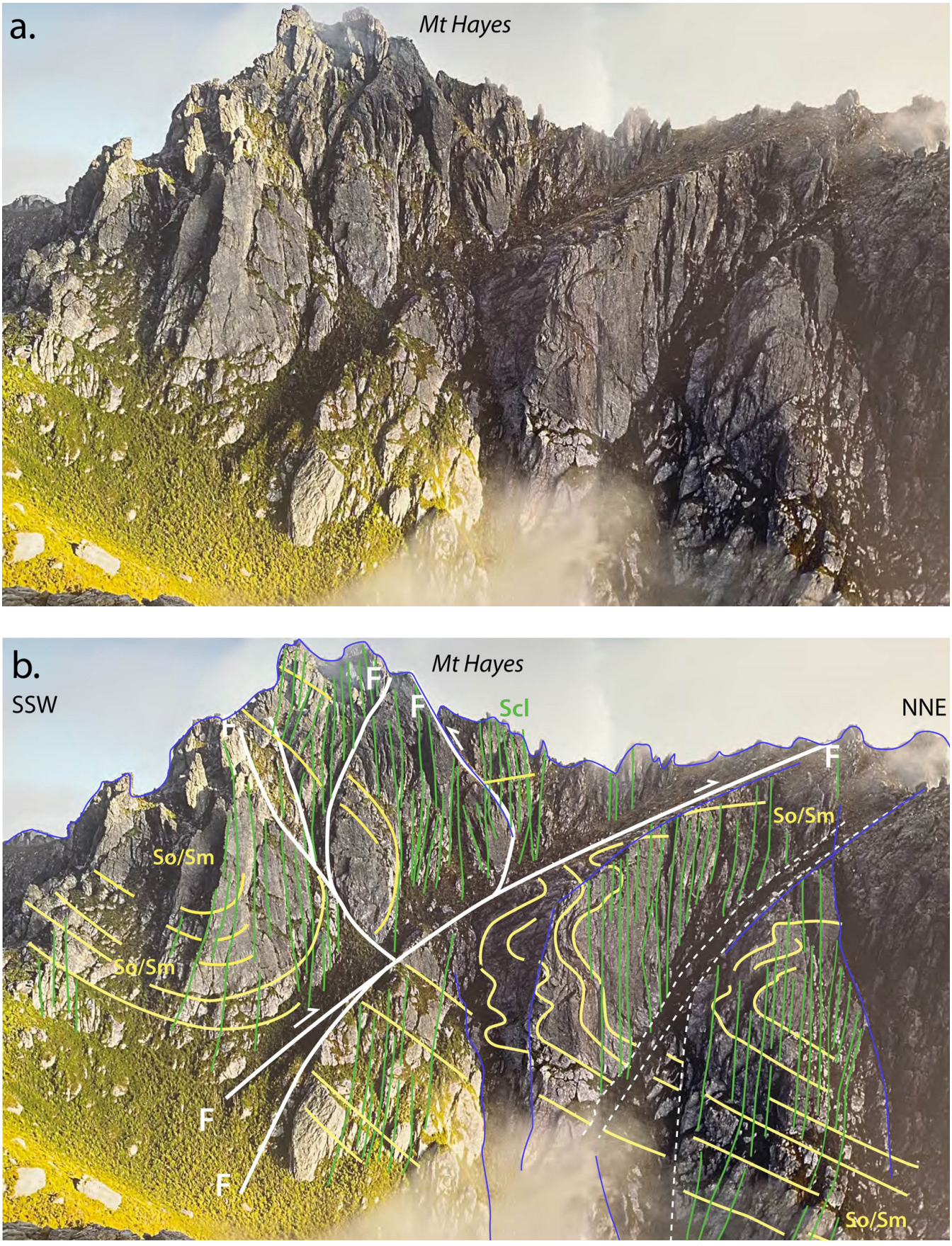

Figure 55. Macro-isoclinal fold pair in the southeastern flank of Mt Hayes (1119 m). View is to the northwest. a) Peter Dombrovskis photo [Peter Dombrovskis, National Library of Australia, nla.cat-vn4937364]. b) Annotated photo with formline interpretation showing the oppositely facing and closing macro-fold hinges cut by a major thrust fault. The position of the photo profile in (b) corresponds to Section P6 in Figure 24. Note the Devonian cleavage (Scl) is enhanced in the more pelitic layers and can be used to define the layering and the So/Sm foliation form lines.

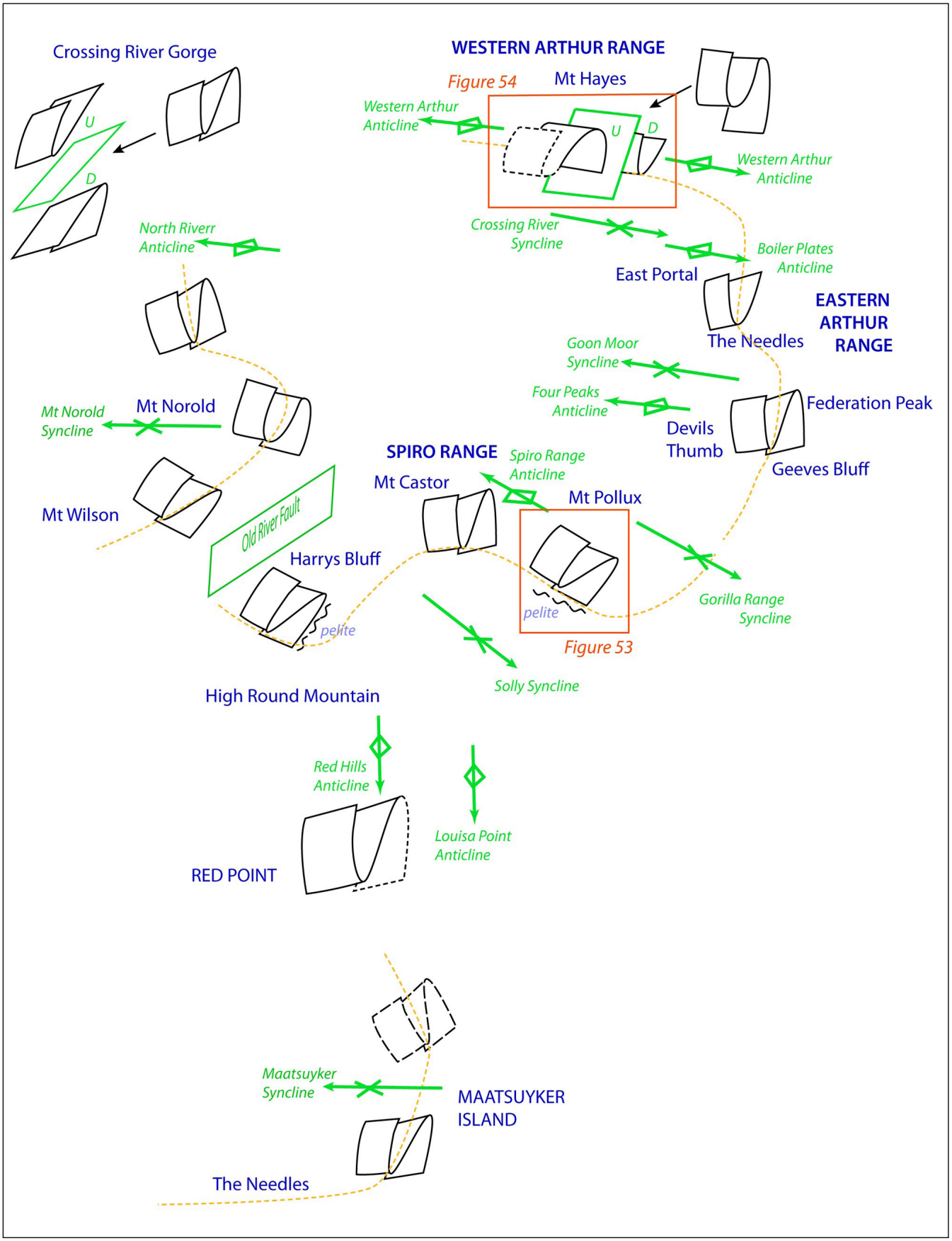

Figure 56. Schematic asymmetric fold-pair diagram showing the 3D geometry and attitude of the S-vergence (down-plunge) fold pair across the eastern Southern Tyennan domain. The spatial positioning reflects an approximate geographic base. Geographic location names are in blue text. Younger, Devonian fold axial surface traces and faults are shown in green and with labeling in green text. The orange dashed line connects the hinge-lines of the structurally higher south-closing macro-isocline across the region.

Length scales are ~60 km from the northern end of the Western Arthur Range in the north to Maatsuyker Island in the south, and ~20 km from Mt Wilson-Mt Norold in the west to Federation Peak in the east.

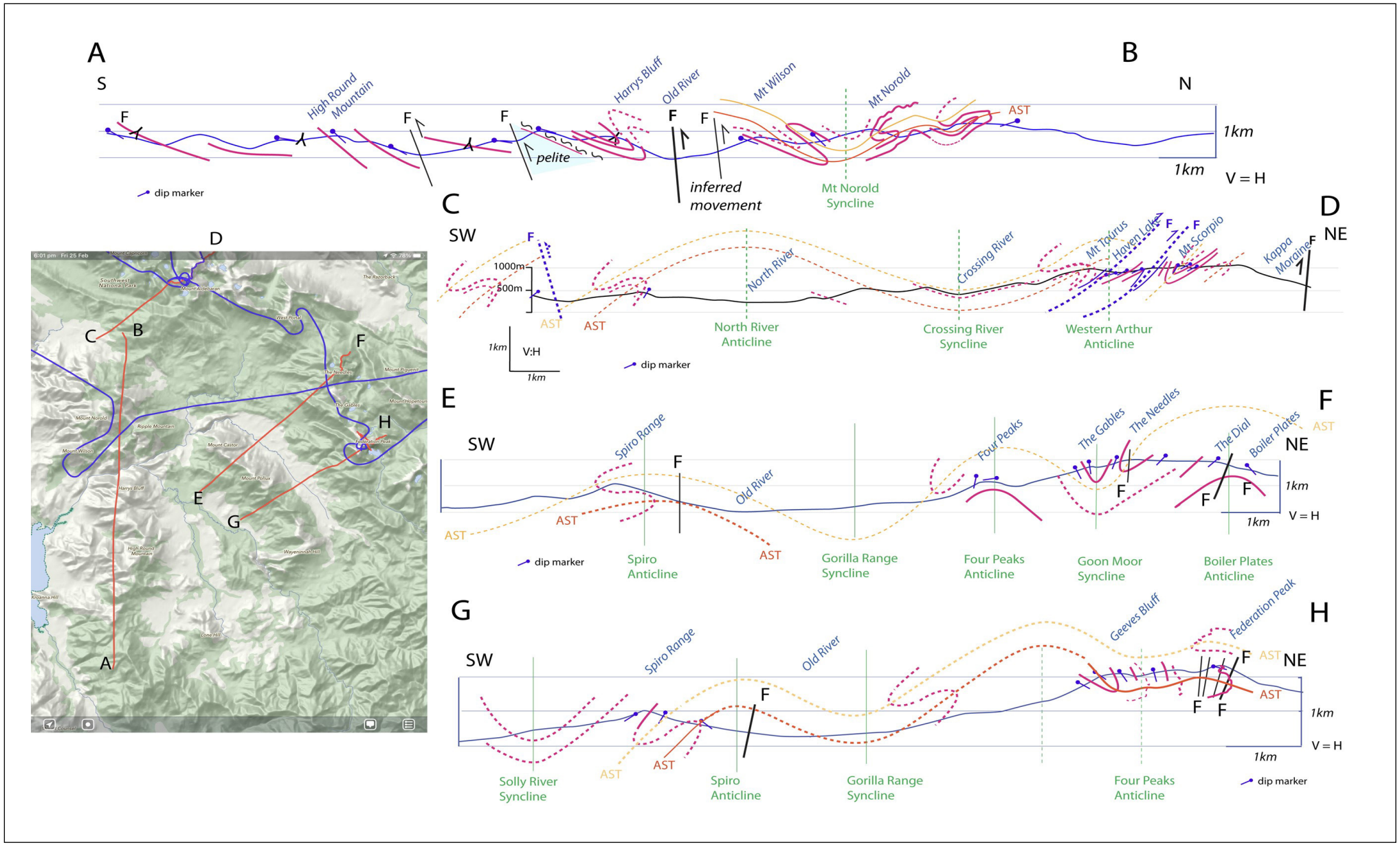

Figure 57. Structural profiles across the eastern Southern Tyennan domain. Section A-B' north-south profile from Mt Norold to High Round Mountain. Section C-D: southwest-northeast profile from Mt Norold to Mt Scorpio and Kappa Moraine. Section E-F: southwest-northeast profile from the Boiler Plates to the Spiro Range. Section G-H: southwest-northeast profile from Federation Peak to the Spiro Range. The blue line traces are the helicopter flight paths during the 2020 flight into the southwest (Figure 24).

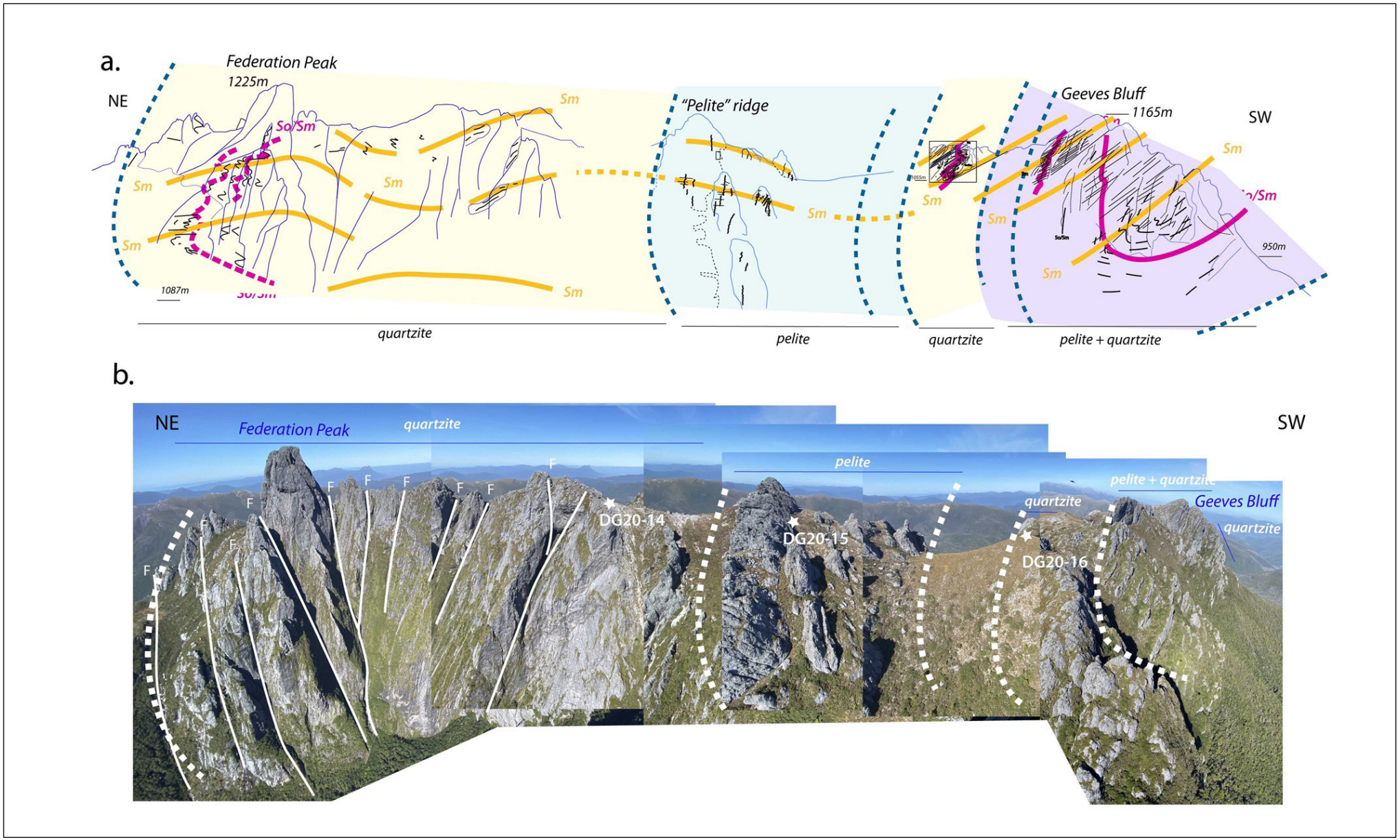

Figure 58. Example of layers or litho-tectonic units folded through a macro-isoclinal fold hinge in the eastern Southern Tyennan domain. a) Federation Peak-Geeves Bluff structural profile with So/Sm form lines (black line traces), layer contacts (blue dashed line traces), axial surface foliation Sm form lines (orange and orange dashed line traces). Lithologies are quartzite (yellow), pelite (light blue) and mixed pelite and quartzite (light mauve). b) Photo collage of Federation Peak-Geeves Bluff ridgeline used to construct the structural profile shown in (a).

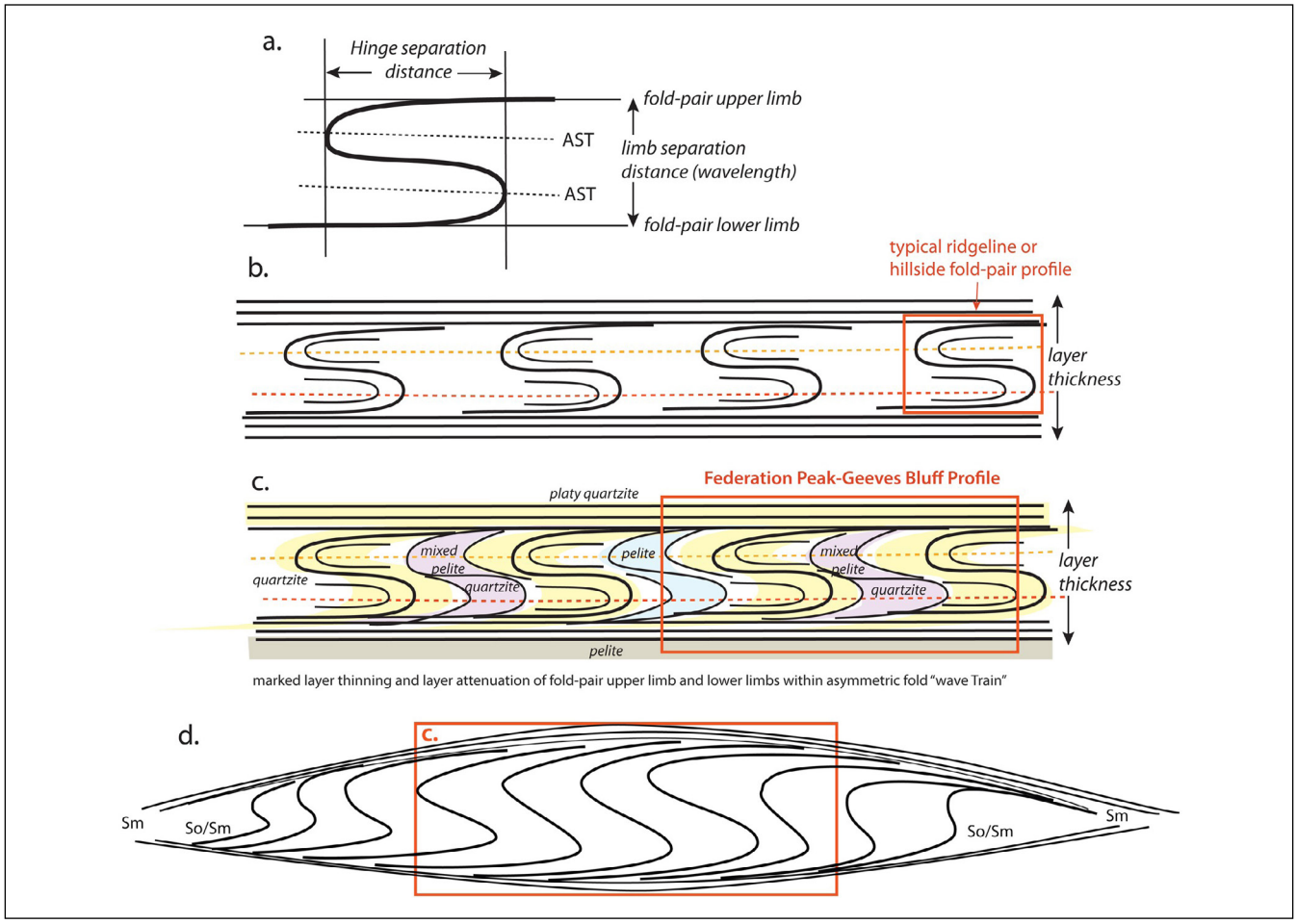

Figure 59. Schematic diagram showing a) asymmetric isoclinal fold-pair dimension parameters, b)"wave couplet train" geometry based on the constructed sections across the eastern Southern Tyennan domain (Figure 57), and c) lithology distribution through the "wave couplet train" fold hinges based on the Federation Peak-Geeves Bluff profile (Figure 58).

The shear lozenge geometry from the initial duplex-like stacking of the low-grade pelite and quartzite is required based on the observed unit relationships and structural character shown in the Geeves Bluff-Federation Peak ridgeline profile (Figure 58). The fold pair duplication as part of the regional fold wave train requires significant repetition of litho-tectonic units and therefore potential duplexing of the quartzite ± pelite throughout the eastern part.

5.0 PORT DAVEY-BATHURST HARBOUR GRABEN

The Port Davey-Bathurst Harbour graben (Williams, 1980, 1989) is a ~20 km long, ~4 km wide, northwest-trending, strike-slip, inverted-pull-apart basin that transects and unconformably overlies the quartzite and platy quartzite of the South West Cape mega-sheath fold (Figures 14 and 60). The basin consists of three sub-basins (Figures 60 and 61) filled with the possible mid-Cambrian Clytie Cove Group, a 2 km thick fining and thinning upwards sequence of conglomerate, sandstone and mudstone (Williams, 1980, 1989). The sub-basins are constrained by a fault-architecture with sub-vertical, northwest-trending, dextral oblique-slip faults linked by north- and northeast-trending growth faults that have controlled deposition within the three sub-basins (Figure 61).

The basin pull-apart geometry reflects east-west extension (Figures 61 and 62a) with the basin fill controlled by the transfer faults (red faults, Figure 61 and 62a) and the interlinking growth faults (blue faults, Figure 62a). Basin inversion is shown by the flexuring against the growth faults (Figure 62c), where the transfer faults acted as abutments.

The model for the evolution of the Port Davey-Bathurst Harbour graben (Figure 62) follows the interpretation of the Clytie Cove Group as middle Cambrian (Corbett and Vicary, 2014, p.173). However, this correlation is poorly constrained. The Clytie Cove Group also shares the marine facies characteristic of parts of the Owen Group, in particular the Newton Cormack Sandstone equivalents, and a Late Cambrian age for this sequence may also be likely.

The northern extrapolation of the Rowitta Fault and the associated northwest-trending structures at the southern end of the Devonian Olga Syncline may also have been active during Late Cambrian sedimentation. The Clytie Cove Group may also be equivalent to the Owen Group in this area. It is likely however, that the two sequences are separated by an unconformity with the Clytie Cove Group underlying the sequence exposed in the Olga Syncline-Crossing River area.

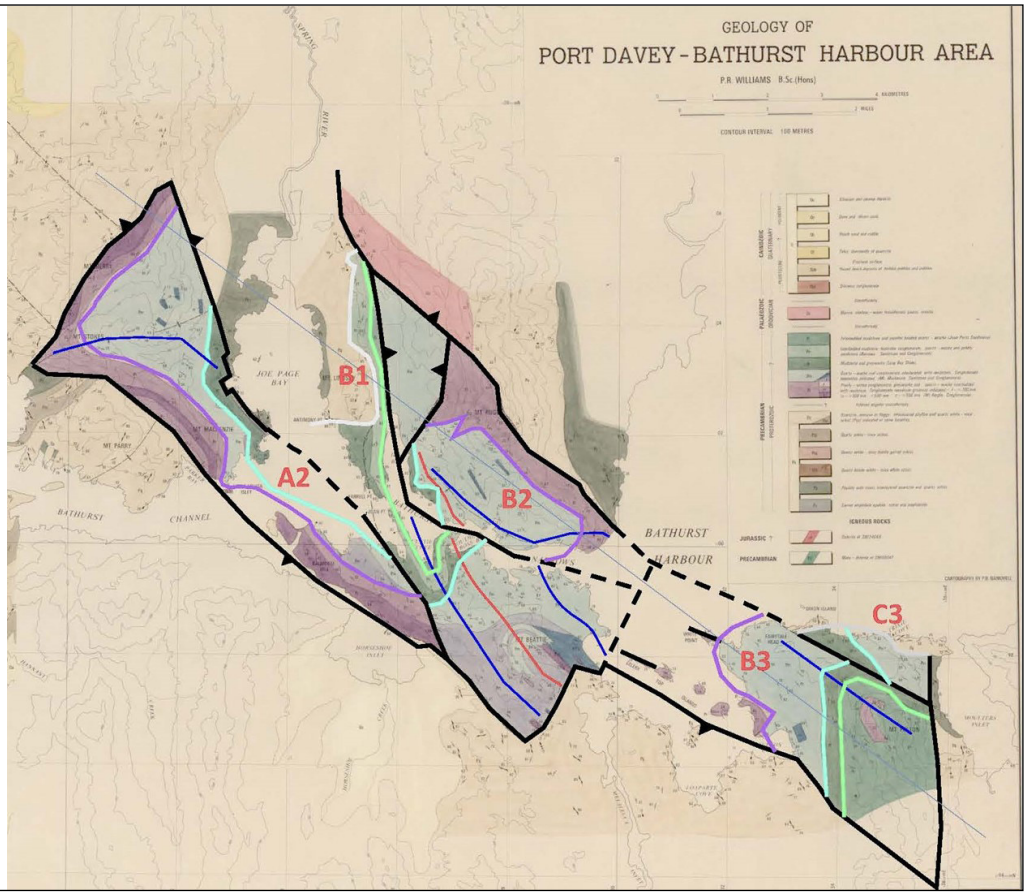

Figure 60. Geological map of the Port Davey-Bathurst Harbour graben showing the internal Clytie Cove Group stratigraphy (Map 1, Williams, 1980). The complex fault pattern of basin-bounding and internal cross faults is highlighted by the heavy black lines. Red lettering A, B and C designate the interpreted three sub-basins (see Figure 62a).

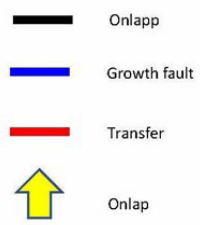

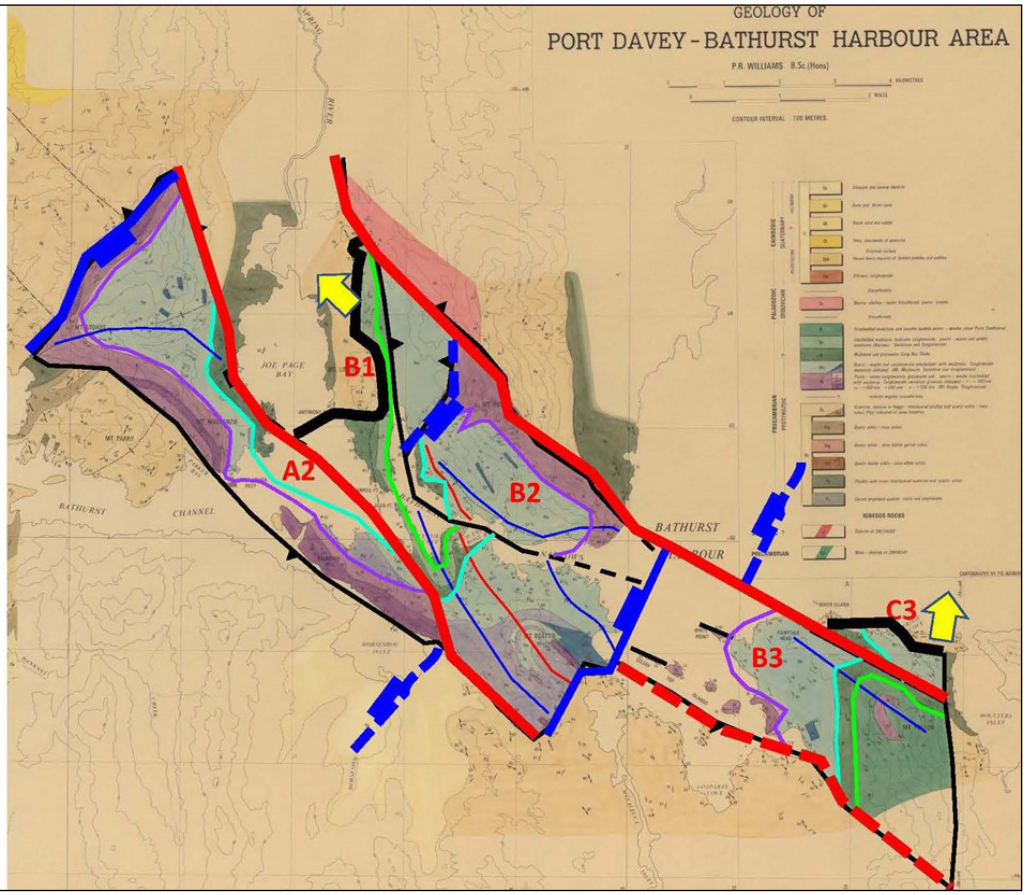

Figure 61. Interpretation map of the Port Davey-Bathurst Harbour basin architecture showing the basin transfer faults (red lines), growth faults (blue lines) and preserved basin-onlap regions (black lines) with directions of onlap shown by the yellow arrows. The base map is Map 1 from Williams (1980).

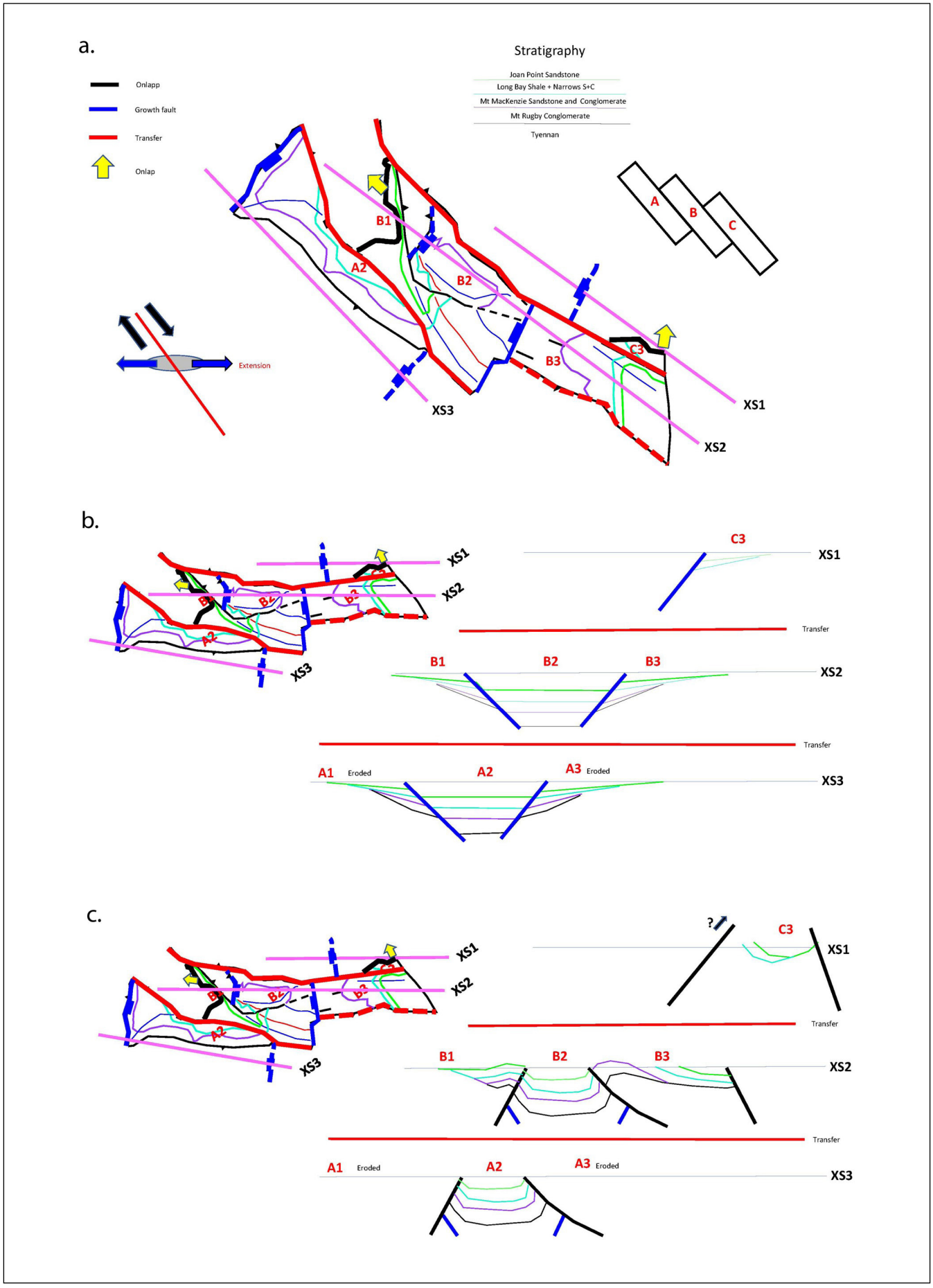

Figure 62. Schematic reconstruction of the Port Davey-Bathurst Harbour graben development. a) Sub-basin definition as three en echelon sub-basins. b) Middle Cambrian basin geometry, and c) Cross-sections following Late Cambrian basin inversion and Devonian deformation.

5.1 Structural Rerlationships within the Port Davey-Bathurst Harbour Graben

The Port Davey-Bathurst Harbour graben has an apparent complex internal structure (Figure 62). An early east-west-trending fold system with a penetrative axial surface cleavage is refolded and overprinted by the dominant northwest-trending folds with an axial surface crenulation cleavage (Williams, 1980, 1989). Both sets of folds are steeply plunging across the graben.

Significantly these fold patterns and overprinting cleavages within the graben preserve structural evidence for episodes of Late Cambrian and Devonian basin inversion. An inferred episode of north-south shortening produced the east-west folds (F2 folds, Figure 63) and penetrative S1 cleavage. This was followed by a younger Devonian inversion involving east-west shortening that produced the northwest-trending folds and associated crenulation cleavage (F3 folds, Figure 63). The ~10°-30° obliquity of the northwest-trending folds to the northwest trending (310°-130°), basin-bounding dextral strike-slip faults suggests refraction of the Devonian stress field across the narrow basin.

6.0 CRUSTAL SCALE IMPLICATIONS OF SOUTHERN TYENNAN DOMAIN STRUCTURE

The Southern Tyennan domain preserves a crustal-scale structural evolution within a, now ~20 km, thick deformed segment of the former subducted continental margin. The structures (Figure 64) and the implications of these structures include:

1. A fold-nappe is preserved at the leading-edge of the uppermost sheet of the Tyennan nucleus.
2. Two complementary, oppositely facing and closing mega-sheath folds define the core of the Southern Tyennan crustal section.
3. Mega-sheath fold evolution includes:
   i. initiation as isoclinal macro-folds from point lobes in the subduction channel about a potentially thickened part of the continental margin sand wedge, and
   ii. sheath-like, lobate form development with increasing shear strain and shear displacement within the subduction channel.
4. The ~20 km sheath-tube form of the complementary mega-sheath folds involves "hinge rolling in shear" within the innermost shell(s) of the mega-sheath folds evidenced by poly-deformation and isoclinal refolding of the early-formed isoclinal folds (see Gray and Vicary, 2022b).
5. The lower part of the Southern Tyennan crustal sequence, exposed in the eastern part, shows second-order macro-folds (e.g. Red Point macro-fold) transitional into a regional-scale zone of third-order asymmetric, "S"-vergent, fold pairs bounded by high strain zones. It is geometrically equivalent to a large-scale shear lozenge in a stacked and repeated, duplex-like low-grade quartzite-pelite sequence (Figures 59 and 68c).
6. The basal part of the quartzite sequence is strongly deformed and overlies a low-grade pelite sequence (Solly River valley) that extends into the Forest Hills and upper reaches of the New River (Dixon and Sharples, 1986). This unit is the likely equivalent of the Scotchfire Metamorphics of the Central Tyennan domain (Gray and Vicary, 2021a, b), as part of the para-autochthonous former continental margin.

6.1 Unit Thickness Determinations

Thickness of litho-tectonic units at different geographic locations and structural positions in the Southern Tyennan domain were calculated utilising both 1) map distances and structural attitudes, and 2) true thickness in cross sections.

6.1.1 Unit Thicknesses of the western and structurally highest part of the Southern Tyennan domain (Nye Bay Fold-nappe).

The Nye Bay fold-nappe (Figures 25, 26 and 27) provides thickness estimates at the leading edge or uppermost part of the Southern Tyennan composite sheet. The western, upper, overturned limb has a quartzite thickness of 1.2 km (Map distance: 1.6 km with dip ~50°) and pelite unit thickness of ~2.4 km (Map Distance: 2.7 km and dip~65°), whereas on the lower eastern limb the flanking quartzite has ~1.8 km (Map Distance: 1.9 km and dip~70°) thickness and the pelite has ~2 km thickness (Map Distance: 2.2 km and dip~65°). The thickness of the high-grade schist is indeterminate as it forms the core of the fold-nappe with attenuation towards Elliott Point where it pinches out.

In summary, the quartzite has a deformed unit thickness of ~1.2 to ~1.8 km and the pelite a unit thickness of ~2.2 to ~2.4 km.

6.1.2 Unit Thicknesses of the central part (core) of the Southern Tyennan domain.

Estimations of the unit thicknesses in the central part of the Southern Tyennan domain have been made from the east-west cross section through the De Witt-Propsting mega-sheath fold (Figure 40). At Wreck Bay (western side of the profile, Figure 40) the quartzite and pelite layers in the carapace to the mega-sheath fold have thicknesses of ~1 km and ~2.5 km respectively.

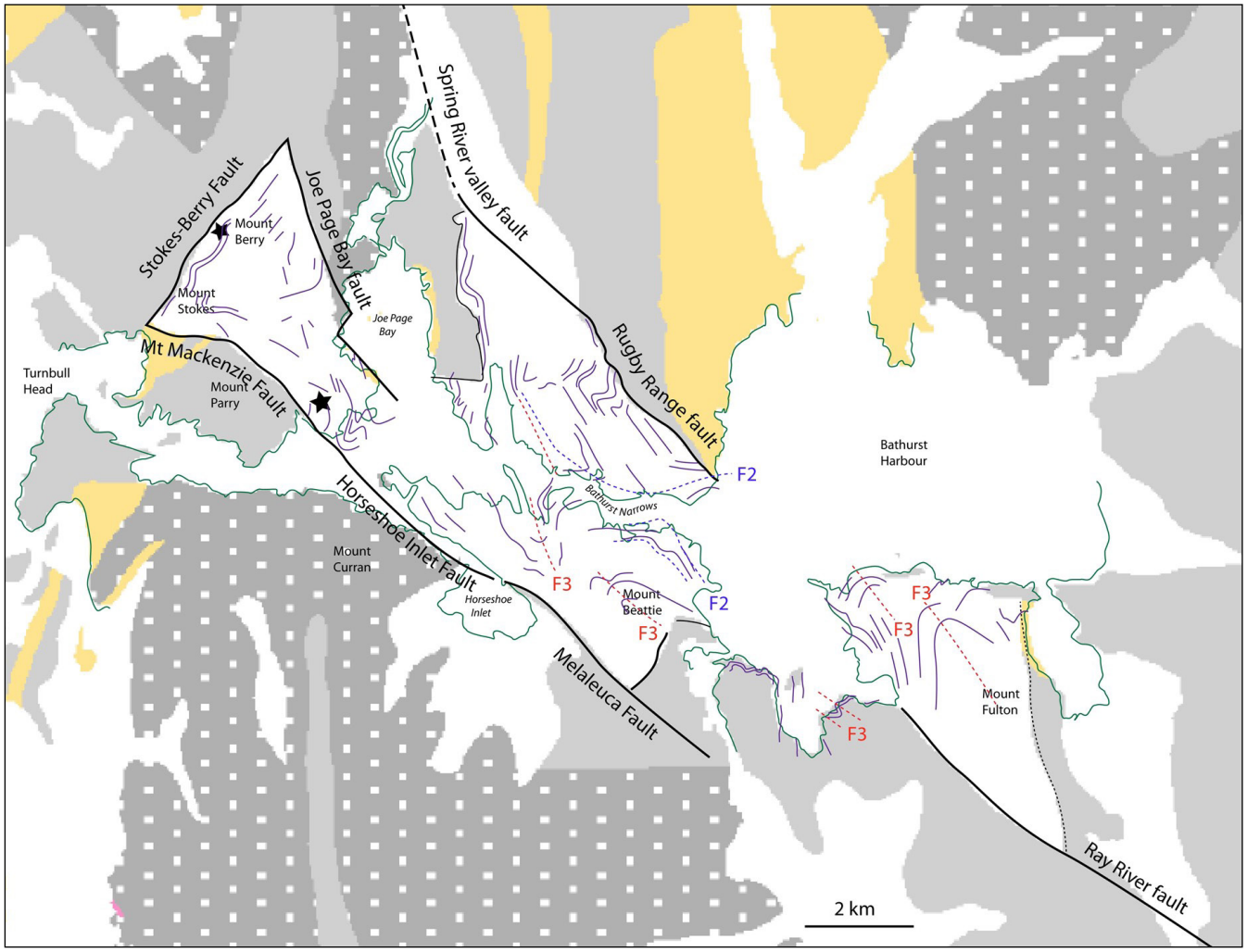

Figure 63. Formline structure map of the Port Davey-Bathurst Harbour graben. The map represents a compilation of the detailed structural maps in Williams (1980). Form line traces in bedding So are the purple line traces. F2 fold axial surface traces are the green dashed lines. F3 axial surface traces are the red dashed lines that have a consistent northwest trend.

The quartzite core of the De Witt-Propsting mega-sheath fold has a deformed thickness of ~3.3 km and the platy quartzite of the lower limb an estimated thickness of ~1 km.

6.1.3 Unit Thickness determinations of the eastern and structurally lowest part of the Southern Tyennan domain.

The Red Point macro-fold (Figure 53), the structurally lowest second-order macro-fold enables thickness determination of the high-grade schist unit (Gray and Vicary, 2022d). High-grade schist on the western limb, the NMGS of Mulder et al. (2015), has a unit thickness of ~1.1 km (Map distance: 1.5 km and dip ~45°), whereas on the lower eastern limb, the SMGS of Mulder et al. (2015), the high-grade schist has ~1 km thickness (Map distance: 1.15 km and dip ~65°).

The thickness of the deformed quartzite unit of the eastern asymmetric fold domain (Element 6, Figure 2) has been estimated in the cliffs at Harrys Bluff to be on the order of ~680 m (Figure 30, Gray and Vicary, 2022c).

6.1.4 Summary

The above litho-tectonic unit thicknesses have been utilised to show 1) how unit thicknesses change across the various macro-folds (Figure 65), and 2) the apparent thickness changes within composite obduction-sheets and between adjacent sheets (Figure 65). The calculated thicknesses are based on the deformed state with observable greatest thicknesses within macro-fold hinges and thinnest units on macro-fold limbs. The actual unit thickness pre-folding should lie somewhere between the two extreme values.

Structural thickening within macro-isoclinal fold hinges and thinning along macro-isocline limbs is responsible for the marked changes in thickness for different litho-tectonic units at different positions in the Southern Tyennan geometric reconstruction (Figures 65 and 66). The largest thicknesses are in the quartzite core of the De Witt-Propsting mega-sheath fold (~3.5 km thickness) and the hinge of the northern culmination of the South West Cape mega-sheath fold (~2.8 km thickness) (Figure 65).

Approximate restoration of the positions of "measured" unit thickness prior to macro-folding and mega-sheath fold development (Figure 66a), as well as utilising the observed stacking order, enables a crude ~8 km thickness estimate of a composite Southern Tyennan "sheet" (Figure 66b).

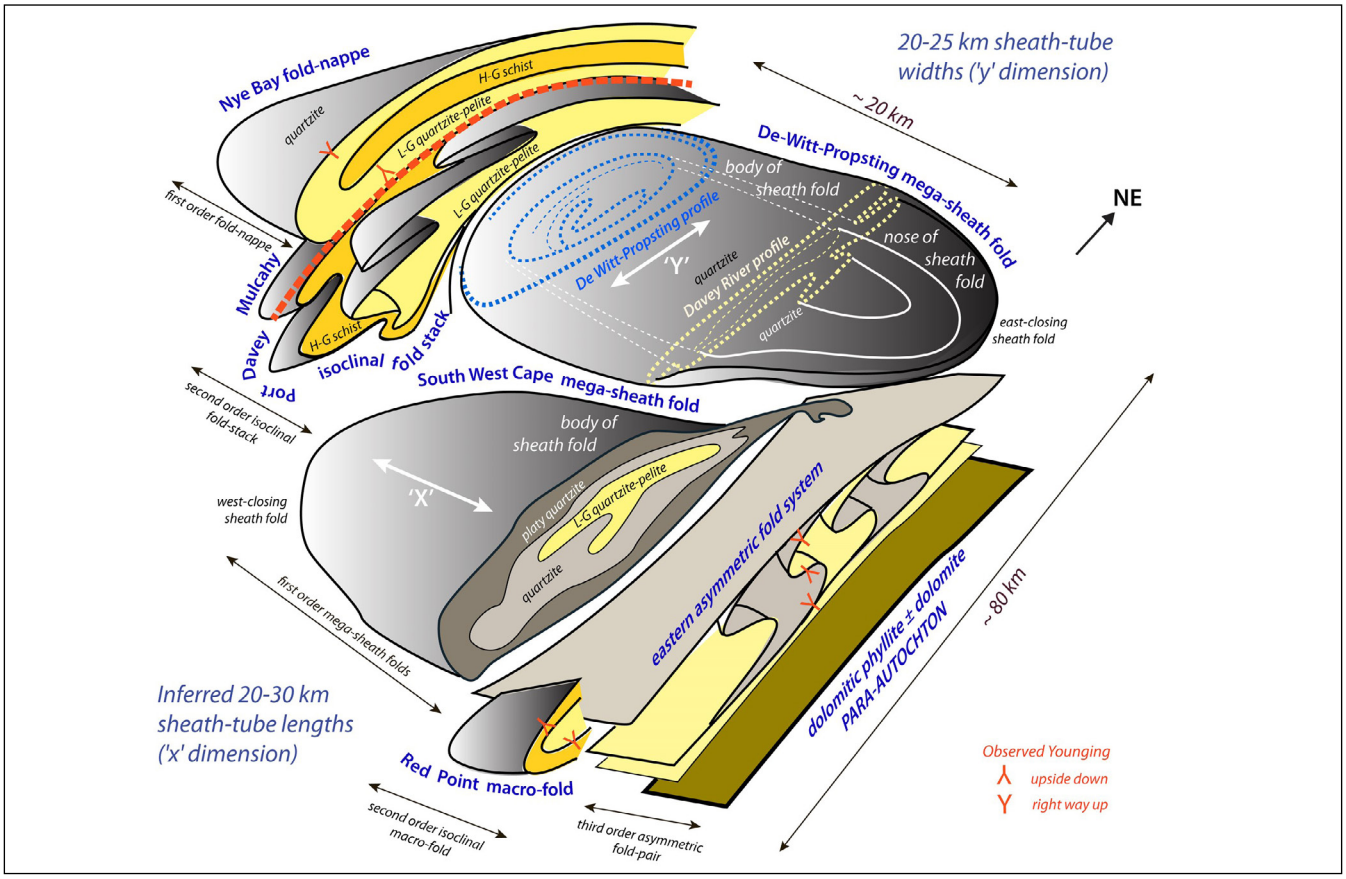

Figure 64. 3D schematic crustal-scale structural architecture of the Southern Tyennan domain. The stacked component structural elements represent a ~20 km crustal thickness. View is to the north. The mega-sheath fold dimensions are on the order of 20-25 km widths ('y' dimension) and ~20 km sheath elongations ('x' dimension). The thick red dashed line is the Mulcahy high strain zone, the shear zone interface across which the unit stacking order changes. The Southern Tyennan structural stack overlies a lower para-autochthonous sheet of dolomitic phyllite and intercalated dolomite (khaki unit). H-G schist: orange unit. Low-grade (L-G) pelite±quartzite: yellow unit. Low-grade quartzite: grey unit. Within the structural stack the positions of the observed younging data are shown by the red 'Y'.

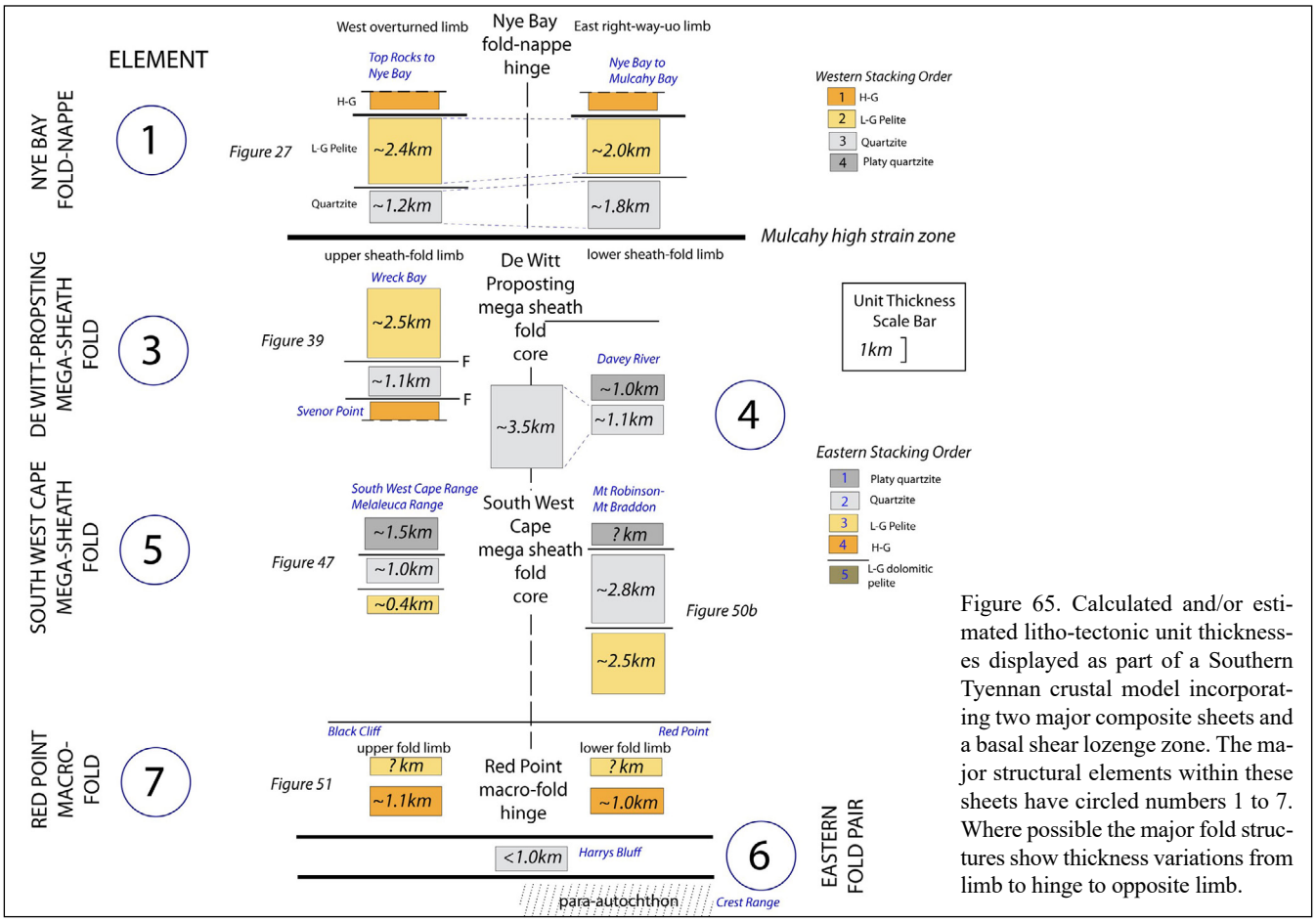

Figure 65. Calculated and/or estimated litho-tectonic unit thicknesses displayed as part of a Southern Tyennan crustal model incorporating two major composite sheets and a basal shear lozenge zone. The major structural elements within these sheets have circled numbers 1 to 7. Where possible the major fold structures show thickness variations from limb to hinge to opposite limb.

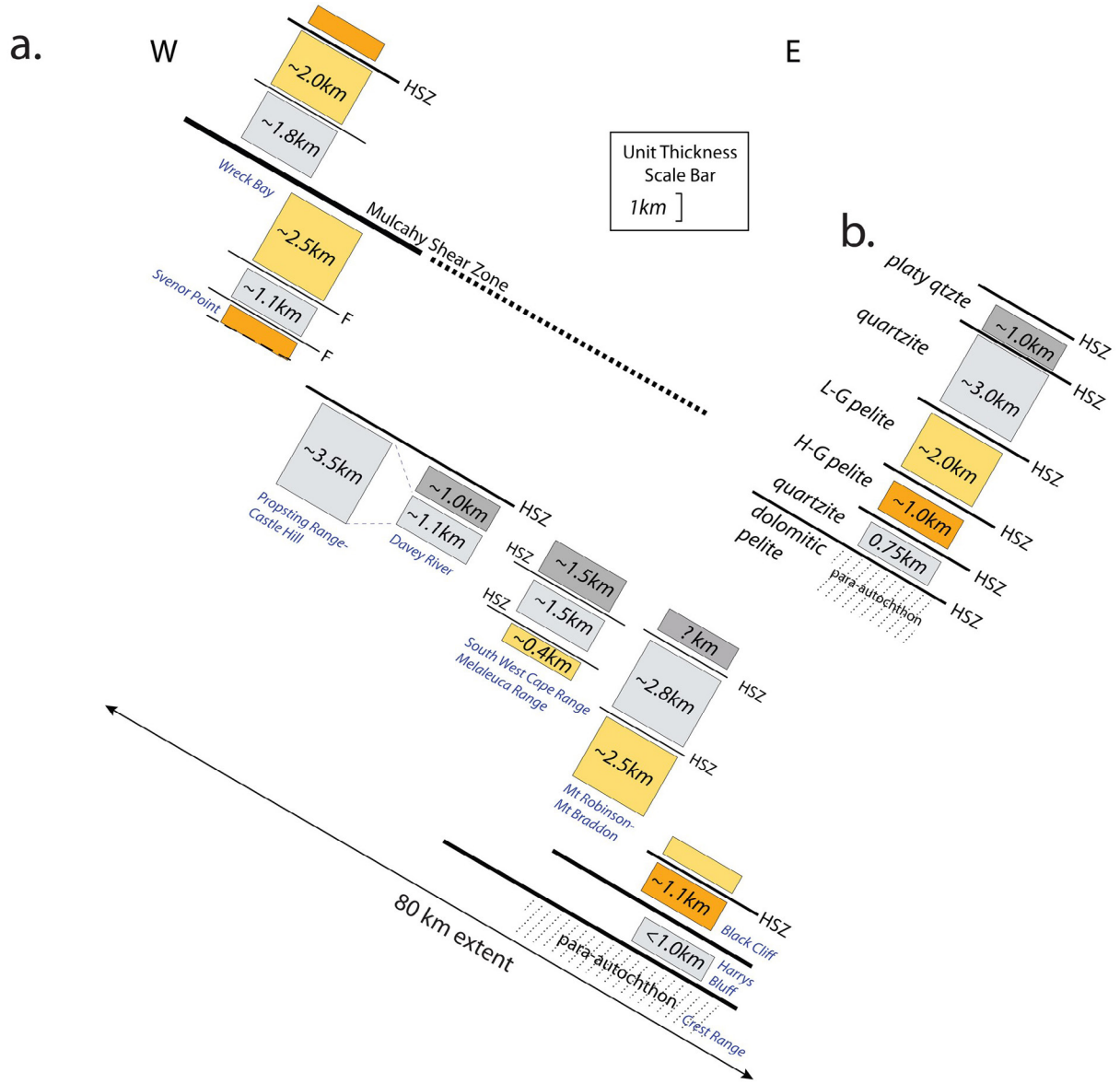

Figure 66. Southern Tyennan litho-tectonic unit thicknesses. a) Attempted reconstruction of the restored Southern Tyennan sheet geometry prior to macro-isoclinal folding with positions constrained by approximate structural position highlighted by the geographic location (blue text). It should be noted that the unit thicknesses are determined from the final deformed state. b) Generalised litho-tectonic unit thicknesses for an idealised Southern Tyennan domain composite sheet with ~8 km total thickness.

For simplicity in the analysis following (Section 6.2) lateral continuity of the litho-tectonic units is assumed, but the map pattern indicates that persistence of individual units varies. For example, in the Lawson Range-Nye Bay area (Figure 25) a black graphitic phyllite from Middle Rocks to Nye Bay occurs on the western limb of the Nye Bay fold-nappe but is absent on the eastern limb (Figure 27). The high-grade schist appears to taper out along the eastern limb of the Lawson Range Anticline and/or lower limb of the Nye Bay fold-nappe. The quartzite at Top Rocks on the upper western limb also appears to thin northwards (Figure 25).

6.2 Geometrical Simulations

Simple geometrical simulations of the Southern Tyennan fold stack (Figures 67, 68 and 69) were undertaken in an attempt to understand the changes in the stacking order as well as the significance of the limited younging data. This was done in relation to the interpreted fold pattern within the defined Southern Tyennan structural architecture.

6.2.1 Simplified Fold Stack Geometry Explanation

A "simple" schematic fold evolution for the Southern Tyennan domain folds is a series of west-verging folds in continuous layering inclined to the east (Figure 67). This interpretation gives the following mechanical explanations for fold evolution:

1. The Nye Bay fold-nappe (circled 1, Figure 67) resulted from "lip-rollover", or bending back on itself, due to frictional resistance by tractional forces along the base of the overlying "sheet". This is somewhat analogous to stubbing-your-toe, as a "toe-stub" fold;
2. The tractional forces at the leading edge effectively pin the front of the sheet such that the structurally lower folds initiate as "catch-up" folds analogous to the wrinkles in a rug sliding on an inclined surface;
3. The mega-sheath folds (circled 3 and 4, Figure 67) initiate as point lobes in the subduction channel about a potentially thickened part of the continental margin sand wedge (cf. Gross et al., 2021).

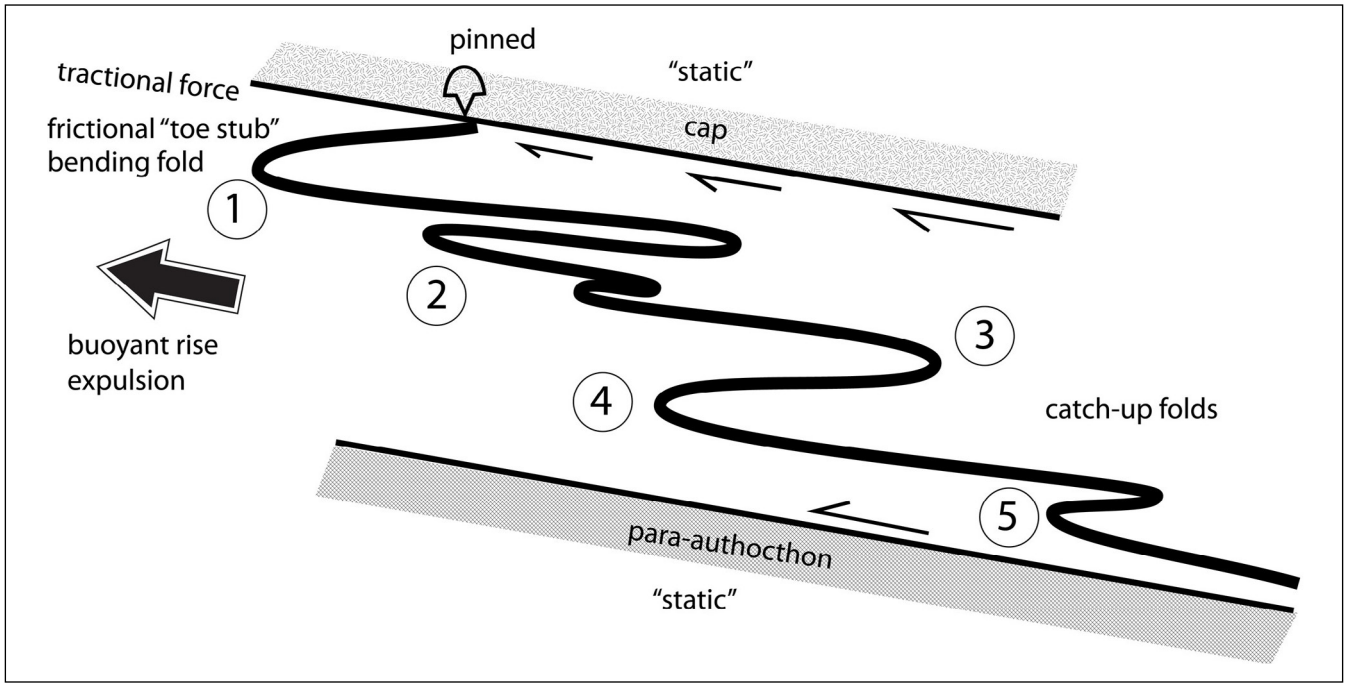

Figure 67. Simple schematic fold evolution diagram depicted as channelised flow within the subduction channel. The channel is bounded by the cap (obducting ophiolite) and the underlying para-autothocthon. Structural evolution and the resultant structures labelled 1 through 5 form as a competition between tractional forces along the channel boundaries and the buoyancy force within the subduction channel.
1: Nye Bay fold-nappe. 2: Mulcahy-Nye Bay isoclinal fold-stack. 3: east-closing De Witt-Propsting mega-sheath fold. 4: west-closing South West Cape mega-sheath fold. 5: Red Point macro-fold.

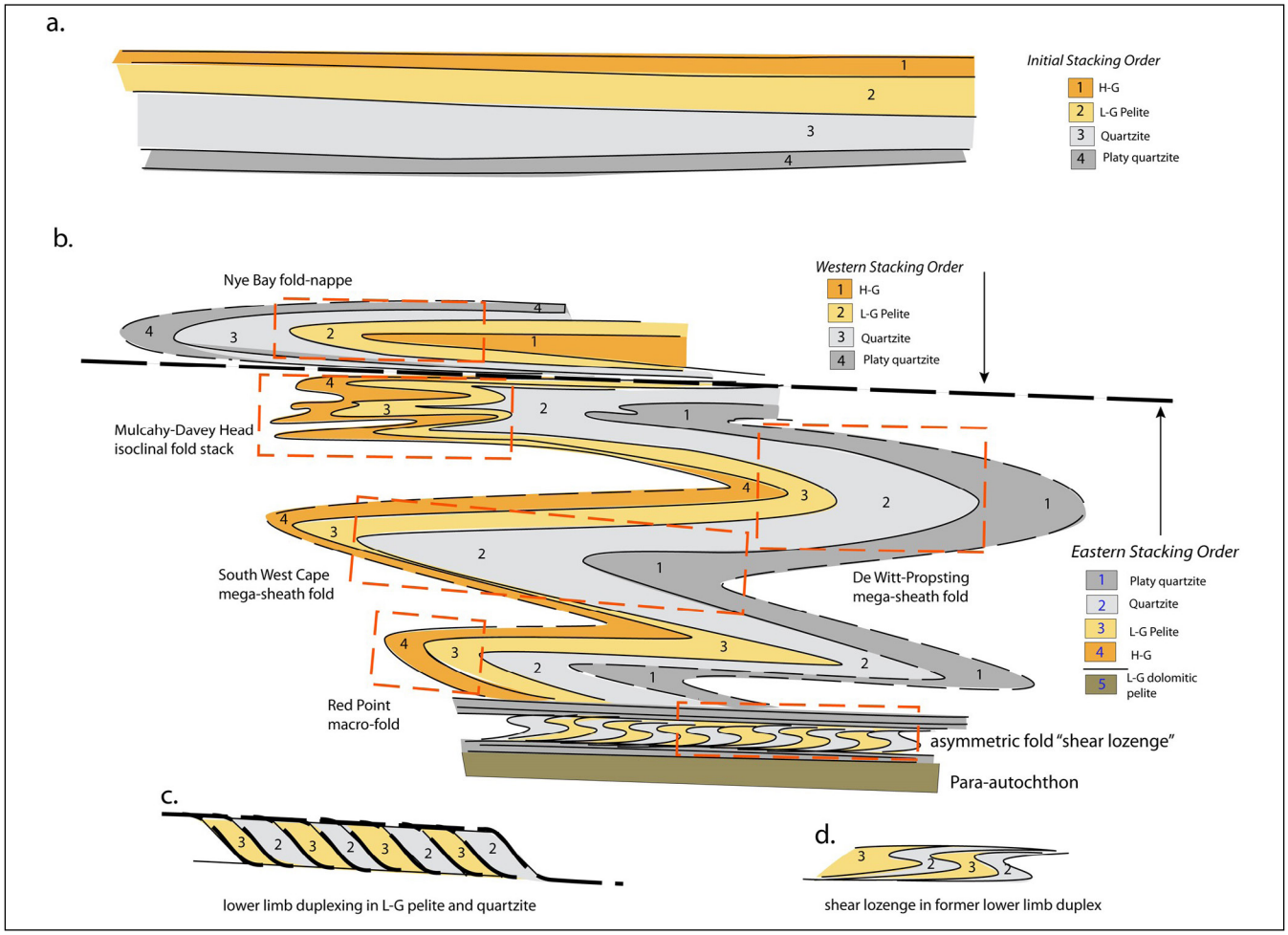

Figure 68. Macro-fold geometry of the Southern Tyennan domain using the observed stacking order and the interpreted structural architecture. a) Initial stacking order based on the uppermost Nye Bay fold-nappe and unit stacking through the Mt Eleanor Anticline. b) Interpreted structural architecture using the unit stacking relationships through the different macro-folds. The red dashed boxes approximate the positions and observed units in the various macro-fold structures. c. Duplex model for low-grade pelite and quartzite duplication in the lower limb of the lowest Red Point macro-fold. d) Final shear lozenge geometry and the observed wave train of asymmetric folds derived by marked shear strain and flattening within the duplex scenario shown in (c).

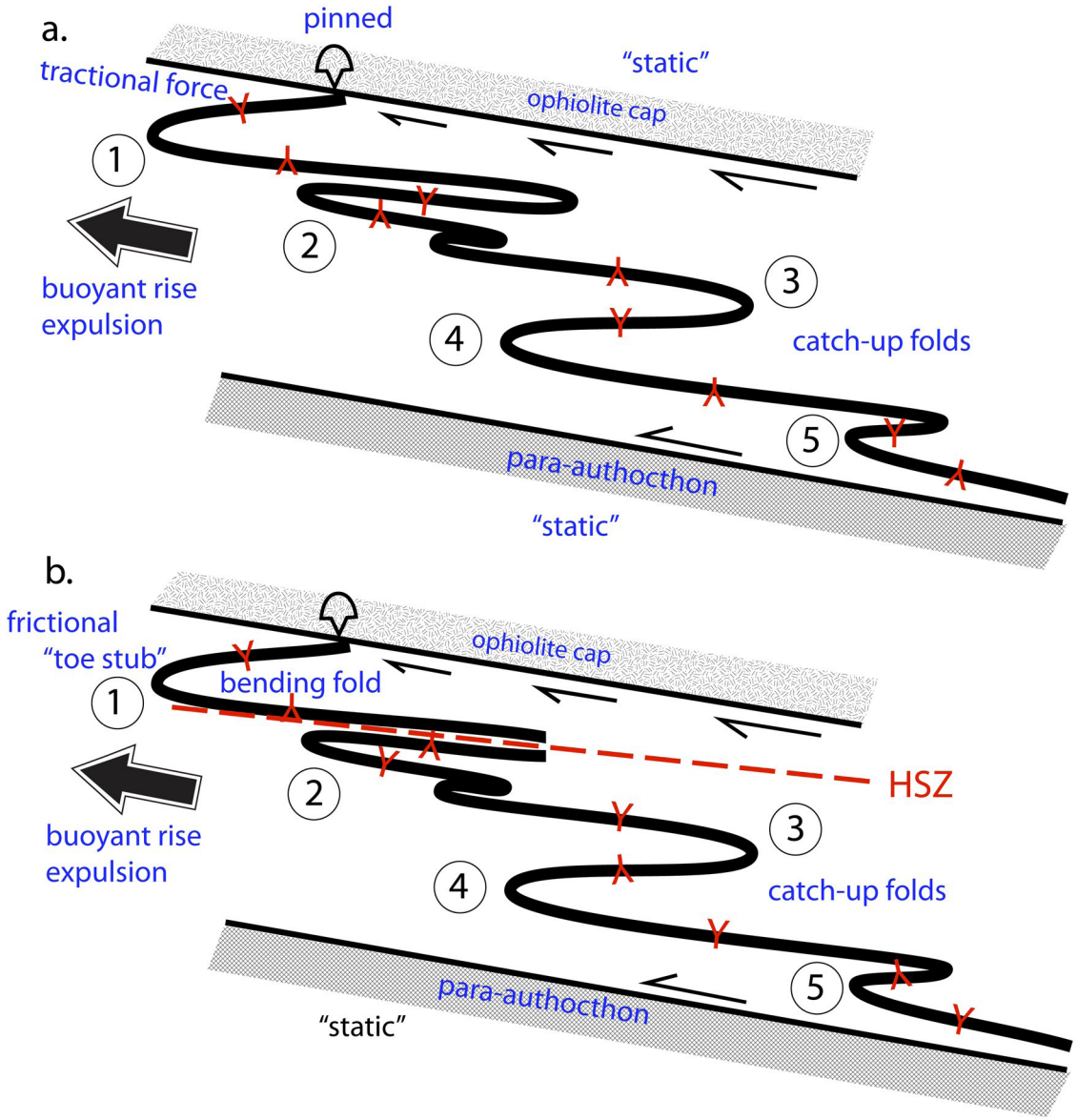

Figure 69. Younging analysis diagrams. a) Younging relationships in a geometry with continuous asymmetric folded layering (Figure 67). b) Younging relationships in a revised geometry based on the observed stacking order relationships (Figure 68).

A possible fold evolution analogy is that of a rug on a table, where the trailing part of the rug "catches up" with an essentially "pinned" or slower moving leading edge, as a fold "wave train" of wrinkles (folds) develops at the rear. The analogy implies a subtle timing difference between the mega-sheath fold development and the lower-limb fold-wave train, with "wave train" development largely post-dating the mega-sheath fold.

6.2.2 Folded Stacking Order Simulation

Stacking order determinations throughout the Southern Tyennan domain provide constraints on the geometry. A simple stacking (Figure 68a) has the composite sheet made up of high-grade schist (top sheet or unit 1) overlying low-grade pelite (unit 2), overlying low-grade quartzite (unit 3) with a basal schistose or platy quartzite (unit 4).

The fold model geometry shown in Figure 68b suggests there is an inverse stacking of units below the interface with the Nye Bay Fold-nappe. Using the unit stacking relationships determined through each of the inferred macro-folds (Figure 68b) there is an apparent change in the stacking order from the structurally highest Nye Bay fold-nappe to the structures below it.

6.2.3 Younging "Test" for Structural Geometry Models

Despite limited younging data throughout the Southern Tyennan domain the stacking order relationships (Figure 65) require an inversion of the stacking order below the Nye Bay fold-nappe. This inversion of the stacking order below the Nye Bay fold-nappe (Figure 65) requires a modification of the simple folded continuous layering model of Figure 67.

Two geometrical models are therefore tested with the available younging data (Figure 69).

6.3 Structural Evolution of the Southern Tyennan Domain

Changes in unit stacking order, the overall sheet younging and macro-fold asymmetry requires overturning of the Southern Tyennan composite sheet. Figure 70 illustrates an interpretative series of stages in the structural and tectonic evolution of the Southern Tyennan domain. The stages are:

Stage 1 (The Subduction Stage): where the continental margin with a simple sedimentary facies system from thick deposits of proximal quartz sands (light grey) to distal, deeper basinal fine grained pelite (light orange and dark orange).

Stage 2 (Ascent and Sheet Stacking): involves segmentation of the metamorphosed subducted margin with a stacking order related to the depth of subduction accompanied by overthrusting and resultant stacking of the deeper sheets on the shallower subducted sheets.

Stage 3 (Crustal-scale isoclinal overfolding): involves pinning at the toe of the composite sheet and subsequent development of an overfold by a rolling hinge mechanism. The lower overfold limb (overturned limb) propagates (see Stage 4) and eventually becomes the Southern Tyennan domain sheet with a 20-40 km length (subduction dip direction), 5-8 km thickness and 100 km width (margin strike direction) dimensions.

Stage 4 (Shear zone propagation): with eventual isolation of sheets along the red dashed line (subsequent break).

Stage 5 (Final Stacking): with resultant geometries that match the right-way-up Eastern Tyennan domain (sheet 1) and the upside-down Southern Tyennan domain (sheet 2). Tractional flexing at the leading edges of sheet 1 (upper sheet) during further buoyant ascent develops the regional scale fold-nappe, whereas internal deformation within sheet 2 produces the mega-sheath fold pair and isoclinal macro-folds.

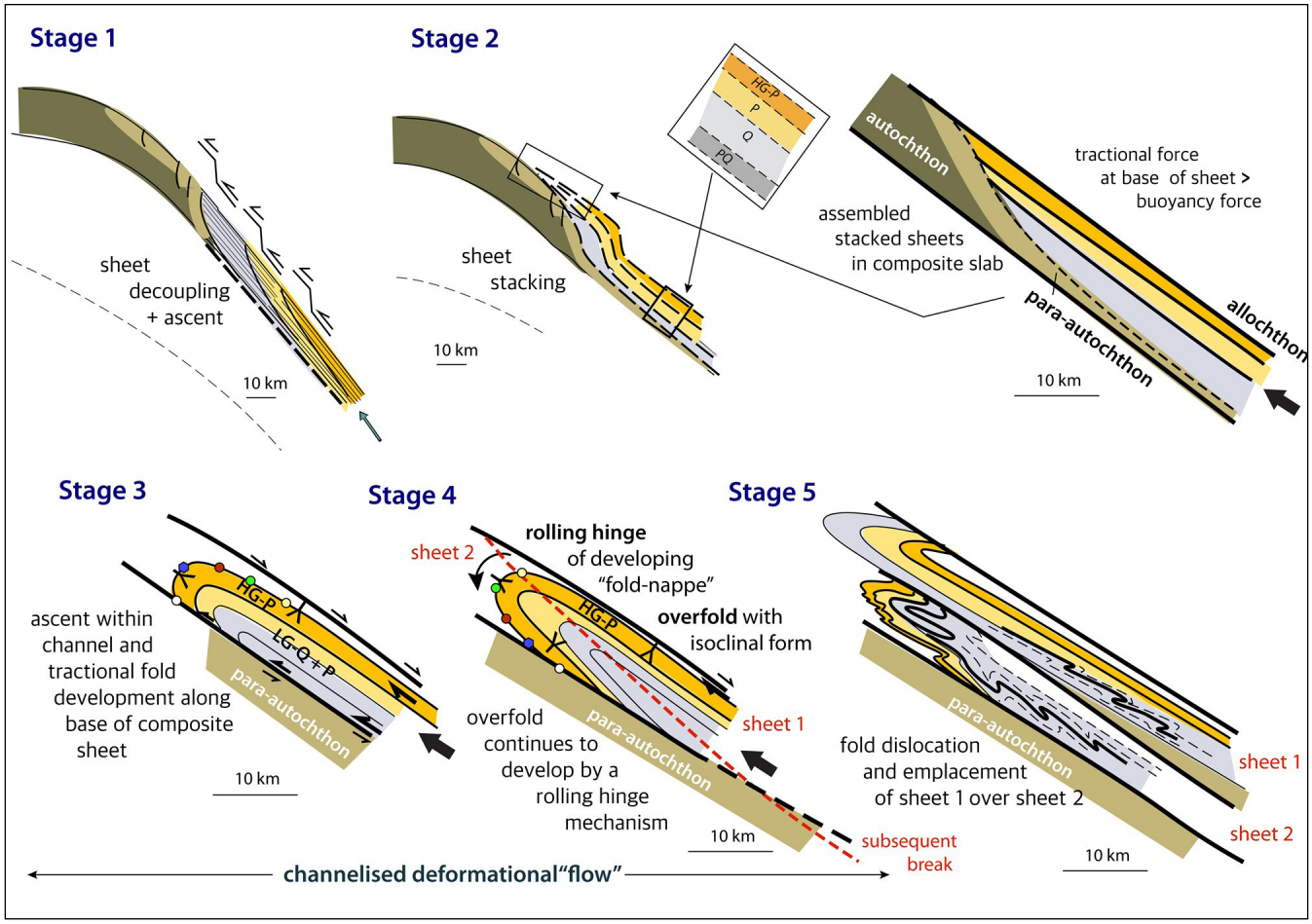

Figure 70. Interpretative structural-tectonic evolution of the Southern and Eastern Tyennan domains. The evolution is presented as a series of stages post margin subduction to depths of 40-60 km. The process involves sheet decoupling facilitated by the normal fault architecture of the rifted margin during Rodinia breakup. This is followed by ascent and stacking of sheets with the high-grade sheet at the top of the assembled stack. Ascent of the composite stacked "sheet" involves development of a tractional-overfold at the base of the sheet via a combined traction-pinning and hinge rolling mechanism within the subduction channel Eventual fault truncation of the overfold results in emplacement of sheet 1 (Eastern Tyennan) over sheet 2 (Southern Tyennan).

7.0 ACKNOWLEDGEMENTS

- Mineral Resources Tasmania (Andrew McNeill) for providing support through the 2016-2020 Geoscience Initiative and critically editing and reviewing the document.
- Mike Hall, Ron Berry, Sebastien Meffre, John Miller, Peter Williams, Paul Lennox, Andrew McNeill and Jacob Mulder for southwest coastal mapping and structural data collection. This compilation would not have been possible without their fieldwork.
- Ron Berry for providing copies of his 1997 field mapping sheets, detailed field notes and field notebook.
- Grant Dixon for providing photographs of the parts of the Southern Tyennan including the Arthur Ranges, the Propsting Range and the Crossing River gorge and for sharing his knowledge of the lithologies west of the Eastern Arthur Range through to the Crest Range.
- Bushwalker photographs by David Noble, Becca Lunnon and Peter Dombrovskis in this and the other companion Southern Tyennan Mineral Resources Tasmania Geological Survey Papers.
- Access to map sheets and/or field notebook copies of Hall, Miller, Williams and Lennox was through Mineral Resources Tasmania and Parks and Wildlife Service (PWS).
- Chris Large for editing and formatting this Tasmanian Geological Survey publication.
- Parks and Wildlife Service (PWS) for allowing helicopter access and landing in the World Heritage Area as well as permits for measurement, sampling and photograph collection.
- Jason Bradbury NRE (Department of Natural Resources and Environment) for assistance with WHA and PWS permits for scientific research.
- Rodney Smith from Rotorlift for helicopter transport into the Tasmanian southwest.
- Rick Allmendinger and Nestor Cardozzo for use of OSX Stereonet.

8.0 REFERENCES

Alsop, G., and Carreras, J. 2007. Structural evolution of sheath folds: a case study from Cap de Creus. *Journal of Structural Geology*, 29, 1915-1930.

Alsop, G. I. and Holdsworth, R. E. 1999. Vergence and facing patterns in large scale sheath folds. *Journal of Structural Geology*, 21, 1335-1349.

Alsop, G. and Holdsworth, R. E. 2004. The geometry and topology of natural sheath folds: a new tool for structural analysis. *Journal of Structural Geology*, 26, 1561-1589.

Alsop, G. and Holdsworth, R. E., 2006. Sheath folds as discriminators of bulk strain type. *Journal of Structural Geology*, 28, 1588-1606.

Berry, R. F. 1997. Unpublished Field Notes.

Berry, R. F. 2014. Chapter 4.2 Cambrian Tectonics – The Tyennan Orogeny. In Corbett, K. D., Quilty, P. G & Calver, C. R. (Editors), Geological Evolution of Tasmania pp 95-110. *Geological Society of Tasmania Special Publication*, 24, Geological Society of Australia (Tasmania Division). 270p.

Berry, R. F. and Crawford, A. J. 1988. The tectonic significance of Cambrian allochthonous mafic-ultramafic complexes in Tasmania. *Australian Journal of Earth Sciences*, 35, 523-533.

Burns, K. L. 1964. *Devonport*, Tasmania.Geological Atlas One Mile Series Map Explanatory Notes. Department of Mines Tasmania.

Chmielowski, R. M. 2009. *The Cambrian metamorphic history of Tasmania*. PhD Thesis, University of Tasmania.

Chmielowski, R. M. and Berry, R. F. 2012. The Cambrian Metamorphic History of Tasmania: The Metapelites. *Australian Journal of Earth Sciences*, 59, 1007-1019.

Corbett, K. D. and Vicary, M. J. 2014. Chapter 4.5.6 Middle Cambrian Sequences to the East of the Tyennan Block. In Corbett, K. D., Quilty, P. G & Calver, C. R. (Editors), Geological Evolution of Tasmania pp 172-174. *Geological Society of Tasmania Special Publication*, 24, Geological Society of Australia (Tasmania Division).

Dixon, G and Sharples, C. 1986 , Reconnaisance geological observations on Precambrian and Palaeozoic rocks of the New and Salisbury Rivers, Southern Tasmania, *Papers and Proceedings of the Royal Society of Tasmania*, 120 , 87-94.

Gray, D. R. and Vicary, M. J. 2021a. Structural Geology of Frenchmans Cap, Central Tyennan Domain, Tasmania. Mineral Resources Tasmania, *Geological Survey Paper*, 6, 44p.

Gray, D. R. and Vicary, M. J. 2021b. Structural Geology of the Central Tyennan Region, Tasmania. Mineral Resources *Tasmania, Geological Survey Paper*, 7, 69p.

Gray, D.R. and Vicary, M. J. 2022a. Structural Geology of the Arthur Range, Central Tyennan Domain, Tasmania. Mineral Resources Tasmania, *Geological Survey Paper*, 8, 79p.

Gray, D. R. and Vicary, M. J. 2022b. Mega-sheath fold core of the Southern Tyennan domain, Tasmania. The De Witt-Propsting and South West Cape mega-sheath folds. *Geological Survey Paper*, 10, 80p.

Gray, D. R. and Vicary, M. J. 2022c. Structural Geology of the eastern Southern Tyennan Domain, Tasmania. Mineral Resources Tasmania, *Geological Survey Paper*, 11, 43p.

Gray, D. R. and Vicary, M. J. 2022d. Structural Geology of the Red Point Metamorphic Complex, Southern Tyennan Domain, Tasmania. Mineral Resources Tasmania, *Geological Survey Paper*, 12, 23p.

Gray, D. R., Vicary, M. J. and McNeill, A. W., 2022. Structure of the High-grade Coastal Belt, Southern Tyennan Domain, Tasmania. Mineral Resources Tasmania, *Geological Survey Paper*, 9, 87p.

Gross, P., Handy, M. R., John, T., Pestal, G. and Pleuger, J. 2020. Crustal-scale sheath folding at HP conditions in an exhumed Alpine subduction zone (Tauern Window, Eastern Apls). *Tectonics*, 39, 22p.

Hall, M. 2005. Unpublished field maps and notes (Top Rocks – Nye Bay - Mulcahy Bay - Wreck Bay - Towterer Beach Area, 2004-05).

Hall, M. 2006. Unpublished field maps and notes (Gilbin River – Lawson Range area).

Hall, M. 2008. Unpublished field maps in the Wreck Bay to Davey Head area.

Hall, W. D. M. 1965. *Report No.1 March-June 1965 for Exploration Licence 13/65 Southwest Tasmania: Geological and geochemical exploration in the area between Bathurst Channel, Cox Bight and South West Cape*. Tasmanian Company Report, 65_0398, 68p.

Hall, W. D. M., McIntyre, M. I., Corbett, E. B., McGregor, P. W., Fenton, G. R, Arndt, C. D. and umstead, E. D. 1969. Report on Field Work in Exploration Licence 13/65, *South-West Tasmania During 1967-68 Field Season.* Tasmanian Company Report, 69_0555.

Hall, M. and Vicary, M., (Compilers). 2010a. Digital Geological Atlas 1:25,000 Scale Series. Sheet 3822. *Mulcahy*. Mineral Resources Tasmania.

Hall, M. and Vicary, M., (Compilers). 2010b. Digital Geological Atlas 1:25,000 Scale Series. Sheet 3823. *Elliott*. Mineral Resources Tasmania.

Hall, M. and Vicary, M. (Compilers). 2010c. Digital Geological Atlas 1:25,000 Scale Series. Sheet 4023. *Propsting*. Mineral Resources Tasmania.

Hall, M. and Vicary, M., (Compilers), 2010d. Digital Geological Atlas 1:25,000 Scale Series. Sheet 4024. Rookery. Mineral Resources Tasmania.

Lennox, P. G. 1980. Unpublished Field Notes (Mineral Resources Tasmania Field Notes F_PLG_3).

Lennox, P. G. 2013. Geology of parts of the Bathurst and Maatsuyker map sheets. *Tasmanian Geological Survey Record*, 2013/03, 30p.

McNeill, A. W. 1985. *The structure and petrology of the Nye Bay area, south west Tasmania*. B.Sc (Hons) Thesis, University of Tasmania: Hobart.

MacLean, C. J. and Bowen, E. A. 1971. Structure of the Precambrian rocks of the Port Davey area, south western Tasmania. *Papers and Proceedings of the Royal Society of Tasmania*, 105, 97-104.

Meffre, S., Berry, R. F. and Hall, M. 2000. Cambrian metamorphic complexes in Tasmania: tectonic implications. *Australian Journal of Earth Sciences,* 47, 971 – 985.

Meffre, S., Berry, R.F., Hall, M. and McNeill, A. 2001. The Structural Style of Cambrian Metamorphic Complexes in Tasmania: SW Tasmanian examples. *Geological Society of Australia Abstracts*, 64, 118-120.

Miller, J. M. 2004. Unpublished Field Notes.

Mulder, J. A. 2013. *The Structure and Metamorphism of the Cox Bight-Red Point Area, South West Tasmania*. Honours Thesis, The University of Tasmania. 76p.

Mulder, J. A., Berry, R. F. and Scott, R. J. 2015. The structure and metamorphism of the Red Point Metamnoirpohic Complex - A newly discovered high-pressure metamorphic complex from the south coast of Tasmania. *Australian Journal of Earth Sciences*, 62, 969-983.

Seymour, D.B. 2014. Chapter 6.1 Middle Devonian Deformation. In Corbett, K.D., Quilty, P.G & Calver, C.R. (Editors), Geological Evolution of Tasmania pp 273-296. *Geological Society of Tasmania Special Publication*, 24, Geological Society of Australia (Tasmania Division).

Spry, A. H. and Baker, W. E. 1965. The Precambrian Rocks of Tasmania, Part VII. Notes on the petrology of some rocks from the Port Davey-Bathurst Harbour area. *Papers and Proceedings of the Royal Society of Tasmania*, 99, 17-26.

Stefanski, M. Z. 1957a Progress Report on Regional Geological Survey of the Port Davey-Cox Bight Area. *Tasmanian Department of Mines Technical Report*, 2, p.87-106.

Stefanski, M. Z. 1957b. Geological Compilation in the Bathurst Harbour Area. Unpublished Map, Mineral Resources Tasmania.

Taylor, A. M. 1959. Precambrian Rocks of the Old River Area. *Tasmanian Geological Survey Technical Report*, 4, p.34-36.

Turner, N. 1989. Precambrian. In: Burrett, C. F. and Martin, E. L. (Editors), Geology and Mineral Resources of Tasmania. *Geological Society of Australia Special Publication*, 15, 5-46.

Williams, P. R. 1976. Unpublished field notebooks. Davey Head 1 and 2. (F_PRW_18 and F_PRW_19). Mineral Resources Tasmania.

Williams, P. R. 1978. Digital Geological Atlas 1:50000 Series. Sheet 8011S. *Davey*. Mineral Resources Tasmania.

Williams, P. R. 1980. *Basin Development, Environment of Deposition and Deformation of a Precambrian? Conglomeratic Flysch Sequence at Bathurst Harbour, SW Tasmania*. PhD Thesis, The University of Tasmania.

Williams, P. R. 1982. Geological Atlas 1:50000 Series. Sheet 91 (8011S) *Davey*. Explanatory Report Geological Survey Tasmania.

Williams, P. R. 1989. Bathurst Harbour Area. . In: Burrett, C. F. and Martin, E. L. (Editors), Geology and Mineral Resources of Tasmania. *Geological Society of Australia Special Publication*, 15, 59-60.

APPENDIX 1

Sugarloaf Rock map and structure interpretation

Appendix

Sugarloaf Rock map and structure interpretation

This appendix consists of series of figures including maps, Google Earth images and photographs (photo credits: E. P. Ambler) used to determine the transport direction (107°).

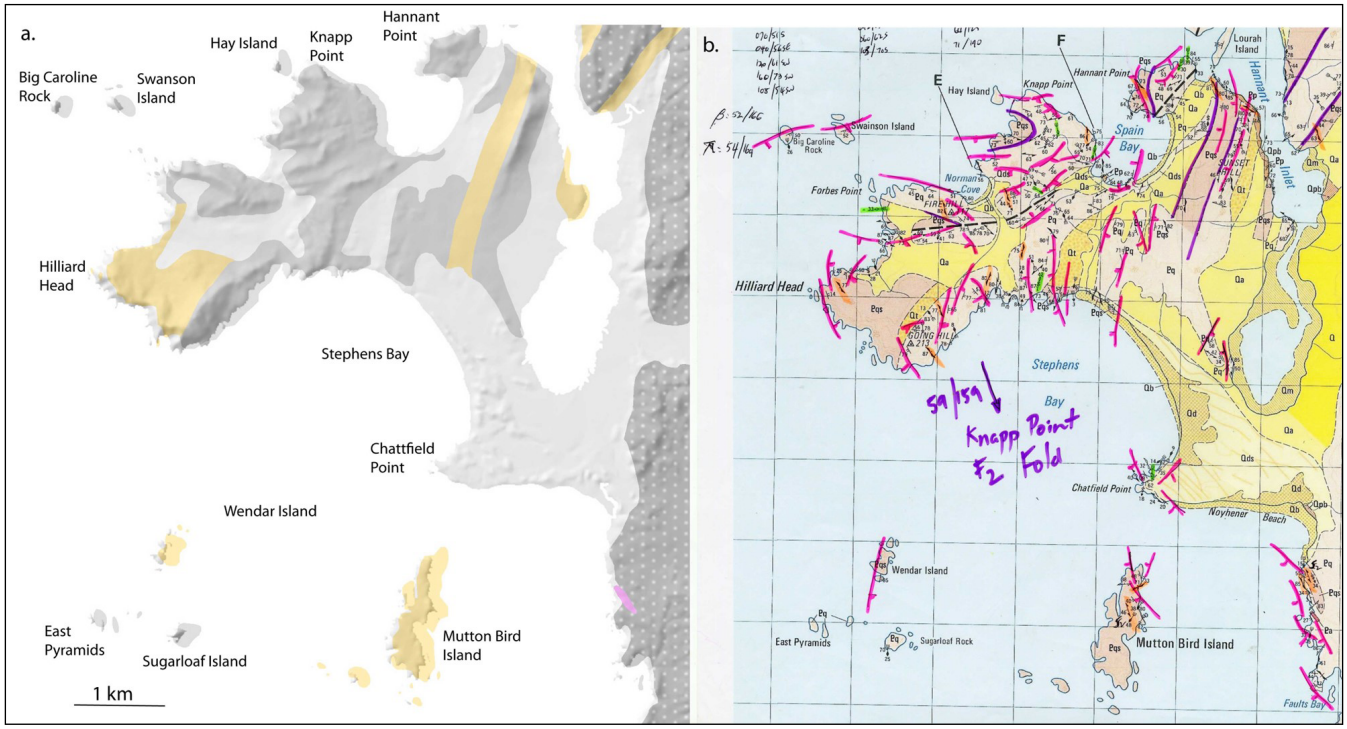

Figure 1. Knapp Point-Hilliard Head Stephens Bay Map with offshore islands. Sugarloaf Rock is shown west of Mutton Bird Island and east of East Pyramids. a) 1:250,000 geological atlas base map draped on ListMap digital elevation model. b) Portion of the Davey 1:50,000 Series Map (Williams, 1976) with formline interpretation.

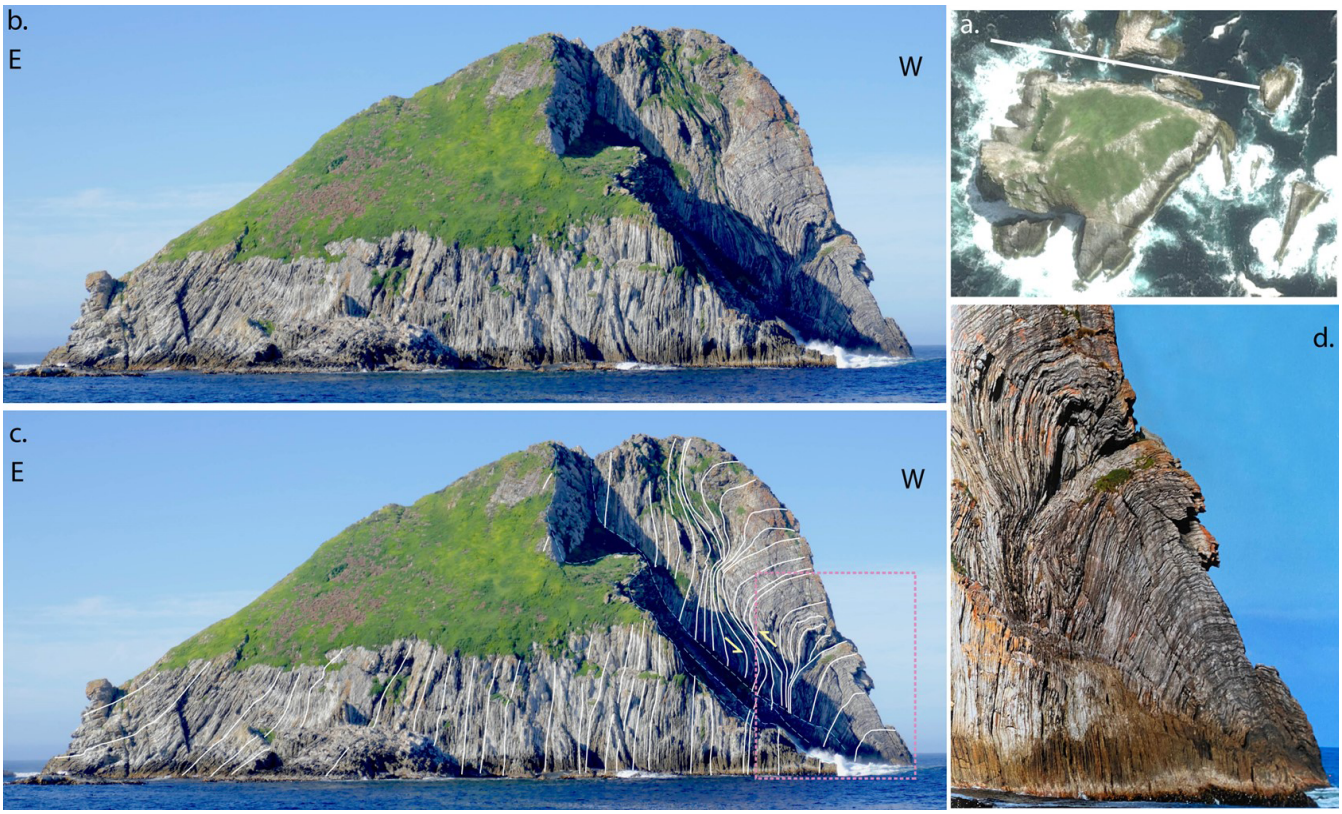

Figure 2. Photograph of the northern face of Sugarloaf Rock. View is to the south. a) Google image of Sugarloaf Rock with b) non-annotated and c) annotated photographs (Photo credit:E.P. Ambler). d) Close up of macro-shear bands (photo credit: Ian Johnston, "The Shank").

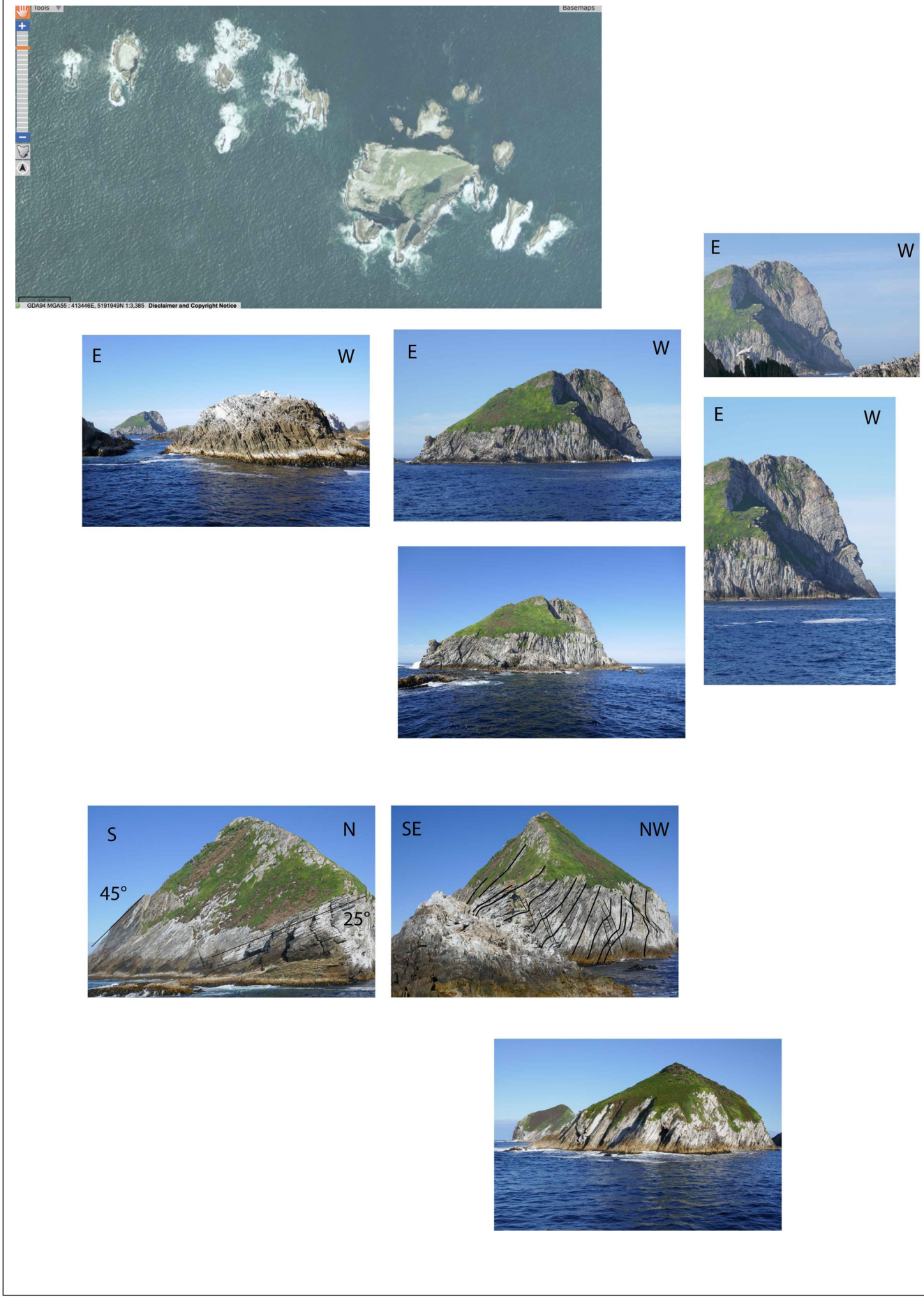

Figure 3. Photo collage of different views of Sugarloaf Rock. (photo credit: E. P. Ambler)

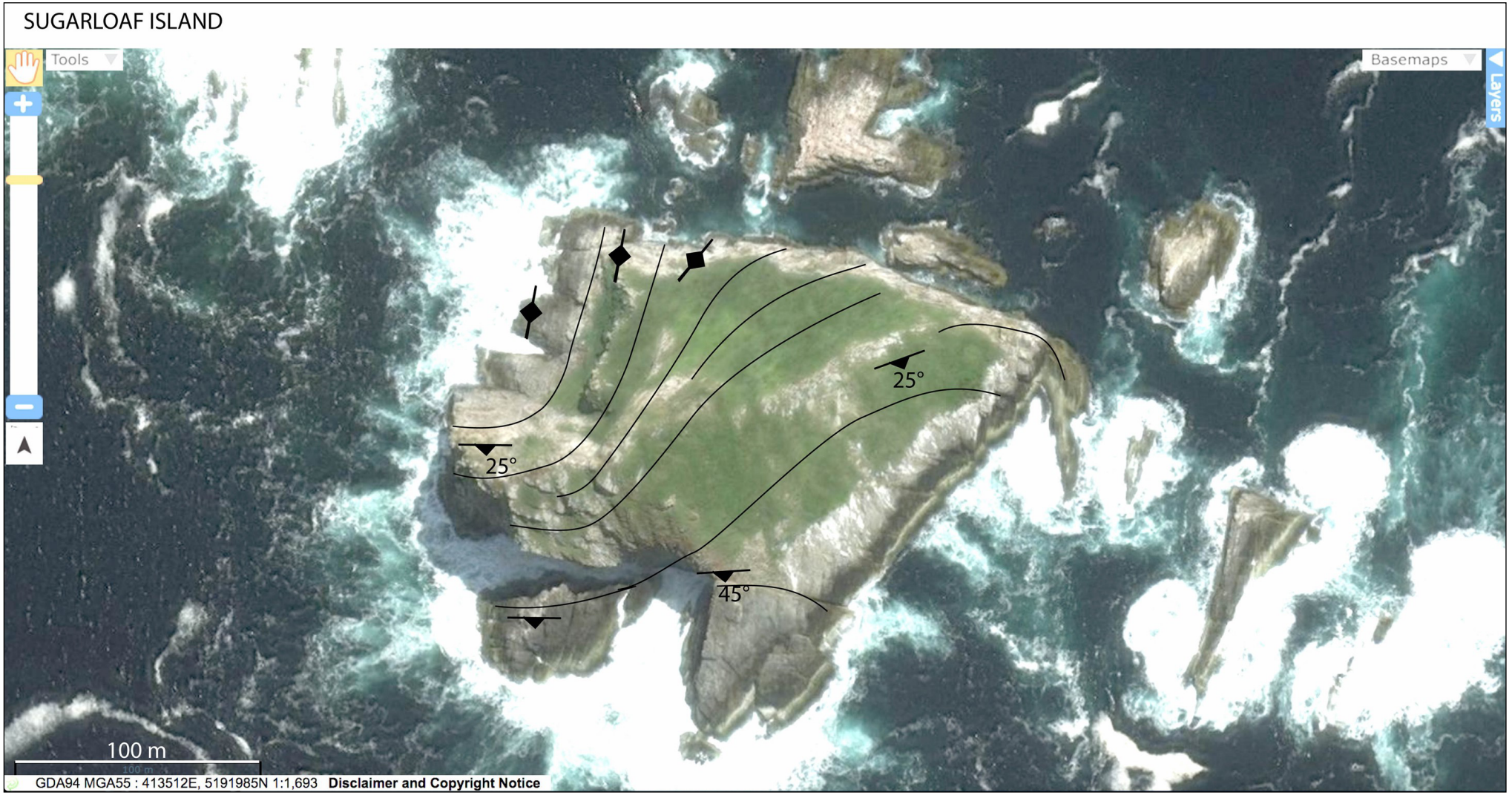

Figure 4. Formline map of Sugarloaf Rock based on the imagery in Figure 3. Note the Google image is rotated so that North is horizontal to the left.

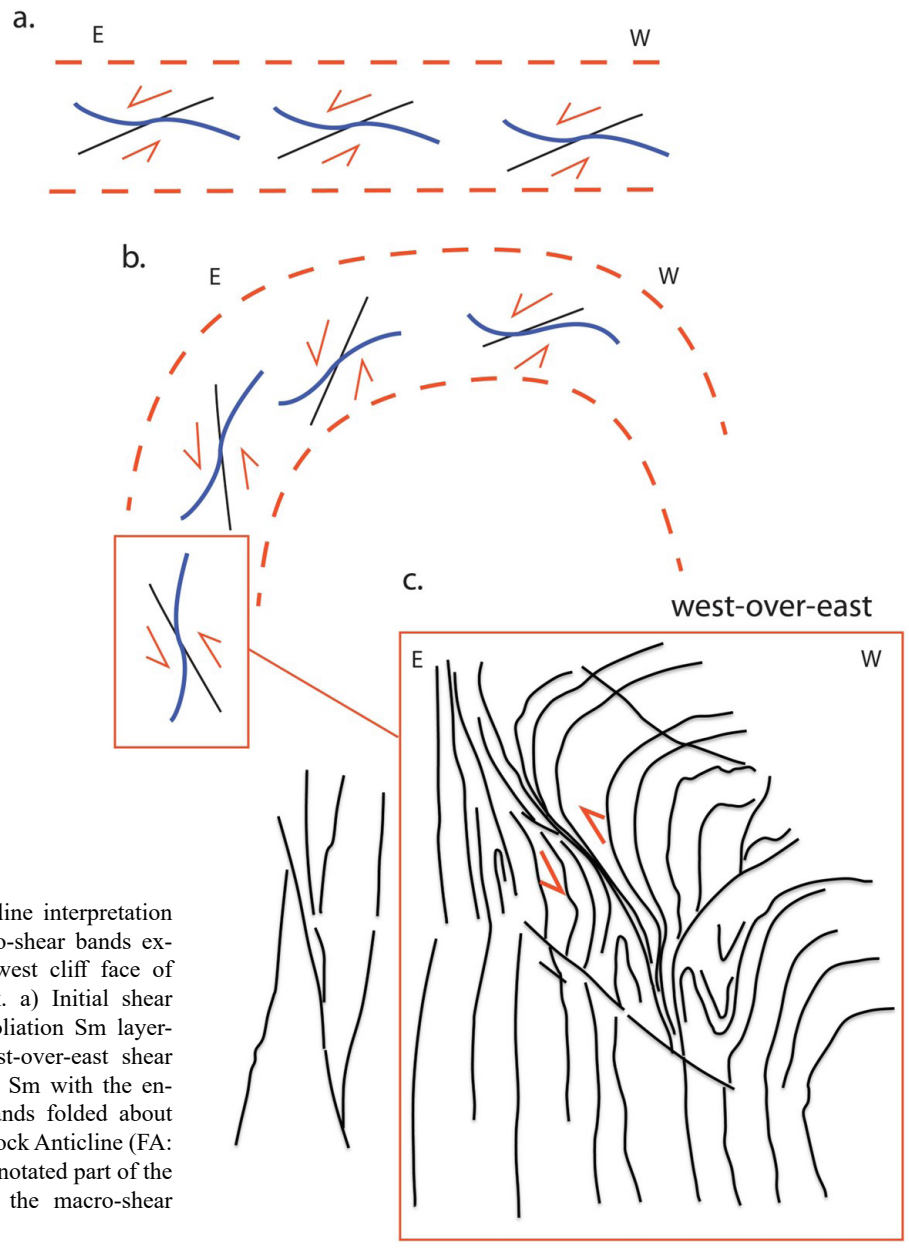

Figure 5. Formline interpretation of folded macro-shear bands exposed on east-west cliff face of Sugarloaf Rock. a) Initial shear bands within foliation Sm layering with a west-over-east shear sense. Foliation Sm with the enclosed shear bands folded about the Sugarloaf Rock Anticline (FA: 25°/178°) c) Annotated part of the cliff face with the macro-shear bands.

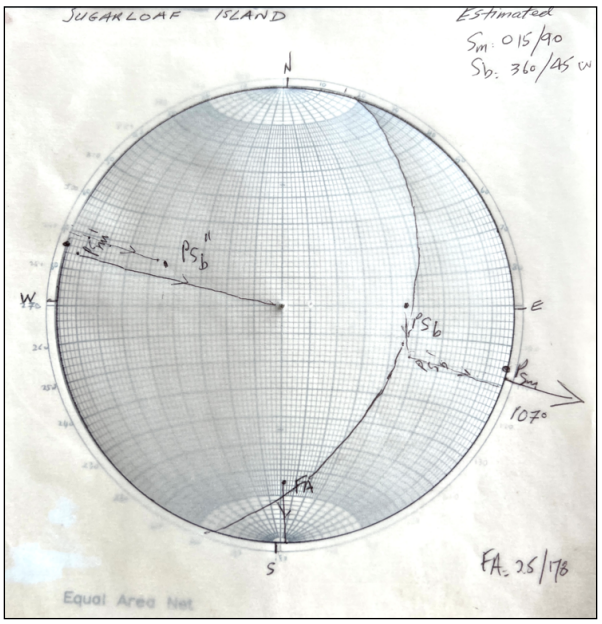

Figure 6. Stereonet showing restored macro-shear bands from the east-west cliff face of Sugarloaf Rock. The fold axis was removed and Sm restored to the horizontal to give a transport direction (TD) towards 107°.

Tasmanian
Government

Mineral Resources Tasmania
PO Box 56 Rosny Park
Tasmania Australia 7018
Ph: +61 3 6165 4800

info@mrt.tas.gov.au www.mrt.tas.gov.au